Diss. ETH No. 19065

Spatial aspects of the large-scale fate and transport of semivolatile organic chemicals

A dissertation submitted to the

Swiss Federal Institute of Technology Zürich

for the degree of
Doctor of Sciences

presented by
Harald Bernd Kurt von Waldow

Master of Environmental Studies, University of Waterloo
born November 26th, 1969
citizen of Germany

accepted on the recommendation of
Prof. Dr. Konrad Hungerbühler, examiner
PD Dr. Martin Scheringer, co-examiner
Prof. Dr. René Schwarzenbach, co-examiner

2010

ISBN 978-3-909386-36-9

Art is the lie that helps us see the truth.

(Picasso)

The same can be said for mathematical modelling.

(Lee A. Segel)

Danksagung

Ich bin vielen Menschen zu Dank verpflichtet, die mich direkt bei der Anfertigung dieser Dissertation unterstützt haben, die meine akademischen Ausbildung geleitet und geprägt haben, und deren Präsenz in meinem Leben sowohl Stütze als auch Motivation war.

Besonderer Dank gebührt Konrad Hungerbühler, der diese Arbeit erst ermöglicht hat, indem er mich als Doktorand in seiner Arbeitsgruppe aufgenommen hat. Neben der Organisation eines exzellenten Arbeitsumfeldes verdankt ihm diese Arbeit auch einige originelle Ideen, die sich zu wichtigen Punkten in der wissenschaftlichen Argumentation entwickelt haben. Ich danke meinem Betreuer Martin Scheringer, der mich nicht nur von seinem Erfahrungsschatz wissenschaftlichen Arbeitens und Schreibens hat profitieren lassen, sondern in fruchtbaren Diskussionen, die, weit über technische Details der täglichen Arbeit hinaus, vor allem auch die Bedeutung unseres Forschungsfeldes im gesellschaftlich Kontext zum Inhalt hatten, meinen Horizont erweitert hat. Martin hat mit seinen Arbeiten zur expositionsbasierten Chemikalienbewertung mittels Reichweite und Persistenz in den 90er Jahren einen Grundstein gelegt, auf dem diese Doktorarbeit fußt. Die Zusammenarbeit mit Matt MacLeod hat diese Arbeit ebenfalls entscheidend geprägt. Matts Tür stand immer offen, um von technische Fragen bis hin zu grundlegenden konzeptuellen Themen alles zu diskutieren, und wertvolle Einsichten des erfahrenen Praktikers einzuholen. Thanks a lot, Matt. Ich danke René Schwarzenbach für die Übernahme des Korreferats.

Kevin Jones, seine Arbeitsgruppe in Lancaster und insbesondere Jasmin Schuster haben mich mit essentiellen Meßdaten versorgt, die es mir ermöglichten, diese konzeptuell - theoretisch geprägte Dissertation empirisch zu untermauern. Ich danke dieser Gruppe auch für fruchtbare Diskussionen und geduldige Erläuterungen der Feinheiten der Messung von Chemikalien in der Umwelt. Während meiner Zeit als Doktorand habe ich von der Zusammenarbeit mit Lara Lamon und Pascal “the hacker” Tay profitiert, denen ich für ihre Kooperati-

on danke. Werner Stahel ist ein ausgezeichneter Pädagoge der Statistik und ich danke ihm und Stefan "WBL-Mami" Oberhänsli für die geduldige aber effiziente Erweiterung meiner Statistikkenntnisse.

Ich danke Prisca Rohr und Erol Dedeoglu, die mir während des Doktorats gekonnt Rückendeckung gegenüber administrativen und IT-bezogenen Problemen gewährt haben.

Das Werkzeug dieser Arbeit war der Computer, ein nutzloses Gerät ohne die große Anzahl hervorragender Programmpakete, die von talentierten Programmierern weltweit in ihrer Freizeit geschrieben, gepflegt, und als Quellcode der Allgemeinheit zur Verfügung gestellt werden. Ohne diese Ressource wäre die Dissertation in dieser Form nicht möglich gewesen.

Die Gemeinschaft aufgeschlossener und talentierter Kollegen und Kommilitonen in der Arbeitsgruppe war eine stetige Quelle der Inspiration und des Ansporns. Immer bereit für fachliche Gespräche und Philosophierereien über Gott und die Welt, haben sie dafür gesorgt, daß sich der HCI G-Stock oft mehr als eine gut funktionierende Wohngemeinschaft denn als ein Arbeitsplatz angefühlt hat. Danke, Andrea, Asif, Bobby, Bojan, Christiane, Christian, David, Fabio, Gilles, Götz, Gregor, Matze, Peter, Sébastien, Stefano und ganz besonders Roland für anregende Gespräche, Tögglimatches, Kaffee und Kuchen, Tennismatches, Freizeitgestaltung, Nachtschichtgesellschaft und alles andere.

Ich danke meinen Eltern für die Unterstützung und das Vertrauen, das sie mir mein ganzes Leben lang geschenkt haben.

Ein ganz besonderer Dank gebührt meiner Frau, die mir durch alle Höhen und Tiefen hindurch den Rücken freigehalten hat. Vielen Dank liebe Suse dafür, daß du mich je nach Bedarf liebevoll aufgepäppelt oder energisch motiviert hast, dafür, daß du das Leben außerhalb der Doktorarbeit für mich gemanaged hast, für Lotte und Fritz, für das Ertragen meiner Nacht- und Wochenendschichten, für deine Liebe und dafür, daß du die beste Ehefrau bist, die ich mir vorstellen kann.

Summary

Chemical contamination of the environment is recognised as a major problem which has to be managed on local, national and international levels to ameliorate and avoid irreparable damage to ecosystems and human health. Of particular concern are persistent and toxic chemicals that may bioaccumulate, travel large distances and contaminate ecosystems far away from emission sources. Substances known to possess these properties are called *persistent organic pollutants* (POPs) and most of them are halogenated hydrocarbons. As a consequence of their phase partitioning behaviour, they can occur in the gas phase to be available for efficient atmospheric long-range transport, but also partition into surface compartments and biota. POPs are used as pesticides, as technical chemicals with a wide range of applications, and might be produced unintentionally as by-products during the production of other chemicals or during other anthropogenic processes such as waste incineration.

International agreements such as the *POP Protocol of the UNECE Convention on Long-Range Transboundary Air Pollution* and the the *Stockholm Convention on POPs* that ban and/or regulate the production and use of POPs require the assessment of chemicals with respect to their toxicity and bioaccumulativity, their persistence in the environment and their long-range transport behaviour.

Mathematical fate- and transport models are indispensable tools to evaluate chemicals with respect to persistence and long-range transport potential. A target variable calculated with these models is the environmental exposure to a chemical. It indicates the part of the potential hazard of a chemical that is caused solely by the chemical's fate and transport behaviour, regardless of toxicological substance properties. Metrics for both, persistence and long-range transport potential are based on exposure. Usually, pulse emissions are assumed to calculate exposure. Here, it is show that exposure does not depend on the shape of the emission function. Exposure calculated for the pulse release of a particular mass of contaminant is equal to exposure calculated for any arbitrary dynamic release of the same mass. This result allows for a more general interpretation of

exposure-based metrics for persistence and long-range transport potential of a chemical. It further extends the meaning of model evaluations at steady-state. Steady-state models yield valid results for certain indicators, without the need to assume that chemical concentrations in the environment have reached or will reach steady-state.

The long-range transport potential of a chemical is the least well defined screening criterium for POPs. Measured levels of a chemical at locations distant from sources can be used as evidence of long range environmental transport, but until now, there has been no quantitative measure of the distance of a location from likely source areas of chemicals. Here an Eulerian atmospheric tracer transport model is employed to calculate a measure of remoteness which describes the effective distance of a location from distributed emission sources, taking into account geographical distance and atmospheric transport pathways. Maps of remoteness for two generic emissions scenarios that represent areas for emissions of industrial and technical chemicals and of pesticides are presented. The results can be used to better interpret spatial patterns of measured and modelled concentrations of chemicals in the global environment, to derive long-range transport potential metrics for specific substances, and to plan future measurement campaigns and extend monitoring networks.

The *global distillation hypothesis* is the dominant paradigm to explain large scale fractionation patterns of semivolatile organic compounds and therefore related to the conceptual understanding of the mechanisms of POP long-range transport. It states that observed fractionation patterns are a result of global patterns of environmental temperatures interacting with the temperature dependencies of the chemicals' phase partition coefficients. Here, an alternative hypothesis is presented, the *differential removal hypothesis*. It proposes that the differences of average atmospheric loss rates, acting along a gradient of remoteness from emission sources, cause observed patterns of global fractionation. A model experiment and a thorough analysis of datasets of concentrations of polychlorinated biphenyls (PCB) in European air are used to compare both hypotheses. The results indicate that the variation of temperature across Europe and into the Arctic has no effect on observed fractionation patterns of PCB congeners in air, but that the *differential removal hypothesis* explains these patterns very well.

Finally, the relationship between measured concentrations and effective distance from emission sources is used to calculate effective residence times in air for a set of PCB congeners. The effective residence times compare well with values calculated by a multimedia mass balance model and can serve as an em-

pirically derived metric for the long-range transport potential of semivolatile organic compounds.

Zusammenfassung

Die Belastung der Umwelt mir Chemikalien ist anerkannterweise ein bedeutendes Problem, das auf lokaler, nationaler und internationaler Ebene bewältigt werden muß, um irreparable Schäden für Mensch und Natur zu mindern und zu vermeiden. Besonders bedenklich sind persistente und toxische Chemikalien, die bioakkumulieren, große Distanzen zurücklegen können und weit von den Emissionsquellen entfernte Ökosysteme belasten. Substanzen, die diese Eigenschaften besitzen, werden als *persistent organic pollutants* (POPs) bezeichnet, und die meisten davon sind halogenierte Kohlenwasserstoffe. Durch ihr Verteilungsverhalten kommen sie in der Gasphase vor, in der sie effizient über weite Strecken transportiert werden können, partitionieren andererseits aber auch in Oberflächenkompartimente und Lebewesen. POPs wurden und werden als Pestizide und als technische Chemikalien mit einem großen Anwendungsbereich genutzt, fallen aber auch unabsichtlich bei der Produktion anderer Chemikalien als Nebenprodukte an oder enstehen bei anderen anthropogenen Prozessen, z.B. bei der Müllverbrennung.

Internationale Abkommen, wie das "POP Protocol of the UNECE Convention on Long-Range Transboundary Air Pollution" und die "Stockholm-Konvention über POPs", die die Produktion und den Einsatz von POPs verbieten und/oder einschränken, verlangen eine Chemikalienbewertung im Hinblick auf Toxizität, Bioakkumulativität, Persistenz und Ferntransportpotential in der Umwelt.

Mathematische Modelle des Stofftransports und Abbaus in der Umwelt sind unverzichtbare Werkzeuge, um Chemikalien im Hinblick auf Persistenz und Reichweite zu beurteilen. Eine mit diesen Modellen berechnete Zielgröße ist die Umweltexposition gegenüber einer Chemikalie. Sie zeigt jenen Teil der potentiellen Gefährdung durch eine Chemikalie an, der ausschließlich durch das Transport- und Abbauverhalten der Chemikalie, unabhängig von deren toxikologischen Eigenschaften, verursacht wird. Maßzahlen für Persistenz und Reichweite basieren auf der Umweltexposition. Normalerweise werden Pulsemissionen angenommen, um die Umweltexposition zu berechnen. Hier wird gezeigt,

daß die Umweltexposition nicht von der Form der Emissionsfunktion abhängt. Die mit der Pulsemission einer bestimmten Masse einer Chemikalie berechnete Umweltexposition ist gleich der Exposition, die sich aus einer Emission der gleichen Masse mit einem beliebigen Zeitverlauf ergibt. Dieses Ergebnis erlaubt eine allgemeinere Interpretation von expositionsbasierten Maßzahlen für Persistenz und Reichweite einer Chemikalie. Weiterhin erweitert es die Bedeutung von Modellergebnissen im Fließgleichgewicht. Das Ergebnis zeigt, daß auf der Fließgleichgewichtsannahme basierende Indikatorberechnungen Gültigkeit besitzen, ohne daß angenommen werden muß, daß Chemikalienkonzentrationen in der Umwelt den Zustand des Fließgleichgewichts erreicht haben, oder erreichen werden.

Die Reichweite einer Chemikalie ist das am schlechtesten definierte Selektionskriterium für POPs. An von den Emissionsquellen weit entfernten Orten gemessene Konzentrationen können als Beleg für den Langstreckentransport einer Chemikalie in der Umwelt benutzt werden. Bis jetzt war allerdings kein quantitatives Maß für die effektive Entfernung eines Ortes von vermuteten Emissionsquellen verfügbar. Hier wird ein Eulersches Tracertransportmodell für die Atmosphäre benutzt, um ein Maß für die effektive Entfernung von räumlich verteilten Emissionsquellen zu berechnen, das sowohl die geographische Entfernung, als auch vorherrschende Muster der Luftströmungen in Betracht zieht. Für zwei generische Emissionsszenarien, die typische räumliche Verteilungen von Emissionsquellen technischer Chemikalien und von Pestiziden beschreiben, werden Karten der effektiven Entfernung entwickelt. Die Resultate können benutzt werden, um räumliche Muster von gemessenen und modellierten Chemikalienkonzentrationen in der Umwelt besser zu interpretieren, um Maßzahlen für die Reichweite von Chemikalien abzuleiten und um Meßkampagnen und die Erweiterung von bestehenden Meßnetzen zu planen.

Die *global distillation hypothesis* ist das dominante Paradigma, um großskalige Fraktionierungsmuster von halbflüchtigen organischen Verbindungen zu erklären. Diese Hypothese ist deshalb eng mit dem konzeptuellen Verständnis des Ferntransports von POPs verbunden. Sie sagt aus, daß beobachtete Fraktionierungsmuster das Resultat der Interaktion von globalen Temperaturgradienten mit der Temperaturabhängigkeit der Verteilungkoeffizienten der Chemikalien sind. Hier wird eine alternative Hypothese, die *differential removal hypothesis*, vorgestellt. Sie besagt, daß globale Fraktionierungsmuster durch Unterschiede der durchschnittlichen Verlustraten aus der Atmosphäre entstehen, die entlang eines Gradienten von zunehmender Entfernung von den Emissionsquellen wir-

ken. Beide Hypothesen werden mittels eines Modellexperiments und mit Hilfe der Analyse eines Datensatzes von Luftkonzentrationsmessungen polychlorierter Biphenyle (PCBs) in Europa verglichen. Im Ergebnis zeigt sich, daß die Temperaturunterschiede in Europa keine Rolle für beobachtete Fraktionierungsmuster der Luftkonzentrationen spielen. Diese Muster können hingegen sehr gut mit der *differential removal hypothesis* erklärt werden.

Die Beziehung zwischen gemessenen Luftkonzentrationen und effektiver Entfernung von Emissionsquellen wird schließlich benutzt, um effektive Verweilzeiten der PCB-Kongenere in der Luft zu berechnen. Die berechneten effektiven Verweilzeiten stimmen gut mit Werten überein, die mit einem Multimedia-Massenbilanzmodell berechnet wurden und können somit als eine aus empirischen Daten abgeleitete Maßzahl für das Ferntransportpotential halbflüchtiger organischer Verbindungen dienen.

Contents

Chapter 1

Introduction

1.1 Persistent organic pollutants

Among the most important environmental challenges today is the continuing pollution of the global environment with anthropogenic chemicals (Meadows et al., 2004; Rockstrom et al., 2009). Of particular environmental concern are organic chemicals that likely cause harm to humans and/or the environment because they are

- toxic and/or bioaccumulative,
- persistent,
- and prone to long-range transport.

Those substances are called *persistent organic pollutants* (POPs) in regulatory texts which restrict or ban their production and use. There is no exact definition for a POP; whether a chemical is classified as such depends not only on the scientifically accessible properties of the molecule but also on politics. Selin and Eckley (2003) observe that the concept "POP" is part of both, the science and the policy worlds and that it can be viewed as a "convenient policy construct around a class of particularly dangerous chemicals". One important international agreement concerning POPs is the *Stockholm Convention on Persistent Organic Pollutants* (UNEP, 2001), and it currently stipulates the elimination, restrictions for production and use, or the reduction of unintentional emissions for 21 substances or substance groups. Here, the substances regulated in the Stockholm Convention are referred to as "recognised POPs".

POPs are a subset of the *semivolatile organic compounds* (SVOCs), defined as organic chemicals with a vapour pressure roughly between 10^{-6} and 10 Pa at environmental temperatures (Bidleman, 1988), corresponding approximately to an octanol-air partition coefficient, K_{OA}, between 10^5 and 10^{12} at 25 °C (Xiao and Wania, 2003; MacLeod et al., 2007). As a consequence of their phase partitioning behaviour, they can occur in the gas phase and sorb to aerosols to be available for efficient atmospheric long-range transport. On the other hand, they do not stay permanently in the air and may partition into surface compartments and biota (Ritter et al., 1995).

All recognised POPs are organohalogens. Many, particularly the older ones, are organochlorines. Organohalogens are chemicals in which at least one halogen atom is covalently bound to a carbon. The comparably high electronegativity of the halogen atoms results in strong carbon bonds, and substituting carbon-bound hydrogens with halogens therefore increases the chemical's inertness and consequently its persistence in the environment. Carbon-bound halogens have only a weak tendency to form hydrogen bonds with H-donors (Schwarzenbach et al., 2003). Therefore, organohalogens that contain the comparatively large halogens chlorine or bromine are hydrophobic and partition easily into organic phases and through biological membranes. In particular aromatic hydrocarbons and organochlorines with a large number of halogens are very persistent, hydrophobic, and bioaccumulative (Schwarzenbach et al., 2003).

Many of the recognised POPs are or were used as pesticides, e.g. DDT, mirex, chlordecone, the toxaphenes, hexachlorocyclohexane, and the cyclodiene pesticides aldrin, dieldrin, endrin, heptachlor and chlordane. Hexachlorobenzene was used as a fungicide. The list of known POPs also includes extremely versatile technical chemicals such as the PCBs, which were used as dielectric fluids in transformers and capacitors, plasticisers in sealants, as heat exchange fluids, hydraulic lubricants, cutting oils, flame retardants, dedusting agents, and in plastics, paints, adhesives and carbonless copy paper (Vallack et al., 1998). Perfluorooctane sulfonic acid (PFOS) and its derivatives are used as a coating material on paper, photographs, packaging, and textile products, in firefighting foam and hydraulic fluids and they play an important role in the semiconductor industry (Tang et al., 2006). Hexabromobiphenyl and tetra-, penta-, hexa- and heptabromodiphenyl ether are used as flame retardants in a wide array of products that range from airplanes to textiles. The Stockholm Convention also covers POPs that are produced unintentionally, such as polychlorinated dibenzo-p-dioxins, polychlorinated dibenzofurans, and chemicals that are or were used as intermediates, such as pentachlorobenzene.

The persistence of POPs, their semi-volatility, and their hydrophobicity have resulted in their globally ubiquitous occurrence in environmental compartments and biota. POPs have been measured on every continent, at locations representative of every climatic zone, and particularly in very remote places like the open ocean, the Arctic and the Antarctic (Ritter et al., 1995). The contamination of the Arctic has received a great deal of attention, not least because the Arctic aboriginal population is extremely exposed to POPs through the consumption of fish

and marine mammals which have bioaccumulated high POP concentrations. Observed deficits in immune function, an increase in childhood respiratory infections and reduced birth weight of Nunavut children were linked to prenatal exposure to organochlorines (Van Oostdam et al., 2005).

1.2 Modelling environmental fate- and transport processes of POPs

Mathematical models play an important role in the attempt to understand the fate- and transport processes of environmental chemicals. The term mathematical model denotes here a particular representation of the real-world system under consideration. The role of mathematical models in science in general and in environmental science in particular is a matter of an ongoing epistemological debate (e.g. see Cartwright, 1997; Morrison, 1998; Humphreys, 2004). A simple conceptualisation of the modelling activity informed by practical needs might distinguish two realms of fate- and transport modelling. Selin and Eckley (2003) propose the distinction between "core science" and "applied science":

core science The use of models is a possibility to conduct controlled experiments in a closed system that contains a limited number of parameters and is shielded from the environment (Haag and Matschonat, 2001). In studying the large scale behaviour of toxic chemicals in the environment, the kind of experiments that could be carried out in the real world is very limited, therefore models have a pivotal role in uncovering cause and effect relationships, discover patterns, and in general advance our understanding by doing what Kuhn (1962) calls the "puzzle solving of normal science".

applied science One important application of research into POP fate- and transport is the generation of input for political and regulatory processes. One main research task is the prediction of future behaviour, or behaviour under conditions not previously encountered, e.g. the release of new chemicals. Another task is the development of indicators that integrate modelling results into quantities that are related to specific needs of the regulatory process, contain normative elements, are easy to communicate to non-scientists, and ideally take the shape of a scalar value. This kind of scientific activity is distinctively different from the traditional view of science

as an activity that produces value-free objective knowledge and functions separately and independently from other groups of society. This kind of science has been termed "post-normal science" (Ravetz, 1999) and calls for new ways to deal with matters like model validation and uncertainty (Haag and Kaupenjohann, 2001). In the context of exposure-based chemical assessment, Scheringer (2002) identified the quantification of *persistence* and of *long-range transport potential* as areas where particular attention has to be paid to the implications of doing scientific work that has to take normative considerations into account.

POP fate- and transport is modelled with *multimedia mass-balance models*, which subdivide the modelling domain into homogeneous environmental compartments. Compartments considered are for example air in the planetary boundary layer of the troposphere, air in the free atmosphere, ocean water, freshwater, soil, vegetation, and sediment. For each compartment, a mass balance it set up that considers degradation processes and advective and diffusive intercompartmental exchange processes like for example wet and dry particle deposition, washout, diffusive exchange between surface compartments and atmosphere, particle sedimentation in the oceans, leaf fall, runoff, and leaching from soils to the water compartments. All these processes are represented as first order kinetics by "process models" (Wania and Mackay, 1999) which are mostly based on empirical relationships. Some mass-balance models are spatially explicit; that means the spatial extent of the modelling domain is partitioned into discrete volumes. The compartments of each volume that represent transport media, air and water, are linked with those of the adjacent volumes through macro-diffusive and advective exchange. The mass balances across all compartments in all volumes of the spatial discretization result in a set of coupled differential equations that are solved numerically. There is a large variety of multi-media mass-balance models, ranging from one-box models like SimpleBox (Brandes et al., 1996) without spatial resolution, over 1-dimensional models like CliMoChem (Scheringer et al., 2000), to the 2-dimensionally resolved BETR-Global (MacLeod et al., 2005).

Besides spatial resolution and processes considered, multi-media models differ with respect to their time resolution. The main division exists between models that are evaluated at steady-state, dynamic models which consider their environmental parameters to be constant in time, and dynamic models which consider seasonally varying environmental parameters, usually with a monthly resolution. Steady state models can be solved much faster than dynamic mod-

els. Furthermore, exposure-based indicators like *persistence* and *spatial range* (see sections 1.5 and 1.6) are calculated from steady-state solutions of multi-media models. In chapter 2 of this thesis, a formal analysis exploiting the common mathematical structure of multi-media models is used to fathom the range of applicability of steady-state solutions.

1.3 Toxicity

The toxicity of recognised POPs has been documented in numerous cases of human poisoning since the beginning of their industrial production in the 1930ies. The earliest published evidence of PCB toxicity stems from an investigation into the cause of the death of three workers that were exposed to PCBs and polychlorinated naphtalenes (PCNs) in 1936. Drinker et al. (1937) concluded that PCBs are harmful at very low concentrations and, together with the PCNs, responsible for the fatal damage of the victims' livers. They also observed that the toxicity of the studied organochlorines increased with the number of chlorine substitutions.

More widely publicised incidences of PCB poisoning are the Yusho accident in 1968 in Japan, where over 1000 people suffered severe illness after ingesting rice oil that was contaminated with PCBs during the manufacturing process, and the Yu-Cheng ("oil-disease") accident in Taiwan in 1979, where 2000 people fell ill after the consumption of PCB-contaminated rice oil (Schantz, 1996). Offspring of Yu-Cheng mothers born up until 14 years after the incident exhibit a plethora of developmental defects and also hormonal effects that might negatively impact the reproductive system functioning (Guo et al., 2004). The PCB mixture of both, the Yusho and the Yu-Chen incident, contained also polychlorinated dibenzofurans (PCDFs), which are more toxic than PCBs. Thus, it could not be determined which groups of toxics were more responsible for the observed health effects (Guo et al., 2004).

Polychlorinated dibenzo-p-dioxins (PCDDs) are closely related to the PCDFs, and the 2,3,7,8-tetra congener (TCDD) is the most toxic one and commonly referred to as "dioxin". Another well publicised mass-poisoning of humans involving dioxin occurred during the Vietnam War between 1961 and 1971, when the U.S. military sprayed more than 70×10^6 litres of herbicide mixture containing 2,4,5-trichlorophenoxyacetic acid which was contaminated with about 300

to 400 kg of TCDD in South Vietnam. Between 2 and 4 million people were sprayed directly (Stellman et al., 2003). This resulted in an increased risk of birth defects in the Vietnamese population (Ngo et al., 2006) and according to Vietnamese estimates, killed or injured 4×10^5 people and contributed to birth defects in 5×10^5children (Dreyfuss, 2000). Effects on U.S. soldiers received more epidemiological attention and different cancers, *spina bifida* in the children of veterans, *diabetes mellitus*, and damage to the peripheral nervous system were linked to the occupational exposure to TCDD containing herbicides during the Vietnam War (Committee to Review the Health Effects in Vietnam Veterans of Exposure to Herbicides, 2004).

In 1976, about 15 km north of Milan, a runaway reaction occurred at a chemical plant manufacturing 2,4,5-trichlorophenol and resulted in the release of several kg TCDD (Homberger et al., 1979). This event became known as "Seveso accident". Results of a mortality study of the exposed population support the cancerogenicity of TCDD and corrobate the hypothesis of cardiovascular- and endocrine-related effects (Bertazzi et al., 2001).

The toxicity of TCDD stems from its interaction with a cytoplasmic receptor protein, the aryl hydrocarbon receptor (AhR). The AhR is involved in regulation of the expression of a large number of genes and is likely a key regulatory protein in normal development and homeostasis (Schecter et al., 2006). The ability to bind to the Ah-receptor is linked to the planar shape of the molecule and to the chlorine substitution pattern. PCDDs and PCDFS with a 2,3,7,8-substitution pattern and PCBs with a minimum of four substitutions at the lateral positions (i.e. 3, 3′, 4, 4′, 5, 5′) and none or one substitution(s) in the ortho positions (i.e. 2, 2′, 6, 6′) are called "dioxin-like", because they also bind to the AhR and cause dioxin-like toxicity, albeit to a lesser extent than TCDD. This class of endocrine disrupting chemical, the AhR agonists, can cause many different biological effects at a number of different life stages and in different species by interfering with different signal transduction pathways (Damstra et al., 2002). AhR mediated toxic effects include *chloracne*, liver damage, cancer, immune deficiency, reproductive and developmental abnormalities, and central- and peripheral nervous system pathology (Schecter et al., 2006).

The mode of action of TCDD is, in a general way, similar to that of most other recognised POPs: The chemical or its metabolite binds to a receptor followed by a complex series of events that lead to changes in gene expression characteristic for a specific hormone. Little is known about the relationship of these initial

events and an observed adverse health response (Damstra et al., 2002). With respect to low-level exposure to xenobiotics, endocrine disruption is arguably considered the most important mechanism of toxic action, or more precisely, a class of mechanisms of action. Damstra et al. (2002) define an endocrine-disrupting chemical (EDC) as "an exogenous substance or mixture that alters function(s) of the endocrine system and consequently causes adverse health effects in an intact organism, or its progeny, or (sub)populations". Therefore endocrine disruption is not a toxicological endpoint in itself, rather it is seen as a functional change potentially leading to various adverse effects (Damstra et al., 2002). There are many different mechanisms through which xenobiotics may act as EDCs. They may mimic naturally occurring hormones, block the binding of hormones to receptors, inhibit or induce enzymes associated with hormone synthesis, metabolism, or excretion. The mechanisms most studied are interactions with the estrogen, androgen, thyroid, and Ah receptor (Goodhead and Tyler, 2009).

There are several problems that complicate linking of low-level POP exposure to observed health effects. Organisms in the environment are exposed to wide range of pollutants, making it difficult to link observed effects to a particular substance. Different POPs may act additively, synergistically, or antagonistically (Hotchkiss et al., 2008). Traditional assumptions about the dose-response relationship, i.e. linearity, monotonicity, and the existence of a non-response threshold, are not valid for EDCs (Welshons et al., 2003). Chemicals of the same group (i.e. PCBs) or even a single chemical may act through different mechanisms and different endocrine systems may influence each other. Timing of exposure is a critical factor, since exposure during early life can induce serious and irreversible effects, whereas the same exposure in a later stage might have no effect (Goodhead and Tyler, 2009). Species, genetic predisposition, age, gender and past exposures might influence the dose-response relationship (Damstra et al., 2002). Nevertheless, many classic POPs could be identified as being responsible for serious population level effects and all classic POPs have been associated with endocrine-disrupting effects (Colborn et al., 1993; Jorgenson, 2001; Lemaire et al., 2006)

Immunotoxic effects have been linked to chronic, low level environmental exposure to several POPs. DDT, aldrin, dieldrin, chlordane, heptachlor, lindane, PCDDs, PCBs, and HCB have been shown to affect the immune system function of experimental animals. Exposure to several organochlorine pesticides and PCB have been found to correlate with reduced T-cell activity and an increased

susceptibility to microbial infections, in whales, dolphins, and seals (Vallack et al., 1998). Immunological symptoms in humans, particularly in Inuit whose diet includes highly contaminated fatty tissues and organs from marine mammals, have been linked to POP exposure (Van Oostdam et al., 2005).

Reproductive and developmental effects of POP exposure in wildlife have been observed for several species. Among the population level effects that have been attributed to POP exposure are declines in the European otter population, eggshell thinning, reduced egg production and hatchability, egg mortality, embryo deformities and shifted sex ratios for different bird populations, reproductive failure of mink and seals, diminished hatching success of lake trout, and feminization of fish, birds and mammals. There is evidence that exposure of children to PCBs *in utero* and through consumption of mother's milk leads to persistently impaired neurological development (Vallack et al., 1998) and that exposure to POPs might induce human testis dysfunction. It has been suggested that the observed increase in testicular cancer and the decrease in sperm quality might be related to low-level POP exposure (Damstra et al., 2002).

This list is by no means complete. Particularly, most of the studies today focus on the classic POPs, and even less is known about new POPs, which are not less likely to exhibit similar effects. Recently for example, evidence has accumulated that polybrominated diphenyl ethers (PBDEs) affect the thyroid hormone homeostasis, cause neurotoxic effects in animals and humans, and that exposure levels of North American infants are close to estimates of the No Adverse Effect Level (NOAEL) (Costa and Giordano, 2007; Schreiber et al., 2010). The global proportion of the problem, the potentially enormous implications, in particular induced by the threat to the reproductive health of many species including humans (Toppari et al., 1996), and the lack of knowledge concerning the identification and the mode of action of EDCs have brought the topic to the attention of a broader audience. Books like *Our Stolen Future* (Colborn et al., 1996) and *Hormonal Chaos* (Krimsky, 2000) set the stage for a paradigm shift in chemical risk assessment. They argue for an interpretation of the precautionary principle that allows to base decisions on the "weight of evidence", rather than to require a scrutinised demonstration of cause-effect relationships.

1.4 Bioaccumulation

Organic chemicals have the ability to accumulate in organisms and reach much higher concentrations than in the surrounding environmental media the organisms inhabit. Therefore, the tendency of a substance to bioaccumulate and biomagnify through the food-chain is an important criterium for the risk assessment of environmental chemicals. The hydrophobicity of a substance is a key parameter for its bioaccumulativity. Compounds with high octanol-water partition coefficient, K_{OW}, move from the aqueous phase into the fatty tissues of the organism and the elimination of these substances depends on the metabolism to water-soluble and readily excretable metabolites (Walker, 2009). For aquatic organisms, a measure of bioconcentration is the *bioconcentration factor*, BCF. Bioconcentration refers to the uptake of the chemical by absorption from the water and the BCF is defined as the ratio of the chemical concentration in the organism to that in water. For hydrophobic organic solutes, the BCF increases linearly with $\log K_{OW}$ for $\log K_{OW} < 6$ (Mackay, 1982), and regulatory screening criteria are based on this relationship. Common thresholds are a $\log K_{OW} > 5$ and/or a BCF > 5000 (Arnot and Gobas, 2006). *Bioaccumulation* refers to the uptake of chemicals through all routes of exposure, including dietary uptake (Mackay and Fraser, 2000). It is the net result of the competing processes of chemical uptake and and chemical elimination (Arnot and Gobas, 2006). *Biomagnification* refers to an increase in chemical concentration with increasing trophic level in food webs, caused by the concentration of chemicals due to food digestion and absorption. For terrestrial food chains, the K_{OA} is also an important predictor for biomagnification (Czub and McLachlan, 2004; Kelly et al., 2007). POP concentrations in polar bears for example may reach 10'000 times the concentrations in primary producers and concentrations in humans may be biomagnified by a factor up to 4'000 (Kelly et al., 2007).

1.5 Persistence

In the context of environmental fate processes of POPs, *persistence* is related to the efficiency of the loss-processes that remove chemicals from the environment.

Loss processes of organic compounds in the atmospheric gas phase include pho-

tolysis, chemical reaction with OH and NO_3 radicals, and with ozone. The OH radical reaction occurs in the troposphere and is the most important loss process for most organic chemicals (Atkinson et al., 1999). The associated loss rate depends on the OH radical concentration, which in turn is a function of the concentrations of ozone, carbon monoxide, nitrogen oxides, hydrocarbons and water vapour, and depends on temperature, cloud cover, and the density of the overhead ozone column (Spivakovsky et al., 2000). Therefore, loss rates from the atmosphere are spatially heterogeneous. In multimedia fate- and transport models, they are modelled as pseudo first-order rate constants by multiplying prescribed OH· concentrations with a 2^{nd} order reaction rate constant. In general, the OH· reaction rate decreases with an increasing degree of halogenation.

Another major loss process from the environment are biological transformations. An organic chemical is taken up by a microorganism, where it binds to an enzyme which facilitates a reaction that transforms the compound into its metabolites. Major strategies to initialise the reaction are hydrolysis, oxidation, reduction, and additions. The rate of biotransformation may depend on the bioavailibility of the chemical to the microorganism, the existence and efficiency of a suitable enzyme, and a change of the microbial population in response to the presence of the chemical. Biotransformation rates might well be the least understood part of chemical fate modelling (Schwarzenbach et al., 2003). In large-scale multimedia fate modelling, one first order rate constant per chemical is assigned, and possible spatial variations due to different environmental conditions are not taken into account.

The dominant model-derived measure of persistence is the overall residence time at steady-state (Scheringer, 1996). It represents a weighted average of the half-lifes in the different environmental compartments, taking into account the tendency of a substance to partition more into some than into other compartments. The main drawback of the residence time at steady-state is its inability to represent clearing rates from the environment after emissions have ceased. In such a scenario, most of the chemical will be present in compartments with slow loss processes after some time, and the residence time at steady-state will underestimate the actual residence time. Stroebe et al. (2004) have put forward the concept of residence time in the "temporal remote state", a state of the system so far in the future that the relative amounts of the chemical in the different compartments do not change anymore.

1.6 Long-range transport potential

The inclusion of the tendency of a chemical to undergo long-range transport in the criteria for the identification of POPs has its base in two concepts related to exposure-based risk assessment. One is the relation of a chemical's spatial range to the quantification of the threat posed by the chemical, which depends on the number of individual organisms, species, populations, ecosystems that are potentially influenced by the chemical's emission. The other concept is a conglomeration of normative principles related to environmental risk assessment, i.e. the *Categorical Imperative*, the principles of *procedural justice* and *impartiality*, the *Polluter-Pays Principle*, and the *Precautionary Principle* (Scheringer, 2002).

The long-range transport potential (LRTP) is the least well defined criterium for POP assessment. The concept of LRTP has a spatial dimension to it, and there is no consensus about how to quantify that dimension. The regulatory wording includes the term "distant from the sources of its release" (UNEP, 2001), but no further information about what is meant by "distant". In practice, the interpretation has been to assign the attribute "distant" or "remote" informally to specific regions like the Arctic or the Antarctic, but no meaningful quantification of "distance" has been proposed in this context. The naïve interpretation as geographical distance neglects the strong influence of airflow-patterns on the spatial distribution of predominantly atmospherically transported substances. Therefore, to interpret measurement data with respect to the LRTP criterium, there is a gap in the current conceptualisation of the relationship between pollutant concentrations at a particular location and that location's position with respect to emission sources and transport pathways. This gap is reflected in a recent guidance document about a global POP monitoring strategy in the context of the *Stockholm Convention* (UNEP, 2007) which states the necessity to consider the influence of airflow patterns on atmospheric POP transport in choosing monitoring sites and interpreting measurement data. The document recommends the use of large-scale tracer transport models but fails to indicate a tangible method to combine tracer transport model results with measured environmental POP concentrations. This thesis introduces a new method aimed at helping to remedy that situation (see chapter 3).

A number of LRTP metrics that are based on the spatial distribution of concentration or exposure have been put forward. Formally, they may be described as

mappings from the domain of concentration distributions over an idealisation of the Earth's surface into the positive rational numbers, which represent a characteristic length or area for the shape of the concentration distribution. Scheringer (2002) derives a necessary requirement for such a LRTP-metric, namely that for a spatially homogeneous concentration distribution, the metric should take the maximum value, which is the area or length associated with the length or area of the whole Earth. Scheringer (2002) analysed the characteristics of five proposed LRTP-metrics and concluded that only one of them, the *spatial range*, SR, fulfils the requirements one would intuitively expect from such a function. However, the *characteristic travel distance*, CTD, is also still widely used in the literature (i.e. Matthies et al., 2009).

SR is defined as the 95% interquantile range of the concentration distribution (Scheringer, 1996). This definition relies on the representation of the Earth's surface as one-dimensional, but it might be possible to extended it in a sensible way to be applicable for a two-dimensional surface. The CTD is defined as the distance from the source where the concentration has dropped by $1/e$ (Bennett et al., 1998). It is only defined for one-dimensional and unidirectional contaminant transport away from a single point source resulting in a monotonically decreasing concentration profile.

1.6.1 Validating metrics of LRTP

In practice, both CTD and SR are calculated with computer implementations of mathematical multimedia fate- and transport models. The model structure, in particular the dimension of the Earth's representation is limited by the respective definition of the LRTP-metric. The main problem with these metrics is that they cannot be linked to empirical data. The success of an indicator that is used for decision-making in the political arena depends on its credibility and the trust it can muster among the stakeholders (Haag and Kaupenjohann, 2001). There are two different features of environmental models that contribute to the perceived validity of their results. One is the *internal validity* of a model, which is a property of its composition. It is based on the manner in which its constituent hypothesis are assembled, the consensus attached to these hypothesis, and the correctness of its technical implementation (Beck et al., 1997). This kind of validity is only accessible to the model developer and to other scientists working in the field. The other feature is the *model performance*, based on the traditional ap-

proach to model validation, i.e. the comparison of model results to data derived from independent sources, for example field measurements or other models. There are established measures for model performance which can be conveyed to non-experts.

This work aims at contributing to a conceptual and methodological framework that makes it possible to relate LRTP metrics to field measurements of chemical concentrations. Figure 1.1 depicts the main idea. The current method to calculate a LRTP metric is to run a multimedia fate- and transport model, which takes substance properties, the specification of an emission source, wind fields, and several other environmental parameters as input. The resulting spatial distribution of contaminant concentrations is then used to calculate the LRTP metric. The choice of the metric is to some extent arbitrary, even if it is carefully constructed to represent the intended meaning. In chapter 3, a method is introduced that utilises an atmospheric tracer transport model to calculate a substance-independent measure of remoteness for all locations on the discretized surface of the Earth from prescribed wind fields and a specification of the spatially distributed emission source. That new measure of remoteness at a particular location is related to the expected contaminant concentration and the substance's LRTP in a way that can be expressed as a closed-form analytical formula. In chapter 4, the method is applied to a set of PCB measurements and the possibilities arising from the relationship between LRTP, remoteness, and measured concentrations are explored.

1.6.2 The global distillation hypothesis

The relative LRTPs of a set of SVOCs that were emitted as a mixture from the same source are related to the shift in the mixture composition observed along the transport pathway in the environment. The *global distillation hypothesis* (Wania and Mackay, 1993, 1996) is a conceptual construct that tries to explain this shift as a result of differing environmental temperatures along the transport path. The hypothesis states that SVOCs of differing volatility partition from the gas into condensed phases at specific ranges of temperature or latitude where they become available for effective deposition (Wania and Mackay, 1996). The *global distillation hypothesis* identifies the interaction of temperature dependent substance properties with spatial gradients of temperature as the underlying cause for observed spatial patterns of fractionation and proposes a particular

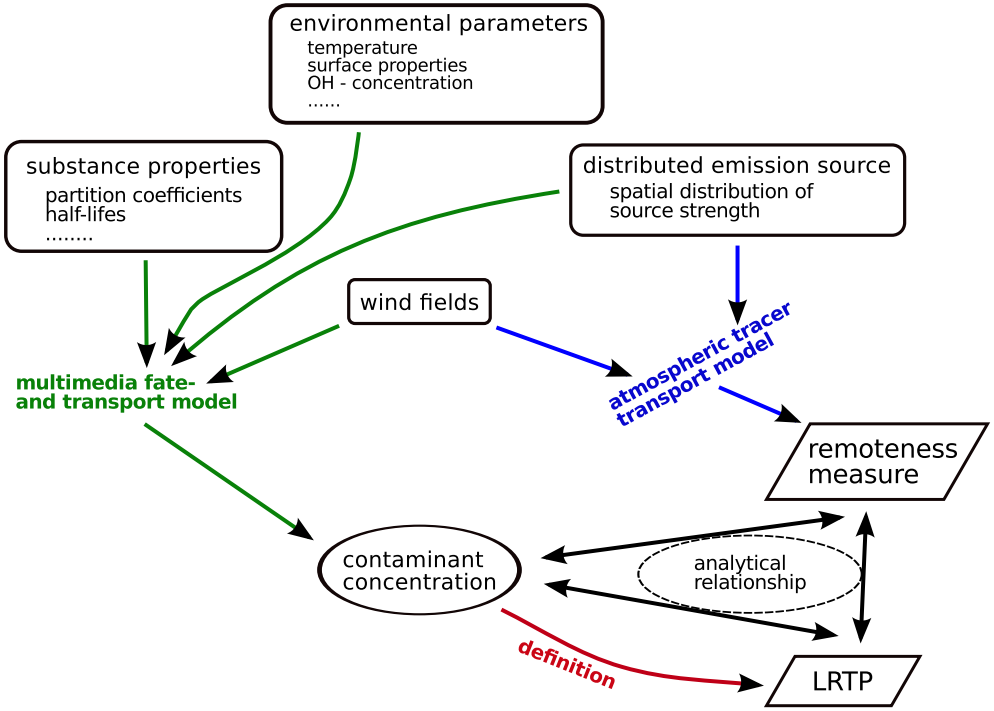

Figure 1.1: Conceptualisation of how this thesis contributes to relating metrics for long-range transport potential to empirical data.

mechanism that controls the LRTP of a chemical.

This hypothesis is tested in chapter 4 in two ways. First, a simple multimedia model experiment is utilised to explores the relative contributions of gradients of remoteness and of temperature, respectively, to modelled fractionation patterns of PCB congeners. Secondly, the tools developed in chapter 3 are used to analyse observed fractionation patterns of PCB congeners with respect to the *global distillation hypothesis*.

1.7 Objectives of the thesis

The objectives of this thesis are

- to examine the interpretability of steady-state solutions of multi-media fate- and transport with respect to indicator calculation and chemical screening for risk assessment,
- to develop a measure for a location's remoteness from spatially distributed emission sources that can be combined with a substance specific measure for long-range transport potential to explain concentrations of that substance in that location.
- to use the remoteness metric to re-examine datasets of atmospheric PCB concentrations with respect to the *global distillation hypothesis*, and
- to use the remoteness metric to calculate an indicator for long-range transport potential for a set of PCB congeners from measurement data and to compare it to model results.

1.8 Structure of the thesis

Figure 1.2 displays the structure of the thesis. It consists of five chapters. The main part in chapters 2-4 has been published in peer reviewed journals or submitted for publication.

Chapter 1, the introduction, gives background information about the topic, with a special focus on the properties and the history of POPs and describes the main problems. This thesis is partly motivated by the needs of regulatory bodies. It is a consequence of this intended area of application that the science cannot be completely separated from normative considerations. The introduction makes reference to some consequences of that situation. Implicitly, these considerations have influenced all the research presented in the following chapters.

Chapter 2 explores the mathematical structure of a common type of POP fate- and transport model. It is formally shown that the evaluation of models at steady-state does not impact the calculation of the underlying target variable of exposure-based chemical assessments. This result is implicitly used in the application of an atmospheric tracer transport model in chapter 3.

Chapter 3 presents a method to derive a measure for the effective distance of a location from spatially distributed emission sources. This result represents the methodological core of the thesis.

Chapter 4 builds on the result of chapter 3 and utilises the new metric to challenge the *global distillation hypothesis* and to better characterise the long-range transport potential of SVOCs.

Chapter 5 closes the thesis with a more general interpretation of the results and suggests directions for further research.

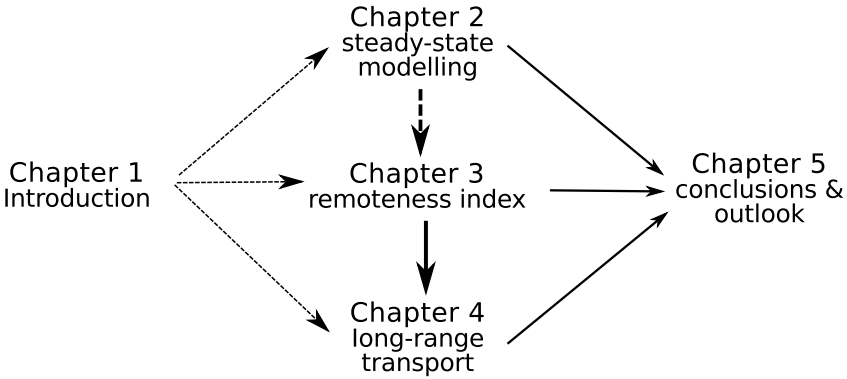

Figure 1.2: Structure of the thesis.

Chapter 2

Modelled environmental exposure to persistent organic chemicals is independent of the time course of emissions: Proof and significance for chemical exposure assessments

Harald von Waldow, Martin Scheringer and Konrad Hungerbühler

Institute for Chemical and Bioengineering, ETH Zürich

Published in:
Ecological Modelling, 2008
Volume 219, Issues 1–2, pages 256–259
DOI: 10.1016/j.ecolmodel.2008.08.016

Abstract

The fate and transport of organic pollutants in the environment is usually assessed with the help of multimedia models. A target variable calculated with these models is the environmental exposure to a substance. It indicates that part of the potential hazard of a chemical that is caused solely by the chemical's fate and transport behaviour, regardless of toxicological substance properties. So far, pulse-emissions are usually assumed in order to arrive at an easy to compute expression for exposure. Here, we show that exposure does not depend on the shape of the emission function. Exposure calculated for the pulse release of a particular mass of contaminant is equal to exposure calculated for any arbitrary dynamic release of the same mass. This result extends the meaning of model evaluations at steady-state. It also allows for a more general interpretation of the *persistence* and the *spatial range* of a chemical, as well as of the *toxicity potential* used in life cycle impact assessment.

2.1 Introduction

Production and use of persistent organic chemicals, which partition into different environmental compartments, degrade slowly, spread over large distances and have the potential to cause harm to humans and ecosystems, are the subject of a number of intergovernmental treaties and regulations (UNECE, 1998; UNEP, 2001; European Parliament and Council of the EU, 2006). Due to an increasing awareness of the problems brought about by the release of synthetic chemicals into the environment as well as the increasing number of new substances in commerce, there is a growing need for chemical risk assessment (Scheringer et al., 2006).

In risk assessment, the fate and transport of organic pollutants in the environment is usually assessed with the help of *multimedia models*. Various model implementations exist that differ in structural characteristics such as spatial and temporal resolution and the processes and compartments considered. An overview is contained in the model inter-comparison study by Fenner et al. (2005).

A basic target variable calculated with these models is the *exposure* of ecosystems and organisms to a substance. It indicates that part of the potential hazard of a chemical that is caused solely by its fate and transport behaviour, regardless of toxicological substance properties. Exposure calculated with multimedia models is the basis for higher-level indicators such as *persistence* (see section 2.4.2) and some varieties of *long range transport potential* (Scheringer, 1996), as well as *toxicity potentials* used in *life cycle impact assessment* (LCIA) to describe the potential chronic effects caused by the emission of toxic substances (see Guinée and Heijungs (1993) and section 2.4.3).

The *exposure*, $\mathcal{E}$, of an organism in contact with a particular contaminated environmental medium over a time period $[t_0, t_1]$ is defined as the time integral of the environmental contaminant concentration $c(t)$ (Lioy, 1990):

$$\mathcal{E} = \int_{t_0}^{t_1} c(t)\, dt \quad . \tag{2.1}$$

The fundamental importance of this expression for chemical risk assessment and toxicology derives from *Haber's Rule*, which states that for a given response in the target organism, the product of concentration and time is constant (Witschi, 1999). There is ample experimental (e.g. see Rozman and Doull, 2001, and references therein) as well as theoretical evidence (e.g. Olson and Cumming, 1981; Gaylor, 2000) that this relationship holds in many cases for subchronic and chronic toxicity and in particular for carcinogenic effects.

When exposure is calculated without a particular target organism in mind, the choice of the time period of exposure $[t_0, t_1]$ is somewhat arbitrary. It is reasonable to start the integration at the beginning of the emissions ($t_0 = 0$). For applications where substances are to be assessed in a general way, the upper integration limit is usually set to $t_1 = \infty$. This is reasonable if the focus lies on chronic long-term effects of low doses. Here, we show that exposure defined in this way does not depend on the time course of contaminant emissions.

2.2 Background and Nomenclature

We consider a discretisation of the spatial domain into n cells. Each cell represents a well-mixed volume in a particular environmental compartment. The elements of the exposure vector $\vec{\mathcal{E}} = (\mathcal{E}_1, \ldots, \mathcal{E}_n)^{\mathrm{T}}$ [MTL^{-3}] and of the vector-valued concentration function $\vec{c}(t) = (c_1(t), \ldots, c_n(t))^{\mathrm{T}}$ [ML^{-3}] represent the exposure and concentration functions in these cells. In the following, all vectors have size n and all matrices are square $n \times n$ matrices. We define *exposure*, $\vec{\mathcal{E}}$, as

$$\vec{\mathcal{E}} = \int_0^\infty \vec{c}(t)\, dt \quad . \tag{2.2}$$

The multi-media mass balance models commonly used to calculate exposure to persistent chemicals take the form

$$\frac{d\vec{m}}{dt}(t) = \mathrm{A}\vec{m}(t) + \vec{q}(t) \quad , \tag{2.3}$$

where $\vec{m}$ [M] is the vector of contaminant masses in all cells and $\vec{q}$ [MT^{-1}] is the vector of emission rates into all cells. The elements a_{ij} $(i \neq j)$ of A are the positive first-order rate constants [T^{-1}] which describe the transport from cell j to cell i. The diagonal elements, a_{ii}, are negative and represent the total loss rate constants from cell i which includes loss to the other cells as well as loss through transformation and physical removal from the system. Consequently,

$$a_{jj} + \sum_{\substack{1 \leq i \leq n \\ i \neq j}} |a_{ij}| < 0 \qquad \forall j \in [1 \ldots n] \quad . \tag{2.4}$$

From the Gershgorin Theorem applied to A^{T} it follows that the real parts of all eigenvalues of A are negative and A^{-1} exists (Hazewinkel, 2002).

Note that this model assumes a time-invariant state-matrix A. The error introduced by fixing A in time to represent an annual average and thereby neglecting seasonal and diurnal changes of the environmental conditions might not be negligible (Lammel, 2004). However, seven out of eight model codes analysed by Fenner et al. (2005) are of this time-invariant type, and are considered credible and useful by the OECD expert working group (Fenner et al., 2005). A constant state-matrix allows to regard multimedia fate models in the form of equation 2.3 as Linear Time Invariant (LTI) dynamical systems and to use results and tools

from linear system theory to explore them. The reader is referred to Hertwich (2001) for the interpretation of some basic properties of LTI systems in the context of chemical fate modelling.

The solution to equation 2.3 is given by

$$\vec{m}(t) = \exp(\mathrm{A}t)\vec{m}(0) + \int_0^t \exp(\mathrm{A}(t-\tau))\vec{q}(\tau)\,d\tau \quad , \tag{2.5}$$

where exp() is the matrix exponential. Because all eigenvalues of A are negative, the solution is asymptotically stable and $\lim_{t\to\infty} \exp(\mathrm{A}t) = \vec{0}$.

To calculate the exposure resulting from a pulse-release into a system with an initial condition $\vec{m}(0) = \vec{m}_0$, the pulse is modelled with

$$\vec{q}(t) = \vec{m}_{\mathrm{e}}^{\mathrm{pulse}}\delta(t) \quad , \tag{2.6}$$

where $\vec{m}_{\mathrm{e}}^{\mathrm{pulse}}$ is the vector of masses emitted into the n cells and $\delta(t)$ $[\mathrm{T}^{-1}]$ is *Dirac's delta* which has the defining property of satisfying

$$\int_{-\tau}^{+\tau} \delta(t) f(t)\,dt = f(0) \tag{2.7}$$

for any $\tau > 0$ and any smooth function $f(t)$ with compact support. Equation 2.5 then reduces to

$$\vec{m}(t) = \exp(\mathrm{A}t)(\vec{m}_0 + \vec{m}_{\mathrm{e}}^{\mathrm{pulse}}) \quad . \tag{2.8}$$

Let V $[\mathrm{L}^3]$ denote a diagonal matrix containing the volumes of the n cells of the spatial discretisation on its main diagonal. The exposure, $\vec{\mathcal{E}}$, can then be calculated as

$$\begin{aligned} \vec{\mathcal{E}} = \int_0^\infty \mathrm{V}^{-1}\vec{m}(t)\,dt &= \mathrm{V}^{-1}\int_0^\infty \exp(\mathrm{A}t)\,(\vec{m}_0 + \vec{m}_{\mathrm{e}}^{\mathrm{pulse}})\,dt \\ &= -\mathrm{V}^{-1}\mathrm{A}^{-1}(\vec{m}_0 + \vec{m}_{\mathrm{e}}^{\mathrm{pulse}}) \quad . \end{aligned} \tag{2.9}$$

This expression is computationally cheap when compared to the general solution of the model (equation 2.5) because only matrix inversions are involved and a matrix exponential needs not be calculated.

2.3 Results

Here we show that equation 2.9 not only holds for a pulse release, but also for any dynamic emission of a finite total mass m_e^i ($i \in \{1 \dots n\}$) into each cell i. In other words, the equation to calculate exposure from a multi-media mass balance model holds for any emission function $\vec{q}(t)$ that has a finite improper integral

$$\int_0^\infty \vec{q}(t)\, dt = \vec{m}_e = (m_e^1, \dots, m_e^n)^T \quad . \tag{2.10}$$

With $\vec{m}(t) = V\vec{c}(t)$, equation 2.3 becomes

$$\frac{d\vec{c}}{dt} = V^{-1}AV\,\vec{c}(t) + V^{-1}\vec{q}(t) \quad . \tag{2.11}$$

Laplace transformation according to

$$\mathcal{L}\{f\}(s) = \int_0^\infty f(t)e^{-st}\, dt \tag{2.12}$$

results in

$$s\mathcal{L}\{\vec{c}\}(s) = V^{-1}AV\mathcal{L}\{\vec{c}\}(s) + V^{-1}\mathcal{L}\{\vec{q}\}(s) + \vec{c}(0) \tag{2.13}$$

$$\Rightarrow \quad \left(sI - V^{-1}AV\right)\mathcal{L}\{\vec{c}\}(s) = \vec{c}(0) + V^{-1}\mathcal{L}\{\vec{q}\}(s)\,, \tag{2.14}$$

where I stands for the $n \times n$ identity matrix. Using the definition of $\mathcal{L}$ (equation 2.12) and evaluating at $s = 0$, we obtain

$$\int_0^\infty \vec{c}(t)\, dt = -V^{-1}A^{-1}V\vec{c}(0) - V^{-1}A^{-1}\int_0^\infty \vec{q}(t)\, dt \tag{2.15}$$

$$\Rightarrow \quad \vec{\mathcal{E}} = -V^{-1}A^{-1}(\vec{m}_0 + \vec{m}_e) \quad . \tag{2.16}$$

A comparison with equation 2.9 shows that this proves the claim.

2.4 Implications

2.4.1 Steady-state modelling

Frequently, the models described by equation 2.3 are evaluated at steady-state (*Level III models*) that results from a constant emission, $\vec{q}_{ss}$. The contaminant

mass present in the model system at steady-state , $\vec{m}_{ss}$, is given by

$$\vec{m}_{ss} = -A^{-1}\vec{q}_{ss} \quad . \tag{2.17}$$

It has been observed previously that the function that maps a constant emission function, $\vec{q}_{ss}$, to the resulting steady-state concentration, $\vec{c}_{ss}$.

$$\vec{c}_{ss} = V^{-1}\vec{m}_{ss} = -V^{-1}A^{-1}\vec{q}_{ss} \tag{2.18}$$

is the same function that maps a pulse-emitted mass, $\vec{m}_e^{pulse}$, to exposure, $\vec{\mathcal{E}}$, (see equation 2.9 with $\vec{m}_0 = \vec{0}$) (Heijungs, 1995; Fenner et al., 2000; Hertwich, 2001).

Our result implies that exposure from any dynamic emission of a finite mass is directly proportional, with a proportionality constant k [T], to the steady-state concentration that results from a set of constantly emitting sources, provided that the vector of dynamically emitted masses equals k times the vector of constant emission rates:

$$\vec{m}_e = k \cdot \vec{q}_{ss} \Rightarrow \vec{\mathcal{E}} = k \cdot \vec{c}_{ss} \tag{2.19}$$

The use of steady-state models to calculate *overall persistence* (see section 2.4.2) and *spatial range* for long-lived chemicals has been criticised because emissions might not occur for a sufficiently long time to cause environmental concentration levels close to the steady-state values (OECD, 2004). Our result, however, shows that the meaning of steady-state concentrations is not limited to an approximation of real concentrations after emissions have continued for a long time. Rather, the steady-state solution can be interpreted as the exposure that results from any realistic release history of a finite mass of contaminant. In other words, results from Level III models pertaining to exposure and exposure-derived quantities such as overall persistence and spatial range are meaningful for any emission history.

The significance of steady-state results for time-varying emission scenarios has been pointed out by Hertwich (2001), who presented a more intuitive argument that complements our formal derivation: Hertwich (2001) used the superposition property of an LTI to interpret the response of the system to a single unit pulse emission into a particular cell (the *impulse response*) as the probability for the presence of a single emitted molecule. That probability is independent of the presence or absence of other molecules of the same kind (Hertwich, 2001).

Because of the time invariance of an LTI, the fate of a molecule does not change for molecules emitted at different times. Since any dynamic emission function can be expressed as the continual sum of weighed unit pulse emissions (Bessai, 2006), the time integral of a system response to any dynamic emission represents, just like the steady state of the system, the "average" fate of a molecule (Hertwich, 2001).

2.4.2 Persistence

Mackay (1979) introduced the overall residence time at steady state (τ^{ss}) as a measure of *overall persistence*:

$$\tau^{ss} = \frac{\|\vec{m}_{ss}\|_1}{\|\vec{q}_{ss}\|_1} \quad , \tag{2.20}$$

where $\| \ \|_1$ denotes the 1-norm defined as $\|\vec{v}\|_1 = \sum_i v_i$. τ^{ss} depends strongly on the *mode of emission*, i.e. the compartments into which the release takes place, and on the geographical locations of the emission sources. It is, however, invariant under the scaling of the vector of constant emission rates, $\vec{q}_{ss}$.

Scheringer (1996) defined the *equivalence width* (τ^{eq}) as a measure of persistence. It can be expressed as the proportionality constant that relates the total emitted mass of a pulse release, $\|\vec{m}_e^{pulse}\|_1$, to the sum of the volume weighted elements of the exposure vector:

$$\tau^{eq} = \frac{\|V\vec{\mathcal{E}}\|_1}{\|\vec{m}_e^{pulse}\|_1} \quad . \tag{2.21}$$

τ^{eq} is equal to τ^{ss} for equivalent release patterns (i.e. $\vec{q}_{ss} = k \cdot \vec{m}_e^{pulse}$ with an arbitrary $k\,[T^{-1}]$) (Fenner et al., 2000; Hertwich, 2001).

Our result shows that the definition of τ^{eq} does not depend on a pulse-emission, but rather is valid for any realistic emission function. Consequently, τ^{eq} and also τ^{ss} can be used as persistence metrics without making reference to either the steady-state or a pulse-emission scenario.

The same conclusion has been reached by Hertwich (2001) via his "single-molecule interpretation" of the superposition principle: The average lifetime of a molecule

does not change for molecules emitted at different times. Since both τ^{eq} for a dynamic emission function and τ^{ss} represent the average lifetime of a molecule, it is plausible that both persistence metrics are identical.

2.4.3 Life cycle impact assessment (LCIA)

Practitioners of LCIA assign *toxicity potentials* to toxic substances that attempt to quantify the chemicals' potential long-term impact per unit emission. To that end, values describing exposure are calculated with multi-media fate models and combined with measures of toxicity (Guinée and Heijungs, 1993). "An LCA is only concerned with the total emission of a substance associated with the entire life cycle of a product, which is regarded as a *pulse* (in kg)" (Guinée and Heijungs, 1993). Consequently, steady-state concentrations are often used as exposure values (e.g. see Huijbregts et al. (2000) and Hertwich et al. (2001) and compare equations 2.9) and 2.18).

Our result shows that the toxicity potentials calculated in this way do not depend on the simplifying assumption of a pulse release. Rather, they can be regarded as based on a realistic and dynamic emission scenario.

Chapter 3

Quantifying remoteness from emission sources of persistent organic pollutants on a global scale

Harald von Waldow, Matthew MacLeod, Martin Scheringer and Konrad Hungerbühler

Institute for Chemical and Bioengineering, ETH Zürich

Reproduced with permission from:
Environmental Science & Technology, 2010
Volume 44, Issue 8, pages 2791–2796
DOI: 10.1021/es9030694

Abstract

One of the four screening criteria that are assessed when a chemical substance is nominated for international regulation under the Stockholm Convention is potential for long range transport. Measured levels of a chemical in locations distant from sources can be used as evidence of long range environmental transport, but until now, there has been no quantitative measure of the distance of a location from likely source areas of chemicals. Here we use a global atmospheric transport model to calculate atmospheric concentrations for a set of volatile tracers that differ in their effective atmospheric residence time. We then derive an empirical relationship to express these concentrations as a function of the atmospheric residence time and a location specific parameter. The location specific parameter can be equated with a measure of remoteness, the *remoteness index RI*. We present maps of *RI* for two generic emissions scenarios that represent areas for emissions of industrial and technical chemicals, and pesticides, respectively. Our results can be used to better interpret spatial patterns of measured and modelled concentrations of chemicals in the global environment and to derive long-range transport potential metrics for specific substances. We thus provide, to our knowledge for the first time, a description of remoteness that is applicable to measurement sites of continental- and global-scale monitoring programmes. Our results can be used to plan future measurement campaigns and extend monitoring networks.

3.1 Introduction

The presence of anthropogenic halogenated organic compounds in the environment and biota far from emission sources is an environmental issue of global concern. Substances such as dichlorodiphenyltrichloroethane (DDT) and polychlorinated biphenyls (PCBs) have been measured in a variety of environmental media in remote regions, including the Arctic (Macdonald et al., 2000; AMAP, 2004) and the Antarctic (Kallenborn et al., 1998; Ockenden et al., 2001a), and are

now regulated globally in the Stockholm Convention (UNEP, 2001) as persistent organic pollutants (POPs). The potential for a chemical to undergo long-range transport (LRTP) is one of the four screening criteria that are considered when new substances are nominated for addition to the Stockholm Convention. Sgpecifically, proposals to add a substance to the Convention should provide evidence from measurements that the substance can be found at levels that are of potential concern "in locations distant from the sources of its release". However, presently there is no quantitatively defined metric of distance from globally dispersed emission sources of known or potential POPs. The guidance document on the global monitoring plan for POPs (UNEP, 2007) acknowledges the need to characterise monitoring sites in terms of large-scale transport pathways.

Here, we present an approach based on a two-dimensional global-scale Eulerian atmospheric transport model. We model steady-state concentrations of a suite of volatile tracers with different residence times in the atmosphere that are emitted from representative source regions. On this basis, we estimate the effective distance of each grid cell from potential sources of chemicals that are spatially distributed based on 1) global light emissions, and 2) global crop areas. Finally, we express our result, remoteness of every location on Earth from these two spatially dispersed emission sources, as a remoteness index, *RI*, at the model resolution of 4° latitude by 5° longitude.

The remoteness index, *RI*, makes it possible to compare substances with respect to their LRTP, based on observed or modelled environmental concentrations. It supports the interpretation of large-scale measurements of POPs and candidate POPs in the environment and helps to guide further measurement campaigns and to define more precisely the meaning of the terms "remoteness" or "distant from the sources " that play a defining role in the wording of international treaties, such as the Convention on Long-Range Transboundary Air Pollution (UNECE, 1998) and the Stockholm Convention (UNEP, 2001).

3.2 Methods

Our measure of remoteness of any location on Earth with respect to a particular spatial distribution of emissions is derived from a atmospheric transport model (see below) used to calculate global steady-state concentrations in the

atmosphere that result from continuous releases of a set of hypothetical, perfectly volatile tracers. The set of tracer substances is assigned rate constants for effective removal from the atmosphere that correspond to atmospheric residence times of $\tau_{\text{eff}} = 2, 5, 10, 20, 50, 100, 200, 500, 1000$ and 2000 days. This range of effective residence times represents the range expected for POPs or POP-like substances (Scheringer, 2002). By definition, these effective residence times represent the average lifetime of each tracer in the atmosphere, regardless of whether it undergoes cycles of deposition and revolatilization from the surface. We then approximate the concentrations calculated with the model as a closed-form function of τ_{eff} and a term that can be identified as the remoteness index, *RI*. *RI* describes the effective distance of each location on Earth from the emission source, at the model resolution. The *RI* is thus only a function of the global atmospheric circulation patterns defined by the model and the spatial distribution of sources.

3.2.1 Atmospheric tracer transport model

The tracer transport model covers the whole surface area of the earth using grid cells of 4° latitude by 5° longitude. To describe long-term advective atmospheric transport, we re-gridded and vertically averaged the long term monthly means of the NCEP/NCAR reanalysis data wind fields (1969–1996) (Kalnay et al., 1996). We parameterised turbulence as eddy-diffusivities D_{xx} and D_{yy} in the zonal and meridional direction. The eddy diffusivities were assumed to be proportional to the variances σ^2_{xx} and σ^2_{yy} of the wind velocities of the 3 hourly NCEP/NCAR reanalysis data. To determine an appropriate factor of proportionality, we matched the zonal average of D_{yy} at 45° northern latitude and a height of 500 hPa with the value of 3×10^6 m^2/s (Murgatroyd, 1969; Czeplak and Junge, 1974; Bratseth, 2003). We used upwind differencing to discretize the advection-diffusion equation in space on the $4° \times 5°$ grid. The resulting system of ordinary differential equations was solved with a standard stiff ODE-solver (Brown et al., 1988).

To evaluate our representation of global scale tropospheric transport, we emitted a pulse of a perfectly persistent and volatile tracer according to a defined emission scenario (the "ECON" scenario defined below), and calculated a time-series of the inter-hemispheric exchange time, τ_{ex}, defined as $\tau_{\text{ex}} = (m_{\text{N}} - m_{\text{S}})/q_{\text{N}\rightarrow\text{S}}$, where m_{N} and m_{S} is the tracer mass in the northern and southern

hemisphere, respectively, and $q_{N \to S}$ is the unidirectional north to south mass flow across the equator. τ_{ex} converged to 0.84 years, which compares well with modelled and observed exchange times for chlorofluorocarbons (Prather et al., 1987) and Kr-85 (Jacob et al., 1987) in the range from 0.7 to 1.1 years.

3.2.2 Emission scenarios

We used two generic emission scenarios that are representative of emissions associated with economic activity and population density (ECON) and of emissions from agricultural pesticide use (CROP), respectively.

Economic activity emission scenario (ECON)

Night-time satellite observations of light emissions in the visible-near infrared (0.4–1.1μm) channel of the Defense Meteorological Satellite Program Operational Linescan System is provided by the National Geophysical Data Center of the US National Oceanic and Atmospheric Administration. We obtained the 1996–1997 radiance-calibrated product that has been processed as described by Elvidge et al. (2001) to represent light emissions from human settlements. The data has a resolution of 30×30 arc seconds. We transformed the digital number of each pixel to radiance [Wm^{-2}] using the equation from the accompanying documentation (NOAA, 2002), regridded the data onto the $4^\circ \times 5^\circ$ degree grid using a conservative remapping algorithm (Jones, 1999) and then calculated the radiative power [W] of each grid cell by multiplying its radiance by its area. Figure 3.5 shows the resulting map of light emissions, which we use as a proxy for likely emissions of technical chemicals.

Pesticide use emission scenario (CROP)

We obtained the $1^\circ \times 1^\circ$ degree global cropland fraction data set from the Meteorological Service of Canada that was produced by Li (1999) from the 1-km resolution land cover characteristics database provided jointly by the U.S. Geological Survey, the University of Nebraska-Lincoln and the Joint Research Centre of the European Commission which in turn is derived from 1-km Advanced

Very High Resolution Radiometer (AVHRR) data spanning the 12-month period from April 1992 to March 1993 (Loveland et al., 2000). As above, we used a conservative remapping algorithm to regrid the dataset onto the $4^\circ \times 5^\circ$ grid and then calculated the cropland area per grid cell. Figure 3.6 shows the resulting map of cropland area per grid cell, which we use as a proxy emission scenario that does not refer to a particular chemical but describes the spatial distribution of potential pesticide emissions.

3.2.3 Derivation of the remoteness measure

We emitted the set of hypothetical, perfectly volatile chemicals at a total rate of 1×10^4 kg/day, spatially distributed according to each of the emission scenarios ECON and CROP and used the atmospheric transport model to calculate the steady-state concentrations, $C_{i,\tau_{\text{eff}}}$, at all 3420 locations, i, of the model grid.

Empirical fitting of several possible relationships between τ_{eff} and $C_{i,\tau_{\text{eff}}}$ led us to the empirical model

$$\ln(C_{i,\tau_{\text{eff}}}) = \alpha - \beta_i(\gamma - (\ln \tau_{\text{eff}})^\theta) \tag{3.1}$$

that describes the data very well. α, γ and θ depend on the emission scenario only, whereas β_i is characteristic of location i (for a given emission scenario). To fit equation 3.1, we used the quasi-Newton algorithm L-BFGS (Liu and Nocedal, 1989). To assess the robustness of a non-linear local optimisation procedure with respect to its initial values, it is necessary to experiment with various initial parameter estimates. In our case, varying 3420 instances of β_i is not feasible. To overcome this problem, we used the non-linear solver only to estimate the parameters γ and θ, and nested the estimation of the linear parameters α and β_i $(i = 1, \ldots, 3240)$ into the objective function. In each step of the L-BFGS algorithm, the current estimates of γ and θ are used to calculate the least squares estimator for α and the β_i, as in an ordinary least squares regression. This way, no initial values for α and the β_i are necessary and we were able to systematically vary the initial values for γ and θ to check the robustness of the optimisation procedure. This method of the separation of linear and non-linear parameters has been described by Maeder and Neuhold (2007)

Since β_i is the only location specific parameter in equation 3.1 that relates steady-state concentrations to effective atmospheric residence times, we equate the β_i

with the measure of remoteness of grid cell i, RI_i:

$$RI_i \equiv \beta_i \tag{3.2}$$

Inspection of equation 3.1 shows that γ represents an upper limit for $(\ln \tau_{\text{eff}})^\theta$: the β_i are positive, and $\gamma < (\ln \tau_{\text{eff}})^\theta$ would, unrealistically, result in increasing concentrations with increasing remoteness. We write γ as $\gamma := (\ln \tau_{\text{max}})^\theta$ and observe that for $\tau_{\text{eff}} = \tau_{\text{max}}$, all log-concentrations are equal to α and independent of location. τ_{max} is an upper limit of atmospheric residence times for which the empirical relationship in equation 3.1 is valid. We interpret τ_{max} as the atmospheric residence time of a substance for which the atmospheric steady-state concentrations are globally homogeneous. In other words, for $\tau_{\text{eff}} = \tau_{\text{max}}$ the troposphere can be regarded as a single, well-mixed compartment. In this case, we can calculate the steady-state log-concentration α from the total source strength, $\|\vec{q}_{\text{ss}}\|_1 = 1 \times 10^4$ kg/day, the model volume of the troposphere, $V_{\text{A}} = 8.32 \times 10^{18}$ m^3, and τ_{max}.

$$\alpha = \ln(C_{\tau_{\text{max}}}) = \ln \frac{\|\vec{q}_{\text{ss}}\|_1 \tau_{\text{max}}}{V_{\text{A}}} \tag{3.3}$$

We now substitute α in equation 3.1 with the right-hand term of equation 3.3 and repeat the fitting procedure for the resulting empirical equation with one less parameter, using only τ_{max}, RI_i and θ as free parameters:

$$\ln(C_{i,\tau_{\text{eff}}}) = \ln \frac{\|\vec{q}_{\text{ss}}\|_1 \tau_{\text{max}}}{V_{\text{A}}} - RI_i((\ln \tau_{\text{max}})^\theta - (\ln \tau_{\text{eff}})^\theta) \tag{3.4}$$

The form of equation 3.4 makes it impossible to consider τ_{eff} shorter than one day. This is an acceptable limitation for the application to persistent contaminants subject to long-range transport.The results of the fit and the assessment of approximation errors as described below are for both emission scenarios indistinguishable from the original fit (equation 3.1) that includes α as a free parameter. We therefore use in the following the results of the fits of equation 3.4.

An evaluation of the quality of the empirical fit is detailed in section 3.6.2. The coefficient of determination in 95% of all grid cells is greater than $r^2 = 0.96$ for both scenarios and 95% of the 32400 residuals are lower than 0.59 and 0.54 for the ECON and CROP scenario, respectively (Figure 3.7). A residual analysis reveals no appreciable bias of the approximation error with respect to the predicted concentration, to the effective residence time and to the remoteness index (Figure 3.8).

3.3 Results

The fit of equation 3.4 leads to $\tau_{max} = 2013$ days and $\theta = 0.6884$ for the ECON scenario, and to $\tau_{max} = 1004$ days and $\theta = 0.5787$ for the CROP scenario. τ_{max} of 5.5 years for ECON is about twice the τ_{max} for CROP. This is a result of the more spatially distributed CROP emission scenario, where the ratio of the emissions in the Northern Hemisphere to the Southern Hemisphere is about 3, as opposed to 12 for the ECON scenario. For a given emission scenario and a fixed τ_{eff}, a unit increase of the remoteness index induces a decrease of $\ln(C)$ by $\left[(\ln \tau_{max})^{\theta} - (\ln \tau_{eff})^{\theta}\right]$. In other words, the larger τ_{eff}, the smaller is the influence of the remoteness on steady state concentrations, which is a plausible relationship. For a fixed location, in turn, a unit increase of $(\ln \tau_{eff})^{\theta}$ implies that $\ln(C)$ at that location increases by the value of the remoteness index of that location. In other words, the more remote a location is, the greater is the influence of a change in atmospheric residence time, which is again a plausible relationship.

3.1 and 3.2 show the remoteness indices for the ECON and CROP emission scenarios, respectively. Since *RI* values are on different scales for the different emission scenarios, we have classified the remoteness index in deciles of the Earth's total surface area to facilitate a direct comparison of the Earth's regions with respect to their remoteness. The corresponding plots with colour-scales linear in the actual values of *RI* appear in section 3.6.3 (Figures 3.9 and 3.10). Because the numerical *RI* values will be used in further applications of the *RI* approach that are based on equation 3.4, we do not normalize them to a common scale. As expected, the spatial centres of regions with low *RI* correspond to the geographical hot spots of emissions (compare Figures 3.5 and 3.6). For the ECON emission scenario these are the Eastern and Western Seaboard of the USA, Central Europe and Mainland Japan. Another, weaker emission centre is located at the Gulf of Guinea, where the sub-Saharan maximum of population density coincides with a high degree of urbanisation in the second largest sub-Saharan economy, Nigeria. Two weak emission centres in the Southern Hemisphere correspond to the economic centre of Brazil around São Paulo and Rio de Janeiro, and the South African region around Pretoria and Johannesburg. The shape of the contours traces the influence of the Westerlies on the long-term global circulation patterns in the Northern Hemisphere. Most of the least remote 20% of the Earth lies between the Arctic Circle and the Tropic of Cancer in the *Northern Hemisphere pollution belt*. The maximum remoteness index of 4.25 with respect to

this emission scenario is reached in the equatorial Pacific Ocean between 150° and 165° west. The most remote 20% of the Earth encompass the Antarctic and the southern Pacific Ocean in both emission scenarios. The average *RI* of about 3.9 for the ECON emission scenario makes the Antarctic the most remote terrestrial region on earth, together with North Australia and New Guinea. The Arctic has an average remoteness index of 2.6 and mainly belongs to the fifth remoteness decile.

The CROP emission scenario is spatially more dispersed. Due to the intensive agricultural land use across western Europe and along the Eurasian Chernozem Belt, on the Indian Subcontinent, and in eastern China, the whole of Eurasia dominates the world map in terms of closeness to cropland-associated chemical emissions. The closeness of the Eastern Seaboard of the United States to potential pesticide emissions stems from the intensive agricultural land use in the Midwestern United States. In the Southern Hemisphere, the agriculturally used land in eastern Brazil, West Africa and eastern Africa dominate the effective distance map. As in the ECON scenario, the influence of the Southern Hemisphere emission centres does not extend much beyond their respective continent, due to their location outside of the prevailing Westerlies.

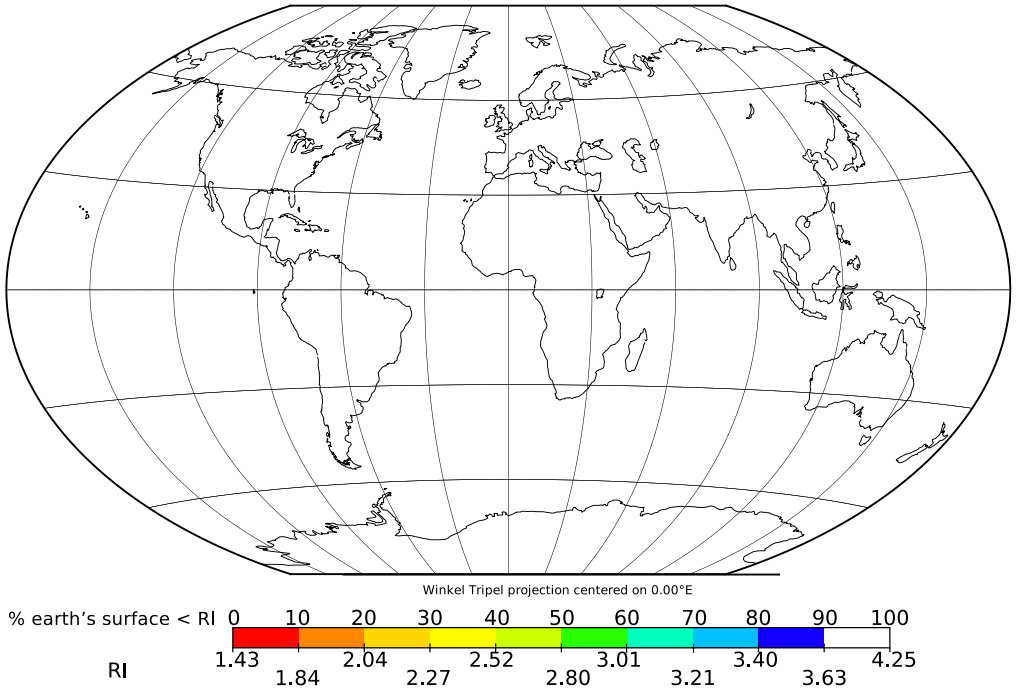

Figure 3.1: Remoteness index *RI* for the ECON - emission scenario

Figure 3.2: Remoteness index *RI* for the CROP - emission scenario

3.4 Implications

In the last decade, several coordinated measurement campaigns were carried out to collect empirical data to characterise the long range transport behaviour of environmental contaminants. Typically, these campaigns measured concentrations of chemicals along spatial transects that cover several thousand kilometres.

For example Shen et al. (2006) examined the spatial variation in PCB congener composition in the atmosphere using passive sampler data from measurement sites along transects ranging from Costa Rica to Ellesmere Island in north-south direction and from Vancouver to Island to Newfoundland in west-east direction. Figure 3.3 depicts the approximate location of these sampling transects superimposed onto a map of *RI* for the ECON scenario (here we use a linear scale to visualize the gradient in *RI*). The part of the north-south transect of Shen et al. that extends from New York into the Arctic traces the steepest *RI*-gradient for the ECON scenario in the Northern Hemisphere. The part extending from Costa Rica into the mid-latitudes exhibits a decreasing *RI* with increasing latitude. The west-east transect runs across a comparatively small range of *RI*. A steeper *RI* gradient in this orientation could have been covered by shifting the west-east transect southward by about 8° latitude.

Muir et al. (2004) studied concentrations of organochlorine pesticides in North American lake water and calculated indicators of atmospheric LRTP from the relation of observed concentration gradients with latitude. In addition to three Arctic sites, the measurement locations are located on a U-shaped path from north-east Manitoba southward to north-west Ontario, westward into New York State and northward towards Labrador. Figure 3.11, bottom left, shows the approximate sampling locations superimposed onto a map of *RI* for the CROP scenario. In the area covered by the measurement sites, the gradient of *RI* is oriented in the north-south direction, therefore the observation of Muir et al. of a correlation of pesticide concentrations with latitude is consistent with the spatial pattern of *RI* from the CROP scenario. A similar concentration gradient in the east-west direction could likely be observed for a transect that would reach from the Great Lakes region in south-west direction into Arizona.

Ockenden et al. (1998b), Meijer et al. (2003), Jaward et al. (2004) and Gioia et al. (2006), used a transect from South England into the Arctic, to evaluate PCB-

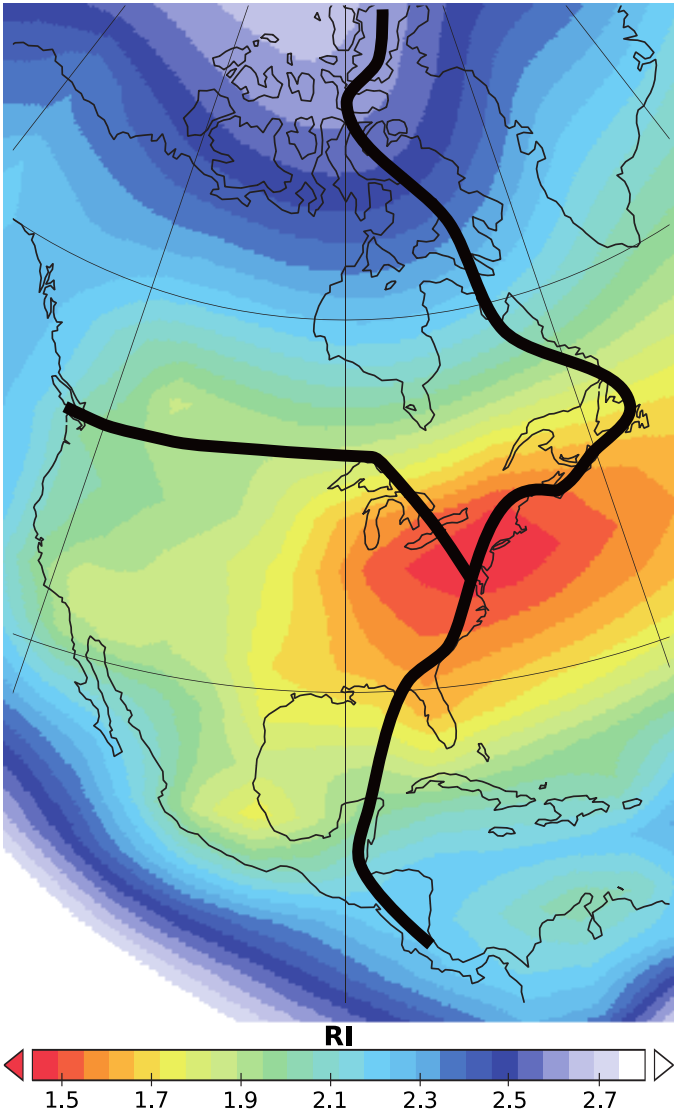

Figure 3.3: Detailed view of the *RI* distribution in North America for the ECON scenario. The fat black lines mark the approximate location of the transects in Shen et al. (2006).

congener fractionation as a function of latitude as part of a long-term monitoring project. Their approximate measurement transect is depicted in Figure 3.11, top right. Here, *RI* also correlates with latitude, but the gradient of *RI* is less steep compared to the same latitude range in the North American transect.

Maps of *RI* can be used as a tool to plan future measurement campaigns designed to empirically assess the LRTP of chemicals. They serve to identify possible transects where steep concentration gradients can be expected. They could also be used to identify observation locations with a similar *RI* but different environmental conditions to elucidate local effects of temperature, precipitation and surface characteristics on chemical concentrations.

Long-term monitoring networks for persistent chemical pollutants have been established to support international conventions. These include the Global Atmospheric Passive Sampling network, GAPS (Pozo et al., 2006), and the European Monitoring and Evaluation Programme, EMEP. In the interpretation of GAPS data, the relative location with respect to emission sources has been characterised in form of a classification into the bins "urban", "agricultural", "remote" and "polar" (Pozo et al., 2006). The first three classes describe measurement locations on a local to regional scale. We propose that, to characterise the locations on a spatial scale that corresponds to the global coverage of the GAPS Network, *RI* provides an appropriate quantitative measure. Figure 3.12 shows the cumulative distribution of *RI* for the earth's surface area in comparison to the 53 GAPS sites. For *RI* values below 2.5 (ECON) and 3.5 (CROP), the GAPS curve in Figure 3.12 is steeper than the curve of the Earth's surface area, i.e. regions with a $RI < 2.5$ (ECON) and $RI < 3.5$ (CROP) are overrepresented in the GAPS monitoring network. New GAPS stations should therefore be established in more remote areas if a representative spatial coverage with respect to *RI* is the objective. Most of the underrepresented range of *RI* belongs to the oceans (compare Figures 3.1 and 3.2). Therefore islands could be considered as possible new sampling locations.

Even though the range of *RI* in Europe is small compared to the global range, enough variation exists to analyze EMEP data for the LRTP of seven PCB congeners. Figure 3.4 shows a plot of the mean atmospheric log-concentrations in the years 2004–2006 at the EMEP stations CZ0003R, FI0036R, FI0096G, GB0014R, IS0091R, NO0001R, NO0042G, SE0012R and SE0014R (EMEP, 2009), versus *RI*. We derived congener-specific *RI*s using the PCB emission scenarios described

below. The error bars indicate three times the standard deviation of the three annual mean log concentrations. We performed a weighted regression for each congener, with weights equalling the inverse variance of the annual log-concentrations for each station and congener. There is no significant linear relationship for PCB-28 (not shown), a weak relationship for PCB-52, and strong negative correlations for PCBs 101, 118, 138, 153 and 180, with r^2 = 0.92, 0.94, 0.81, 0.86 and 0.70, respectively. Since heavier PCBs tend to have shorter effective atmospheric residence times, this is to be expected.

Tables 3.1 and 3.2 list *RI* for the EMEP and GAPS stations, respectively. We provide there *RI* for the ECON and CROP emission scenarios as well as for emission scenarios of the PCB congeners 28, 52, 101, 118, 138, 153 and 180. For the PCBs, we used the average of the "high" scenarios estimated by Breivik et al. (2007) for the years 2007 and 2008.

Another application of *RI* is the the estimation of atmospheric residence times and associated LRTP indicators such as the characteristic travel distance from empirical data. According to equation 3.4, the slope of the regression line of measured atmospheric concentrations at different observations locations against *RI* equals $(\ln(\tau_{max}))^\theta - (\ln(\tau_{eff}))^\theta$. Since τ_{max} and θ are known, τ_{eff} can be calculated and compared among different substances that are emitted according to a similar pattern.

3.5 Discussion

The derivation of our remoteness index is based on steady-state concentrations calculated with a 2-dimensional global atmospheric tracer transport model. The spatial resolution is coarser than that of state-of-the-art atmospheric chemistry transport models, however, given the uncertainties of emissions and transport data, we consider this resolution as appropriate. The use of long-term averages to describe atmospheric circulation and the evaluation of the model at steady-state limits its applicability to the assessment of phenomena related to the long-term exposure to environmentally distributed chemicals. Since the application in the context of this work aims at a time-independent characteristic, *RI*, this approach is appropriate. Individual short-time measurement data, for example, from high-volume active samplers, will be influenced by short-term wind conditions and therefore cannot be interpreted in terms of *RI*.

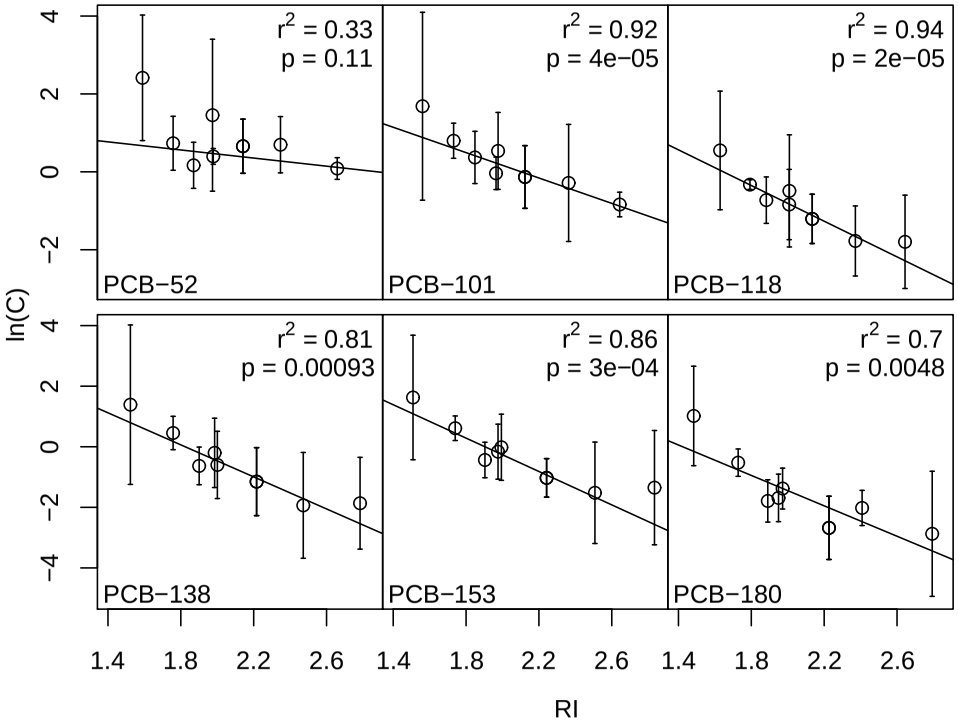

Figure 3.4: PCB congener annual mean concentrations in air for the years 2004–2006 at 9 EMEP stations as a function of *RI*. Error bars indicate 3 times the standard deviation of the three annual mean log concentrations.

It is important to recognize that our method for deriving *RI* does not depend on the type of model used to calculate long-term atmospheric concentrations. The only limit to the model's complexity is calculation time. Our simple but fast model was selected to enable us to efficiently develop the concept by experimenting with various emission scenarios and 10 hypothetical substances. Should our method be used with a different atmospheric transport model, it is possible that the optimal form of the empirical equation will be different from equation 3.4.

RI is a function of emission pattern and atmospheric circulation only, and is formulated to be independent of the properties of any particular substance. *RI* represents a metric on the Earth's surface that reflects the geographical distance from emission sources interacting with atmospheric circulation patterns. Normal geographical distance, in contrast, does not reflect the spatially inhomogeneous atmospheric circulation. Therefore, *RI* can be used to replace geographical distance in the identification of remote regions and in the interpretation of spatial concentration gradients in the context of long-range transport of chemicals. *RI* does not represent spatial distribution patterns of particular chemicals. Only in the limiting case of a substance that has a very long residence time in air, the distribution of *RI* might mirror real concentrations. An example is the spatial distribution of CO_2 with a residence time of about 7 years (Siegenthaler and Oeschger, 1978) in the atmosphere which, according to data from the Atmospheric Infrared Sounder exhibits global spatial patterns determined by source locations and large-scale circulation patterns (Chahine et al., 2008), just like *RI*.

A set of possible applications of the *RI* approach includes the evaluation of transects for field camaigns and the calculation of effective residence times from equation 3.4. These applications involve the implicit comparison of concentrations of real substances to modelled concentrations of the hypothetical airborne tracer substances used in the derivation of *RI*. The atmospheric residence times of real substances, however, might exhibit considerable spatial variations due to varying environmental conditions. It is therefore essential, in the applications mentioned above, to limit the the region containing the observation locations to a size where the spatial variations of the atmospheric residence time can be neglected in comparison to uncertainties associated with measurements of atmospheric concentrations of persistent chemicals. The strong correlation of *RI* with PCB concentrations in air (Figure 3.4) indicates that this assumption is valid in a region encompassing the EMEP stations, reaching from 20° West to 15° East

and from 50° to 78° North.

To make the concept of the hypothetical airborne tracer substances clearer, we have assigned them "perfect volatility" and an unspecified mechanism of removal from the atmosphere in the description of the method for calculating *RI*. However, when τ_{eff} is calculated from *RI* values and measured concentrations according to equation 3.4, real substances are compared with the hypothetical tracers. This comparison is possible, because the removal rate assigned to the hypothetical tracers can be interpreted as representing the net removal rate of real substances from the atmosphere, including loss through various deposition processes and gain through re-volatilization from surface compartments.

Since *RI* values for different emission scenarios are on different scales, caused by differing fitting parameters θ and τ_{max}, the *RI*s for different source patterns need to be rescaled to enable a comparison of *RI* for different emission patterns. We suggest the rescaling to the Earth's surface area as exemplified in the colour coding of Figures 3.1 and 3.2 as suitable approach, in line with the objective of introducing a graduation of the globe according to remoteness from emission sources. For applications that involve actual concentrations measured in the field, *RI* cannot be re-scaled, because this would invalidate *RI*'s relationship with concentrations and τ_{eff} expressed in equation 3.4.

Acknowledgements

We thank Kevin Jones for valuable discussions and Bobby Neuhold for his advice on the optimisation procedure.

3.6 Supporting Information

3.6.1 Emission scenarios

Figures 3.5 and 3.6 depict the data from which the two emission scenarios for this work were derived. Figure 3.5 shows the radiative power [MW] of the emitted light per grid cell, derived from a 1996–1997 radiance-calibrated satellite composite of night-time satellite observations (NOAA, 2002). Figure 3.6 shows

the cropland area per grid cell derived from a 1-km resolution land cover characteristics database that in turn was derived from satellite based Advanced Very High Resolution Radiometer data (Li, 1999). We use two emissions scenarios to represent technical emissions of chemicals (ECON), on the one hand, and pesticide emissions (CROP), on the other hand. They have been selected to represent general global usage patterns of chemicals that are identified POPs, and those that have the potential to be considered as candidate POPs in the future. Both scenarios are based on satellite imagery. The night-time satellite imagery that forms the basis of the ECON scenario has been shown to correlate with Gross Regional Product (Doll et al., 2006), electric power consumption, carbon dioxide emissions (Elvidge et al., 2001) and population density (Sutton et al., 2001). These indicators have been used previously to establish emission scenarios of specific technical pollutants. In the construction of a PCB emission dataset, for example, Breivik et al. (2002) used the Gross Domestic Product as a surrogate to distribute PCB imports over countries where no import data was available and observed that PCB consumption is linked to the use of electrical equipment. To produce a gridded map of PCB emissions, they used population density data as a surrogate. The other emission scenario, CROP, describes areas of potential pesticide use and is based on a global land cover classification derived from satellite based AVHRR data. It has been used previously to create gridded emission inventories for hexachlorocyclohexane (HCH) (Li, 1999) and DDT (Semeena et al., 2006).

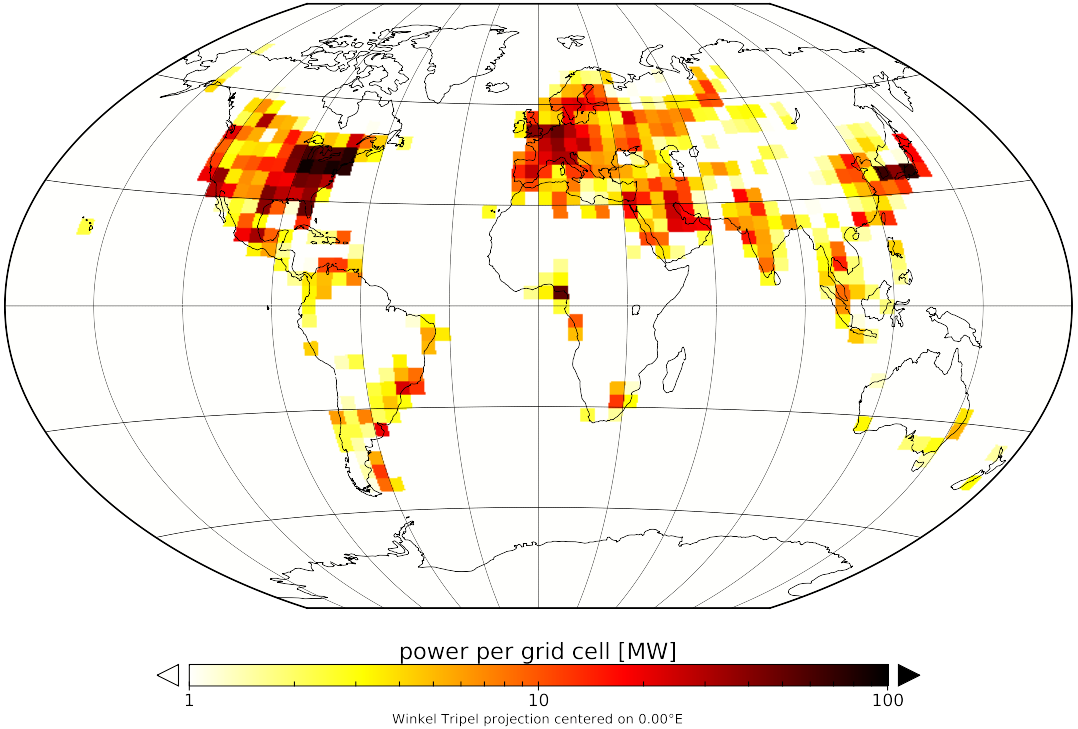

Figure 3.5: World map of light emission power per grid cell on a $4° \times 5°$ grid

Figure 3.6: World map of cropland [km^2] per grid cell on a $4° \times 5°$ grid

3.6.2 Quality of the empirical fit

Figures 3.7 and 3.8 are diagnostic graphics to assess the quality of the fit of equation 3.4 for the ECON and CROP scenario. Figure 3.7 shows the accuracy of the empirical approximation (equation 3.4) to the modelled steady-state concentrations. Figure 3.8 shows plots of the residuals versus fitted $\ln(C[\mathrm{pg/m^3}])$, versus atmospheric residence time $\tau_{\mathrm{eff}}[\mathrm{days}]$, and versus remoteness index *RI*. The black line in each sub-plot represents the robust smoothing function `loess` with smoothing parameter $\alpha = 0.75$ (Cleveland et al., 1992). It indicates that no appreciable systematic bias of the approximation exists with respect to the predicted concentration, to the effective atmospheric residence time and to the remoteness index. The largest deviations of the fit occur for low concentrations (compare Figure 3.8) that are a result of an atmospheric residence time of 2 days. The range of the residuals increases for τ_{eff} between 5 and 50 days and becomes smaller for larger effective residence times.

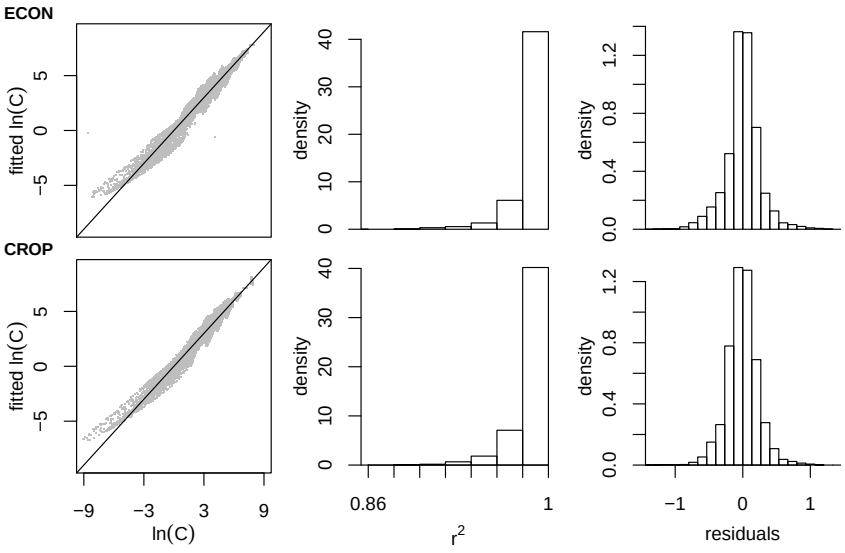

Figure 3.7: Accuracy of the empirical approximation to steady state concentrations for the ECON (top) and CROP (bottom) scenario. From left to right: fitted $\ln(C[\mathrm{pg/m^3}])$ vs. actual $\ln(C[\mathrm{pg/m^3}])$, histogram of the r^2 for the individual fits in all 3240 grid cells, histogram of the residuals for all 32400 fitted values.

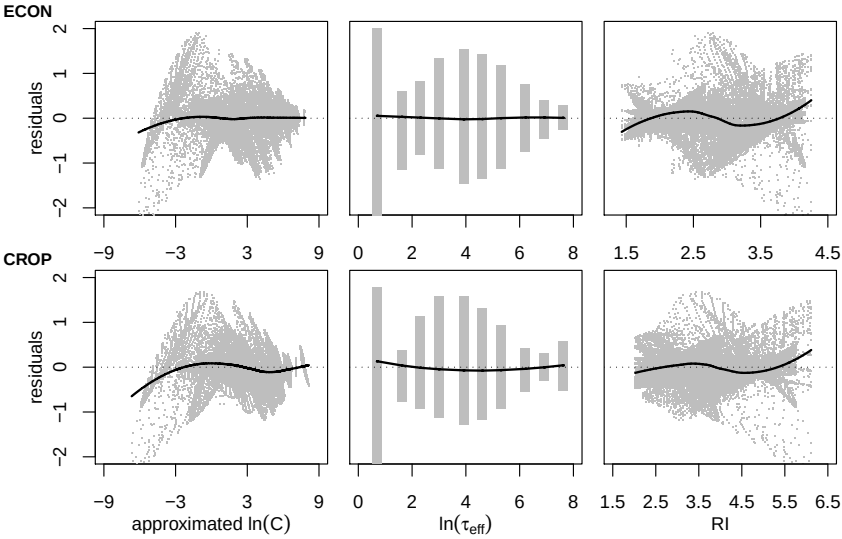

Figure 3.8: Residuals of the empirical approximation to steady state concentrations for the ECON (top) and CROP (bottom) scenario. From left to right: versus fitted $\ln(C[pg/m^3])$, versus atmospheric residence time τ_{eff}[days], versus effective remoteness index *RI*.

3.6.3 Global distribution of RI

Figures 3.9 and 3.10 depict the global distribution of *RI* for the ECON and CROP scenario, respectively. These figures differ from Figures 3.1 and 3.2 only in their colour scale, which here represents the original scale of both *RI* variants.

3.6.4 Interpretation of POP measurement transects using *RI*

Figure 3.11 depicts the *RI* distribution in North America (left column) and Europe (right column) for the ECON (top row) and CROP (bottom row) scenario.

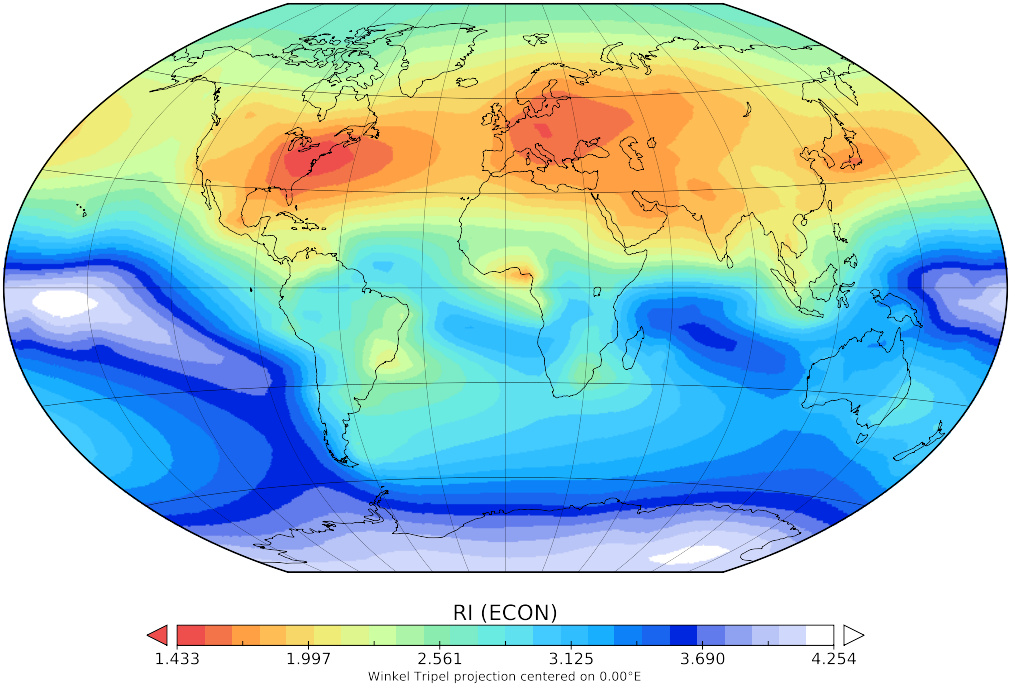

Figure 3.9: Map of *RI* with respect to the ECON scenario.

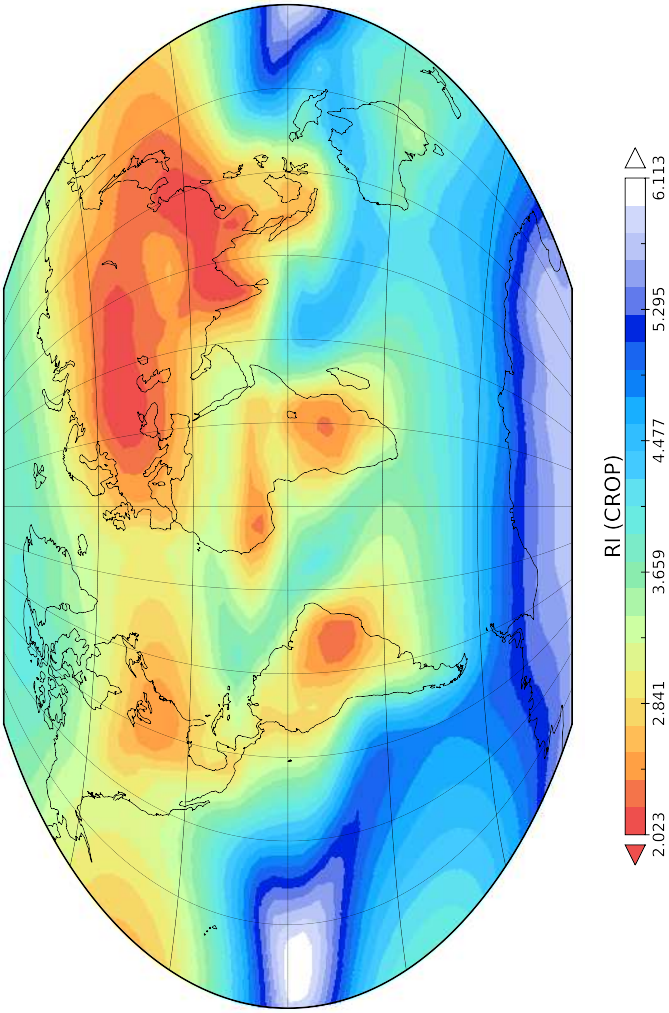

Figure 3.10: Map of *RI* with respect to the CROP scenario.

Superimposed onto the maps are the transects of selected POP sampling campaigns: Shen et al. (2006) top left, Muir et al. (2004) bottom left, Gioia et al. (2006) top right.

3.6.5 Remoteness Index for monitoring network stations

Figure 3.12 shows the cumulative distribution of *RI* (ECON and CROP) for the Earth's surface area and for the 53 GAPS sites. It indicates that regions with an $RI < 2.5$ (ECON) and $RI < 3.5$ (CROP) are overrepresented in the GAPS monitoring network.

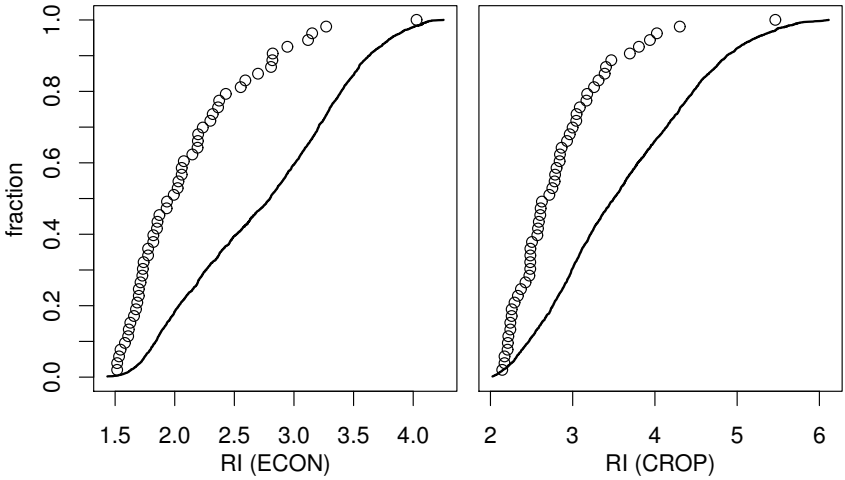

Figure 3.12: Cumulative distribution of *RI* for the Earth's surface area (line) and for the 53 GAPS sites (circles).

Tables 3.1 and 3.2 list the *RI* values for EMEP and GAPS monitoring sites and for the ECON, CROP and seven PCB emission scenarios. The PCB emission scenarios are based on the average of the "high" emission scenarios for the years 2007–2008 estimated by Breivik et al. (2007).

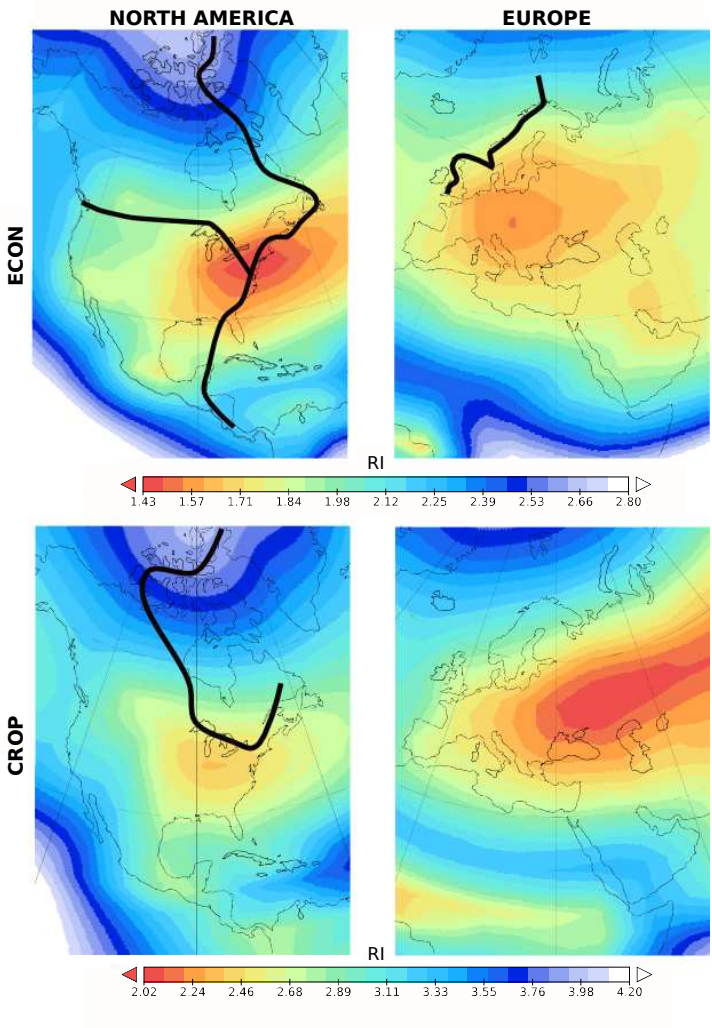

Figure 3.11: Detailed views of the *RI* distribution in North America (left column) and Europe (right column) for the ECON (top row) and CROP (bottom row) scenario. Superimposed onto the maps are transects of selected measurement campaigns described in the text.

STATION		remoteness index *RI* for different emission scenarios								
				PCB emission scenarios for congeners						
Code	Location	ECON	CROP	28	52	101	118	138	153	180
BE0004R	Knokke	1.628	2.573	1.831	1.849	1.853	1.888	1.832	1.812	1.798
BE0014R	Koksijde	1.628	2.573	1.831	1.849	1.853	1.888	1.832	1.812	1.798
CZ0003R	Kosetice	1.543	2.292	1.552	1.575	1.550	1.623	1.526	1.493	1.492
DE0001R	Westerland	1.674	2.627	1.884	1.892	1.885	1.930	1.895	1.878	1.863
DE0009R	Zingst	1.622	2.554	1.806	1.811	1.792	1.850	1.811	1.791	1.780
DK0031R	Ulborg	1.674	2.627	1.884	1.892	1.885	1.930	1.895	1.878	1.863
ES0008R	Niembro	1.749	2.660	2.013	2.016	2.033	2.049	2.038	2.035	1.988
FI0096G	Pallas,Särkijärvi	1.860	3.024	2.204	2.183	2.168	2.186	2.250	2.270	2.246
GB0014R	High Muffles	1.772	2.750	2.092	2.088	2.097	2.121	2.136	2.139	2.090
IE0002R	Turlough Hill	1.566	2.473	1.693	1.713	1.707	1.758	1.686	1.656	1.657
IS0091R	Storhofdi	2.023	3.259	2.397	2.365	2.383	2.389	2.502	2.542	2.434
LT0015R	Preila	1.613	2.372	1.730	1.728	1.701	1.749	1.736	1.730	1.712
LV0010R	Rucava	1.613	2.372	1.730	1.728	1.701	1.749	1.736	1.730	1.712
LV0016R	Zoseni	1.620	2.267	1.678	1.660	1.633	1.654	1.699	1.717	1.710
NL0091R	De Zilk	1.628	2.573	1.831	1.849	1.853	1.888	1.832	1.812	1.798
NO0001R	Birkenes	1.733	2.795	2.044	2.042	2.036	2.073	2.071	2.067	2.038
NO0042G	Spitsbergen	2.362	3.694	2.712	2.672	2.658	2.660	2.798	2.848	2.802
NO0099R	Lista	1.733	2.795	2.044	2.042	2.036	2.073	2.071	2.067	2.038
SE0002R	Rörvik	1.622	2.554	1.806	1.811	1.792	1.850	1.811	1.791	1.780
SE0012R	Aspvreten	1.628	2.676	1.928	1.924	1.905	1.948	1.946	1.941	1.924
SE0014R	Råö	1.622	2.554	1.806	1.811	1.792	1.850	1.811	1.791	1.780

Table 3.1: Remoteness indices for EMEP monitoring sites

STATION			remoteness index *RI* for different emission scenarios								
					PCB emission scenarios for congeners						
Country	latitude	longitude	ECON	CROP	28	52	101	118	138	153	180
Ghana	8.0	-2.0	2.19	2.369	2.661	2.685	2.675	2.711	2.666	2.653	2.664
Malawi	-14.18	33.12	2.806	2.425	3.507	3.53	3.51	3.552	3.521	3.516	3.534
South Africa	-30.67	24.0	2.817	3.404	3.217	3.248	3.23	3.274	3.22	3.206	3.229
South Africa	-25.87	22.9	2.82	3.042	3.338	3.366	3.347	3.391	3.345	3.335	3.356
China	30.67	104.07	2.057	2.257	2.297	2.273	2.241	2.224	2.321	2.358	2.392
China	40.98	122.05	1.87	2.207	2.046	1.984	1.949	1.909	2.112	2.205	2.281
China	45.73	126.63	1.933	2.21	2.026	1.957	1.924	1.881	2.106	2.213	2.3
China	30.97	103.52	2.057	2.257	2.297	2.273	2.241	2.224	2.321	2.358	2.392
India	28.67	77.23	1.775	2.24	2.061	2.066	2.054	2.067	2.067	2.066	2.083
India	28.67	77.23	1.775	2.24	2.061	2.066	2.054	2.067	2.067	2.066	2.083
Indonesia	-0.2	100.32	2.192	2.472	2.486	2.522	2.512	2.555	2.472	2.445	2.473
Japan	32.78	130.7	1.819	2.216	2.095	2.086	1.986	1.981	2.205	2.239	2.277
Korea	37.58	127.02	1.697	2.17	1.946	1.928	1.886	1.874	1.984	2.014	2.056
Korea	36.02	129.32	1.697	2.17	1.946	1.928	1.886	1.874	1.984	2.014	2.056
Kuwait	29.33	47.9	1.731	2.963	2.052	2.075	2.069	2.102	2.044	2.026	2.029
Malaysia	4.95	117.85	2.552	2.752	2.777	2.801	2.789	2.827	2.779	2.762	2.787
Philippines	14.65	121.07	2.297	2.625	2.659	2.673	2.65	2.671	2.665	2.662	2.685
Australia	-40.68	144.68	3.117	3.804	3.852	3.86	3.825	3.876	3.869	3.873	3.873
Australia	-12.37	130.87	3.269	4.302	3.736	3.742	3.71	3.754	3.759	3.766	3.771
Costa Rica	9.7	-83.87	2.234	2.84	2.627	2.652	2.644	2.681	2.633	2.617	2.627
Cuba	22.75	-83.53	1.818	2.93	2.194	2.173	2.214	2.222	2.301	2.328	2.201
Mexico	19.2	-96.13	1.737	2.803	2.242	2.262	2.263	2.293	2.257	2.242	2.237
Canary Isl.	27.98	-15.37	2.029	3.313	2.334	2.318	2.345	2.352	2.403	2.424	2.332
Czech Rep.	49.58	15.08	1.543	2.292	1.55	1.59	1.561	1.629	1.523	1.509	1.484
Finland	61.05	25.67	1.626	2.484	1.775	1.739	1.715	1.712	1.817	1.857	1.872
France	48.87	2.37	1.656	2.504	1.678	1.705	1.71	1.752	1.658	1.624	1.628

Table 3.2: Remoteness indices for GAPS monitoring sites (continued on next page)

STATION			remoteness index *RI* for different emission scenarios								
					PCB emission scenarios for congeners						
Country	latitude	longitude	ECON	CROP	28	52	101	118	138	153	180
Iceland	63.4	-20.28	2.023	3.259	2.376	2.347	2.363	2.371	2.472	2.507	2.408
Ireland	55.37	-7.33	1.849	2.864	2.092	2.088	2.097	2.121	2.136	2.139	2.09
Italy	37.97	12.07	1.727	2.609	1.804	1.833	1.835	1.871	1.779	1.751	1.751
Norway	78.9	11.88	2.362	3.694	2.699	2.659	2.643	2.644	2.784	2.834	2.793
Poland	54.22	18.38	1.613	2.484	1.73	1.728	1.701	1.749	1.736	1.73	1.712
Russia	54.9	37.8	1.608	2.142	1.518	1.458	1.433	1.401	1.581	1.668	1.736
Spain	41.38	2.18	1.711	2.587	1.785	1.814	1.823	1.85	1.756	1.727	1.724
Turkey	38.42	27.13	1.673	2.332	1.719	1.747	1.733	1.771	1.697	1.684	1.677
Bermuda	32.37	-64.65	1.684	2.785	2.026	1.993	2.043	2.044	2.162	2.208	2.035
Canada	82.45	-63.5	2.591	3.938	2.961	2.908	2.89	2.879	3.077	3.15	3.095
Canada	50.2	-104.72	1.93	2.715	2.325	2.294	2.271	2.274	2.405	2.444	2.402
Canada	45.22	-78.93	1.515	2.483	1.855	1.828	1.859	1.866	1.958	1.989	1.857
Canada	43.78	-79.47	1.515	2.483	1.855	1.828	1.859	1.866	1.958	1.989	1.857
Canada	63.52	-116.0	2.317	3.388	2.675	2.628	2.574	2.56	2.793	2.866	2.864
Canada	49.22	-123.12	1.99	3.046	2.208	2.174	2.16	2.158	2.307	2.352	2.292
Canada	50.07	-122.95	2.074	3.086	2.351	2.315	2.283	2.278	2.45	2.501	2.468
USA	33.37	-83.48	1.58	2.577	1.919	1.888	1.941	1.94	2.057	2.102	1.925
USA	71.32	-156.6	2.427	3.469	2.756	2.692	2.633	2.604	2.892	2.998	3.033
USA	34.27	-118.77	1.854	3.166	2.045	2.008	2.035	2.029	2.182	2.239	2.095
USA	63.7	-170.48	2.371	3.175	2.571	2.508	2.445	2.415	2.702	2.808	2.871
Argentina	38.75	-62.25	1.531	2.605	1.843	1.812	1.86	1.861	1.97	2.011	1.844
Bolivia	-16.27	-68.13	2.697	2.779	3.337	3.362	3.343	3.385	3.348	3.34	3.358
Brazil	-23.15	-47.17	2.195	2.569	2.74	2.779	2.765	2.812	2.727	2.701	2.729
Chile	-45.58	72.03	3.151	4.023	3.781	3.802	3.777	3.819	3.801	3.802	3.818
Chile	-18.22	-69.17	2.943	2.998	3.528	3.549	3.527	3.568	3.543	3.54	3.556
Colombia	7.02	-70.75	2.146	2.844	2.498	2.526	2.519	2.556	2.5	2.481	2.493
Antarctica	-74.7	164.12	4.027	5.464	4.872	4.871	4.832	4.874	4.925	4.956	4.955

Table 3.2: Remoteness indices for GAPS monitoring sites (continued)

Chapter 4

Remoteness from emission sources explains the fractionation pattern of polychlorinated biphenyls in the Northern Hemisphere

Harald von Waldow*, Matthew MacLeod*, Kevin Jones‡,
Martin Scheringer* and Konrad Hungerbühler*

*Institute for Chemical and Bioengineering, ETH Zürich
‡Lancaster Environment Centre, Lancaster University

Reproduced with permission from:
Environmental Science & Technology
Submitted for publication, April 2010

Abstract

The *global distillation hypothesis* states that fractionation patterns of persistent semivolatile chemicals in the environment are determined by differences in the effect of varying environmental temperature on the temperature-dependent phase partition coefficients of different chemicals. Here, we a use model experiment and an analysis of monitoring data for polychlorinated biphenyls (PCBs) to explore an alternative hypothesis, the *differential removal hypothesis*, which proposes that fractionation results from different loss rates from the atmosphere, acting along a gradient of remoteness from emission sources. Our model calculations for a range of PCB congeners demonstrate that fractionation occurs with distance from sources, regardless of the temperature gradient. We have assembled two independent datasets of PCB concentrations in European air that show fractionation, and quantified the remoteness of monitoring sites from PCB sources using the remoteness index, RI. Regression analysis of these empirical data against RI and temperature demonstrates that RI determines fractionation patterns. Based on this result, we calculate empirical effective residence times in air for a set of PCB congeners from the relationship between measured concentrations and RI. These empirical effective residence times agree well with values calculated by a multimedia mass balance model. Our conclusion from both our model experiment and analysis of monitoring data is that temperature is not a driver of the fractionation of PCBs, but rather that fractionation reflects differential removal from the atmosphere by deposition processes.

4.1 Introduction

The long-range transport of persistent organic chemicals in the global environment is recognised as a major environmental problem. Of particular concern is the presence of toxic organochlorines in environmental media and biota in ecosystems far away from the emission sources, especially in the Arctic (Scheringer, 2009). Accordingly, the potential of a chemical to undergo long range transport

(LRTP) is important in the assessment of environmental pollutants and constitutes one of the four screening criteria used to identify new persistent organic pollutants (POPs) in the Stockholm Convention (UNEP, 2001).

If two chemicals are emitted in equal amounts from the same source, the chemical causing higher environmental exposure in remote locations has a greater LRTP. The relative LRTPs of a set of chemicals that were emitted as a mixture from the same source are therefore related to the shift in the mixture composition observed along the transport pathway. These compositional shifts have been observed in the field, mainly for PCBs (e.g. Meijer et al., 2003; Ockenden et al., 2003; Shen et al., 2006), and that phenomenon is referred to as *global fractionation* (Scheringer, 2009). In other words, *global fractionation* is an observable manifestation of differing LRTPs.

The dominant paradigm to explain global fractionation patterns is the *global distillation hypothesis* or *cold condensation hypothesis* (Wania and Mackay, 1993, 1996). It states that global fractionation patterns of semivolatile organic compounds (SVOCs) are determined by the latitudinal structure of global temperature zones interacting with temperature-dependent partitioning of SVOCs between the atmosphere and water, soil and vegetation on the Earth's surface. The temperature dependence of this partitioning is largely determined by the substance's volatility (MacLeod et al., 2007). Thus, the hypothesis is that SVOCs of differing volatility "environmentally condense", i.e. partition from the gas into condensed phases, at specific ranges of temperature or latitude (Wania and Mackay, 1996). However, it is intuitively evident that fractionation of chemical pollutants can also result from the competition between removal processes and transport in the atmosphere. Removal of pollutants from the atmosphere occurs by chemical reactions, mainly with the OH radical (Atkinson, 1990), and through deposition processes, which depend on the partition coefficients between octanol and air, K_{OA}, and between air and water, K_{AW} (Scheringer, 2009). Less persistent and less volatile chemicals are removed at a faster rate from the atmosphere than more persistent and more volatile ones. This leads to a progressive fractionation in the atmosphere with effective distance from the emission source, driven by differences of overall loss rates of different chemicals. The atmospheric fractionation pattern might also be reflected in the surface compartments, because deposition fluxes are proportional to atmospheric concentrations. We refer to this alternative explanation for fractionation patterns as the *differential removal hypothesis*. It asserts that substance-specific loss rates from the atmosphere that act along a gradient of remoteness from emission sources

determine observed fractionation patterns.w

The global fractionation phenomenon is most closely associated with studies of the homologous series of PCB congeners because globally resolved emission estimates are available and indicate that sources of all congeners are highly correlated (Breivik et al., 2007). PCBs cover a wide range of volatility and of rate constants for OH radical reaction in air. Environmental concentrations of PCBs in soil (Meijer et al., 2002; Ockenden et al., 2003), air (Agrell et al., 1999; Meijer et al., 2003; Shen et al., 2006), water (Sobek and Gustafsson, 2004), cetaceans (Minh et al., 2000) and lake sediments (Muir et al., 1996) have been plotted against latitude in studies that searched for evidence of global fractionation. In most cases, a significant correlation is observed, where the decrease of concentration with increasing northern latitude or with decreasing average temperature of the sampling location differs for PCBs with different volatilities. Generally, more volatile PCBs exhibit shallower (less negative) regression slopes than less volatile congeners. The observed patterns are usually interpreted as support for the *global distillation hypothesis* and this interpretation of concentration - latitude trends is also prevalent in modelling studies (Wania and Su, 2004; Scheringer et al., 2000).

Most of the empirical studies that show latitudinal fractionation of PCBs are based on measurement transects that cover a latitudinal range from the industrialised regions of the temperate Northern Hemisphere towards the Arctic. And, most of the modelling studies examining global fractionation rely on models that represent horizontal transport as one-dimensional eddy-diffusion in the North-South direction (Scheringer et al., 2000, 2004; Wania and Su, 2004). The latitudinal or temperature gradient in these studies thus coincides with a gradient of remoteness or distance from emission sources. Therefore, the relative contribution of the processes controlled by temperature and by remoteness to the observed fractionation patterns cannot be easily distinguished.

In this study we explore the relative importance of two mechanisms that could lead to the observed fractionation patterns of PCB congeners in the atmosphere, focussing on the region between Northern Hemisphere mid-latitudes and the Arctic: 1) the temperature dependency of phase partitioning properties acting along a gradient of environmental temperatures (*global distillation hypothesis*), and 2) the differences of average atmospheric loss rates, acting along a gradient of remoteness from sources (*differential removal hypothesis*). Atmospheric removal rate constants might also be influenced by spatially variable environ-

mental temperatures because of the temperature dependency of the OH radical reaction. This is a confounding factor for both hypotheses and our assessment will evaluate its impact.

We find strong evidence that differential removal controls the spatial patterns of PCB concentrations in air and the observed fractionation. This implies that chemical-specific removal rate constants can be calculated from concentration data measured in the field. We apply this method to datasets of PCB measurements in European air to derive atmospheric removal rate constants and their inverses, effective atmospheric residence times in air.

4.2 Methods

4.2.1 The CliMoChem experiment

In previous model experiments that examined the *global distillation hypothesis*, fractionation occurs along a gradient of decreasing temperature and concomitantly with increasing distance from emission sources (e.g. Scheringer et al., 2004; Wania and Su, 2004). To isolate the effects of temperature and distance from sources, we used CliMoChem (Scheringer et al., 2000) to model the fractionation of 35 PCB congeners in the atmosphere for two different emission scenarios:

1. in the Northern Temperate Zone (CliMoChem zone 15, 45°– 48° N),

2. in the Arctic Polar Zone (CliMoChem zone 1, 87°– 90° N).

The congeners span from tetra- to octa-chlorinated biphenyls and CliMoChem was run for 100 years with the PCB mixture continuously emitted. The first experiment is similar to the experiment conducted in (Scheringer et al., 2004), whereas in the second experiment, the temperature increases with the distance from the emission source.

4.2.2 Empirical data I

In an ongoing field measurement programme, amounts of 31 PCB congeners sequestered in passive samplers exposed to air over 2-year periods at 11 remote locations along a South-North transect from southern England to northern Norway were measured (Ockenden et al., 1998b). Figure 4.1 shows the locations of the sampling sites; more information about the stations is listed in Table 4.1. Amounts of PCBs sequestered at each location during five sampling campaigns 1998–2000, 2000–2002, 2002–2004, 2004–2006 and 2006–2008 were reported by Meijer et al. (2003); Jaward et al. (2004); Gioia et al. (2006) and Schuster et al. (2010). The samplers are Standard U.S. Geological Survey semi-permeable membrane devices (SPMDs) that were deployed in Stevenson Screen Boxes, two at each site. Details about sampling method, extraction and cleanup procedure and GC-MS analysis are reported elsewhere (Meijer et al., 2003). We removed the PCB congeners 18, 22, 31, 123, 194, 199 and 203 from the dataset because they were not detected frequently enough to yield robust estimates of mean concentrations. We removed the data for hexa- and hepta-chlorinated congeners measured at sites 7 and 8 during the 1998—2001 campaign, because these values were considered outliers in the original study (Meijer et al., 2003). We calculated concentrations in air, C_{air}, from the SPMD-sequestered amounts, m_S, according to

$$C_{\text{air}} = \frac{m_{\text{S}}}{V_{\text{S}} K_{\text{SA}}} \left(1 - \exp\left(\frac{-R_{\text{S}}}{V_{\text{S}} K_{\text{SA}}} t\right)\right)^{-1} \tag{4.1}$$

based on the description of SPMD chemical uptake from the air as flux across a bottleneck boundary (Huckins et al., 2006). $V_S = 4.525 \times 10^{-6}$ m^3 is the SPMD volume (Meijer et al., 2003; Jaward et al., 2004; Gioia et al., 2006) and $t = 730$ d is the length of the sampling period. We calculated the SPMD-air partition coefficient, K_{SA}, from the relationship given by Shoeib and Harner (2002):

$$\log K_{\text{SA}} = 0.8113 \log K_{\text{OA}} - 4.8367 \tag{4.2}$$

and the apparent air sampling rate, R_{S} [m^3/d], was calculated according to the empirical relationship given by Huckins et al. (2006):

$$\log R_{\text{S}} = 0.154 \log K_{\text{OA}} - 0.80 \tag{4.3}$$

In equations 4.2 and 4.3 we used temperature-corrected $\log K_{\text{OA}}$ values calculated from K^0_{OA} at standard temperature T_0 for the average annual temperatures

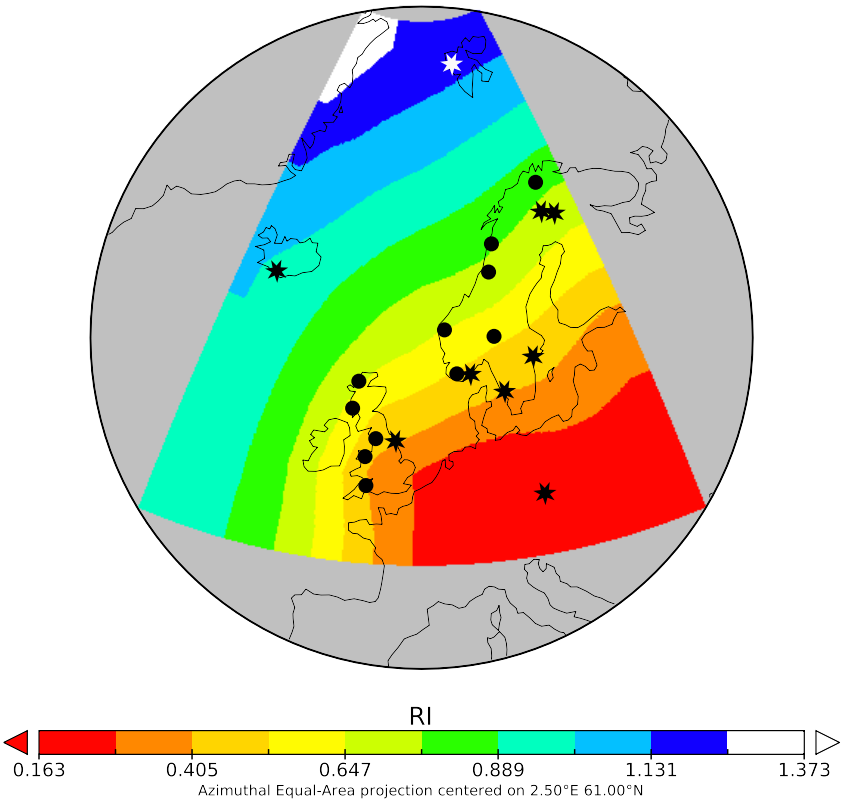

Figure 4.1: Map of measurement locations. Circles mark the TRANS - SPMD sites, and the stars mark the EMEP - HiVol sites. The colour scale represents the remoteness index, RI, which is a measure of the effective distance from PCB emission sources.

at the sampling sites, $\overline{T}_i$, according to Schwarzenbach et al. (2003):

$$\ln K_{OA}(\overline{T}_i) = \ln K^0_{OA} + \frac{\Delta U_{OA}}{R}\left(\frac{1}{T_0} - \frac{1}{\overline{T}_i}\right) \quad (4.4)$$

where ΔU_{OA} is the internal energy of octanol-air transfer and $R = 8.3145\,JK^{-1}mol^{-1}$ is the gas constant. To apply the empirical equations 4.2 and 4.3, we employed the $\log K_{OA}$ and ΔU_{OA} values used by the respective researchers. Background information about the derivation of atmospheric concentrations from SPMD-sequestered amounts is given in section 4.6.

To derive representative average long-term concentrations, we conducted for all locations a regression analysis of the logarithmized concentration of each congener in air vs. time. The absolute residuals of the the 2002–2004 campaign were significantly higher than for other years, which indicates that these data are less representative of the long-term conditions between 1998–2008 than those measured in the other four campaigns (Figure 4.4). We therefore dropped the 2002–2004 campaign from the dataset. To calculate for each location a robust estimate of concentrations representative for the whole period, we first replaced the 8% of the data that were missing values with predictions from the regression model of log-concentration vs. time and then calculated geometric mean concentrations for each congener at each location. More detailed information about the time trend analysis is provided in section 4.6. The final dataset consists of 264 values representing the average air concentrations between 1998 and 2008 of PCBs 28, 44, 49, 52, 70, 74, 87, 90/101, 95, 99, 105, 110, 118, 138, 141, 149, 151, 153/132, 158, 170, 174, 180, 183 and 187 at 11 locations. We refer to this dataset as "TRANS".

4.2.3 Empirical data II: EMEP stations

In the data of PCB concentrations in air available from the European Monitoring and Evaluation Programme (EMEP) we identified the longest sequence of years in which there is a complete and continuous record of the seven routinely measured congeners, PCBs 28, 52, 101, 118, 138, 153 and 180, at the maximum number of EMEP stations. That is the case for the years 2004—2006 and the nine stations CZ0003R, FI0036R, FI0096G, GB0014R, IS0091R, NO0001R, NO0042G, SE0012R and SE0014R. The location of these EMEP stations is depicted in Figure 4.1 and more information about the stations is listed in Table 4.2. We obtained

the annual averages of total concentrations of each PCB congener in air and on aerosol particles, determined in samples collected with high volume air samplers from the EMEP Chemical Coordinating Centre (EMEP, 2009). We refer to this dataset as "EMEP".

4.2.4 Remoteness index and temperature data for measurement locations

To quantify the remoteness of measurement locations from PCB emission sources, we use the *remoteness index*, RI (von Waldow et al., 2010). For a particular spatially distributed emission source, RI is a function of location only and is independent of substance properties. RI is defined as a fitting parameter of an empirical equation for atmospheric log-concentrations, $\ln(C_{i,j})$, of a hypothetical tracer substance, j, at location i:

$$\ln(C_{i,j}) = f(RI_i, \tau^j_{\text{eff}}, \vec{\vartheta}) \tag{4.5}$$

where τ^j_{eff} is the effective atmospheric residence time of substance j, and $\vec{\vartheta}$ is an emission scenario specific parameter vector. We used an atmospheric tracer transport model to calculate the spatially resolved atmospheric concentrations at steady-state of a set of hypothetical tracers with differing atmospheric residence times; we used the "high" emission scenario of the sum of 22 PCB congeners reported by Breivik et al. (2007) as boundary condition for the transport model. The details of the tracer transport model and the fitting procedure of equation 4.5 are given in (von Waldow et al., 2010). Here we implemented three modifications:

1. We used an atmospheric tracer transport model that includes two atmospheric layers, one representing the planetary boundary layer between the surface and a height of 850 hPa, and one representing the free troposphere between 850 hPa and 100 hPa.

2. Instead of considering the whole globe, we restricted the geographical area of the concentrations that were considered in the fitting procedure, to an area that encompasses all measurement locations described below, i.e. between 48° and 80° northern latitude and between 23° western and 28° eastern longitude (Figure 4.1).

3. Within this restricted geographical area, the explicit form of equation 4.5 could be simplified compared to that utilised in (von Waldow et al., 2010). The explicit form of equation 4.5 used to derive the RI values used in this study is:

$$\ln(C_{i,j}) = \vartheta_0 - RI_i \left(\vartheta_1 - \ln\left(\tau_{\text{eff}}^j\right)\right) \tag{4.6}$$

The quality of the fit is better than for the fit considering the whole globe as reported in (von Waldow et al., 2010). The emission-scenario- specific fitting parameter ϑ_1 equals 5.98 for the modified procedure and for τ_{eff} given in units of days. The numerical value of ϑ_0 depends on arbitrarily selected units, and will not be used here. Figure 4.1 shows the distribution of RI calculated by this procedure for the study area.

We calculated the average annual temperatures in the study area $\overline{T}_i$ at 2 m height from the monthly mean temperature of the ERA-Interim reanalysis dataset for the years 1998–2008 (Berrisford et al., 2009).

4.2.5 *RI* and temperature as explaining variables for the spatial variation of PCB concentrations in air

We plotted $\ln(C)$ of all congeners separately against RI and against $\overline{T}$ for TRANS (Figures 4.9 and 4.10) and for EMEP (Figures 4.11 and 4.12). Both RI and $\overline{T}$ are, individually, well correlated with measured log-concentrations.

To compare the relative power of RI_i and $\overline{T}_i$ to explain $\ln(C_{i,j})$ for PCB congeners j at locations i, we used both variables as covariates in a nested multiple regression model that we fitted separately to each dataset, TRANS and EMEP.

$$\ln(C_{i,j}) = \alpha_j + \beta_j RI_i + \gamma_j \overline{T}_i + \epsilon \tag{4.7}$$

α_j, β_j and γ_j are the congener-specific regression parameters intercept, effect of remoteness, and effect of temperature, respectively, and ϵ is the error term.

4.2.6 Effective residence times τ_{eff}

We fitted ordinary linear regression models

$$\ln(C_{i,j}) = \alpha_j + \beta_j RI_i + \epsilon_j \tag{4.8}$$

separately for each congener j for both datasets. The regression coefficient estimates $\widehat{\beta}_j$, serve as estimates for the derivative $\mathrm{d}\ln(C_j)/\mathrm{d}RI$. From the definition of the remoteness index (equation 4.6) follows that this derivative can be used to calculate the logarithmized effective atmospheric residence time of substance j:

$$\ln(\tau_{\text{eff}}^j) = \vartheta_1 + \frac{\mathrm{d}\ln(C_j)}{\mathrm{d}RI} = 5.98 + \widehat{\beta}_j \tag{4.9}$$

The difference of the regression models in equation 4.8 from the model in equation 4.7 is firstly that the term $\gamma_j \overline{T}_i$, which turned out to be not significant (see section 4.4), was dropped. Secondly, the error variance was estimated separately for each congener, as opposed to the previous regression model, where the variance is pooled.

Finally, to examine the relationship of τ_{eff} to substance properties, we built a regression model aiming to explain $\ln(\tau_{\text{eff}})$ as a function of the physicochemical substance properties $\log K_{\text{OA}}$, $\log K_{\text{AW}}$ and the log-rate constant for removal from the atmosphere by reaction with OH radicals, $\log(k_{\text{reac}})$. We used $\log(k_{\text{reac}})$ values extrapolated for all congeners from the data reported by Anderson and Hites (1996) and partitioning properties and internal energies of phase change calculated with the QSPR regressions by Schenker et al. (2005). All substance properties were temperature corrected to 6.4 °C, the mean temperature of the region and time span under consideration. Since the variance $\sigma^2(\widehat{\beta}_j)$ of the coefficient estimates from equation 4.8 varies among congeners j, the derived effective residence time τ_{eff}^j is known with a different precision for each congener. To account for that, we performed a weighted regression of $\ln(\tau_{\text{eff}})$ vs. chemical properties with the weights $\omega_j = \left(\sigma^2(\widehat{\beta}_j)\right)^{-1}$ for each congener j.

4.3 Modelling Results

Figure 4.2 displays the atmospheric fractionation of the PCB mixture, modelled with CliMoChem, after 100 years of continuous emissions from the Northern

Temperate Zone (a) and from the North Pole (b) as a function of latitude. The fraction of each homologue is quantified as $\ln(C^{\text{hom}}/C^{\text{PCB118}})$, where C^{hom} is the average homologue concentration and C^{PCB118} is the concentration of PCB-118, which we use as a reference substance. For the emission in the Northern Temperate Zone (a) we observe the typical pattern of global fractionation reported for similar experiments and measurement data (Scheringer, 2008), characterised by an increasing fraction of tri-, tetra- and penta-chlorinated PCBs and a decreasing fraction of hepta-, octa- and nona-chlorinated congeners with increasing latitude.

The fractionation pattern resulting from emissions at the North Pole (b) is almost identical, qualitatively and quantitatively, albeit with a reversed x-axis that runs from north to south, i.e. from high latitudes to low latitudes, and from a colder environment to a warmer one. According to this model experiment, the fractionation pattern occurs as as a function of distance from the emission source regardless of the temperature gradient.

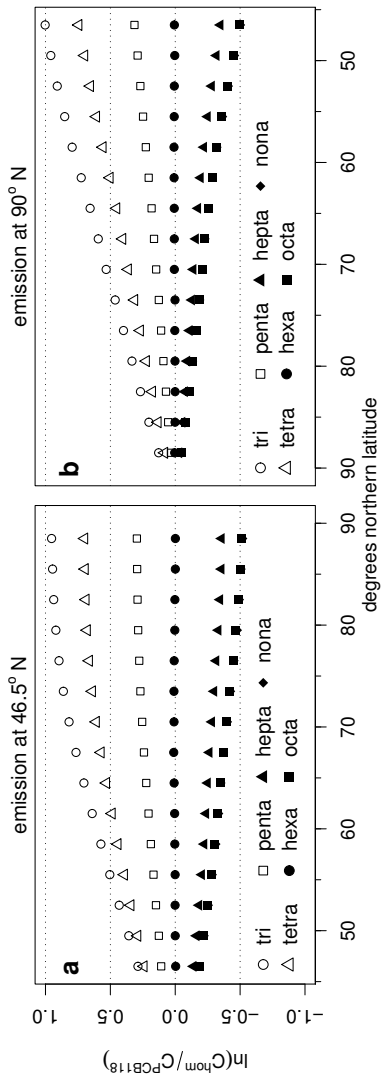

Figure 4.2: Fractionation of a PCB mixture after 100 years of continuous emissions in the Northern Temperate Zone (a) and at the North Pole (b).

4.4 Empirical Results

To examine the relevance of each explanatory variable, RI and $\overline{T}$, if both are taken into account as possible explanans, we fitted multiple regression models (equation 4.7), separately for TRANS and EMEP. They fit very well for TRANS ($R^2 = 0.9503$) and for EMEP ($R^2 = 0.847$). Temperature $\overline{T}$ has no significant effect on $\ln(C)$ in either dataset ($p = 0.86$ for TRANS and $p = 0.99$ for EMEP). That indicates that neither the temperature dependency of partitioning properties nor the temperature dependency of removal rate constants from the atmosphere by reaction with OH radicals contributes to the explanation of the observed concentration patterns. The effect of RI, in contrast, is highly significant ($p < 10^{-27}$ for TRANS and $p < 10^{-3}$ for EMEP). The estimated coefficients $\widehat{\beta}_j$ are negative ($-6.89 \leq \widehat{\beta}_j \leq -2.27$ for TRANS and $-3.81 \leq \widehat{\beta}_j \leq -0.097$ for EMEP) and their correlation with degree of chlorination is negative, with Spearman's $\rho = -0.74$ for TRANS and $\rho = -0.75$ for EMEP, and significant ($p = 2.7 \times 10^{-5}$ and $p = 0.027$). The negative sign of the $\widehat{\beta}_j$ means that concentrations decrease with increasing remoteness. This is in concordance with the *differential removal hypothesis*. The negative correlation of the $\widehat{\beta}_j$ with the degree of chlorination means that the decrease of concentrations per unit RI is greater for heavier PCB congeners than for lighter ones.

Thus, the multiple regression analysis does not support the *global distillation hypothesis*, but indicates that remoteness from emission sources, measured as RI, determines observed fractionation of PCB congeners in European air.

Since, according to our regression analysis, the effect of $\overline{T}$ on PCB concentrations is not significant, we can use equations 4.8 and 4.9 to estimate τ_{eff} for each congener from field measurement data and RI. Before fitting the regression model of equation 4.8, we dropped site 3 (Hazelrigg) from the TRANS dataset, because it is an outlier with unusually high concentrations (Figure 4.13a). The reason might be that this location is relatively close to the city of Lancaster, whereas the other locations are far away from potential local PCB sources.

The results of the model fit of equation 4.8 along with the derived values for logarithmized atmospheric residence times for TRANS, $\ln(\tau_{\text{eff}}^{\text{TRANS}})$, and EMEP, $\ln(\tau_{\text{eff}}^{\text{EMEP}})$, and the associated 95% confidence intervals (CI) are reported in Table 4.3. The estimated medians of $\tau_{\text{eff}}^{\text{TRANS}}$ range from one day for PCB-170 to 80 days for PCB-28 and the medians of $\tau_{\text{eff}}^{\text{EMEP}}$ range from 13 (PCB-138) to 189 days (PCB-

28). The CI for the five congeners common to TRANS and EMEP overlap, but $\ln(\tau_{\text{eff}}^{\text{TRANS}})$ is systematically lower than $\ln(\tau_{\text{eff}}^{\text{EMEP}})$, with an average difference of 1.44.

For comparison, we also calculated effective residence times, $\tau_{\text{eff}}^{\text{ELPOS}}$, from characteristic travel distances reported by Beyer et al. (2003), based on calculations with the ELPOS model for Europe at 5 °C. Those values are also included in Table 4.3. Figure 4.15 shows that $\tau_{\text{eff}}^{\text{ELPOS}}$ differs by factor 2 and 0.5 from $\tau_{\text{eff}}^{\text{TRANS}}$ and $\tau_{\text{eff}}^{\text{EMEP}}$, respectively.

To determine the substance properties that control τ_{eff}, we considered $\log K_{\text{OA}}$, $\log K_{\text{AW}}$ and $\log(k_{\text{reac}})$ as explaining variables. In the regression analysis $\log K_{\text{AW}}$ has no significant effect on $\ln(\tau_{\text{eff}})$, if $\log K_{\text{OA}}$ is considered at the same time as an explaining variable ($p = 0.2$ for both datasets). Since $\log K_{\text{OA}}$ and $\log(k_{\text{reac}})$ are highly correlated ($r < -0.96$ for both datasets), only one of them can be included in the same regression model. $\log(k_{\text{reac}})$ is positively correlated with $\ln(\tau_{\text{eff}})$ ($r = 0.89$ for TRANS and $r = 0.97$ for EMEP). This is not a causal relationship, because it would imply that higher degradation rate constants cause a longer residence time in air. Therefore, $\log K_{\text{OA}}$ remains as explaining variable and indicates that deposition processes dominate the differential removal of PCBs from the atmosphere in the area of study. Figure 4.3 shows the regression results of $\ln(\tau_{\text{eff}})$ on the temperature-corrected $\log K_{\text{OA}}$ for EMEP (a) and TRANS (b). Both relationships are strong, with $R^2 = 0.88$ for EMEP and $R^2 = 0.92$ for TRANS. The estimated regression slope of -1.1 (CI $= [-1.6, -0.6]$) for EMEP is not significantly different from -1, however the slope of -1.4 (CI $= [-1.5, -1.2]$) for TRANS is. If removal from the atmosphere were indeed controlled by deposition processes dependent on K_{OA}, an atmospheric residence time inversely proportional to K_{OA} would be expected, because those deposition fluxes are proportional to K_{OA} (Wania and Mackay, 1995; Scheringer, 1996). This is in concordance with the relationship between $\log K_{\text{OA}}$ and $\ln(\tau_{\text{eff}})$ for EMEP but not for TRANS.

4.5 Discussion

Our first main finding is that, for PCBs in temperate to polar latitudes, temperature is not a driver of the fractionation process. This is demonstrated in our analysis of field data and by the CliMoChem experiment that yields the same

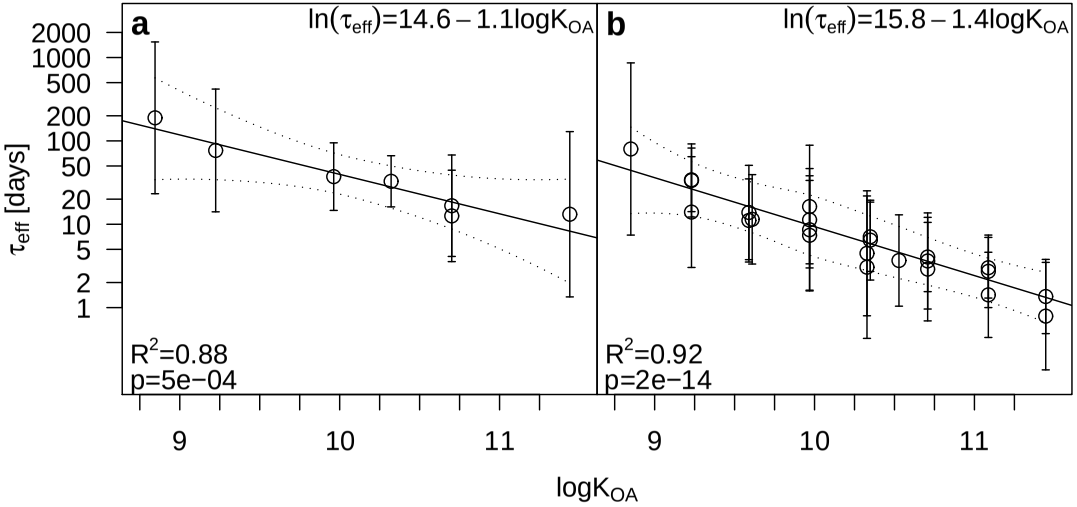

Figure 4.3: The estimated median of the effective residence time in air, τ_{eff}, on a log scale versus temperature corrected $\log K_{\text{OA}}$ for EMEP (a) and for TRANS (b). The error bars indicate the 95% confidence interval for the estimate of $\ln(\tau_{\text{eff}})$. The dotted lines mark the smoothed 95% prediction intervals of the regressions. The x-axis positions in (b) are slightly scattered around the real $\log K_{\text{OA}}$ values to improve readability.

fractionation pattern independent of the direction of temperature gradient. The CliMoChem experiment also demonstrates that previous modelling results were often mis-interpreted because the correlation of temperature with remoteness was overlooked.

In the analysis of the PCB field data, we assumed a linear relationship between $\ln(C)$ and both RI and temperature. Under this assumption, we demonstrated that RI explains fractionation patterns better than $\overline{T}$. When we remove the assumption of a linear relationship between $\ln(C)$ and RI and $\overline{T}$, we can assess the strength of the monotonic relationship between $\ln(C)$ and RI and $\overline{T}$ using Spearman's rank correlation coefficient, ρ. Figure 4.14 shows a comparison of ρ for all congeners and both datasets. Only for four congeners out of 24 in TRANS and for two out of seven in EMEP is there a slightly better rank-correlation of $\ln(C)$ with $\overline{T}$ than with RI.

In conclusion, our analysis supports the *differential removal hypothesis* and not the *global distillation hypothesis* to explain patterns of PCB fractionation in the Northern Hemisphere. The interpretation of modelling and empirical data for PCBs as supporting the *global distillation* hypothesis appears to be erroneous, and stems from overlooking the correlation of temperature with remoteness gradients.

Our second main result is the derivation of τ_{eff} from concentrations measured in the field. The two sets of PCB concentrations measured at different locations with different sampling methods and analysed in different laboratories yield two sets of effective residence times that differ from each other by a factor of four. It is unlikely that this difference between $\tau_{\text{eff}}^{\text{TRANS}}$ and $\tau_{\text{eff}}^{\text{EMEP}}$ is caused by a systematic error in the calculation of RI, since the geographical coverages of TRANS and EMEP overlap (Figure 4.1). One possible explanation could be a systematic, temperature-related error in the calculation of air concentrations from SPMD sequestered amounts of chemicals. If, for example, SPMD uptake was slower at lower temperatures, or during periods when the triolein is frozen (below -4° C), air concentrations in colder environments would be underestimated. Since colder environments correspond to increasing RI in our dataset, the underestimated concentrations occur at locations with high RI; in other words, the slope of $\ln(C)$ vs. RI would be too steep. This, in turn, would imply too low values of $\tau_{\text{eff}}^{\text{TRANS}}$ (equation 4.9). However, considerable uncertainty surrounds the mechanisms of chemical sequestration by SPMDs from air, and we summarise the sources of this uncertainty in section 4.6. To determine reli-

able values for τ_{eff} from passive sampling, the gaps in current knowledge about the correct characterisation of passive samplers with respect to environmental variables such as temperature needs to be addressed.

Another question concerns the relationship of τ_{eff} and $\log K_{\text{OA}}$. For the EMEP data, this relationship has a slope of -1, as expected, but for the TRANS data, the slope is steeper than -1. This finding may be related to the fact that SPMDS only sample the gas-phase and not the particle-sorbed fraction. That fraction can be high for heavier congeners and it might increase with decreasing temperature and, consequently, with increasing RI. If this fraction is underrepresented in the SPMD samples from locations with high RI, $\tau_{\text{eff}}^{\text{TRANS}}$ is systematically underestimated for heavier PCBs, which leads to a relationship in Figure 4.3b that is too steep.

Finally, our relationship between concentrations measured in the field and τ_{eff} makes it possible to evaluate estimates of τ_{eff} derived from multimedia mass balance models against the empirical record. Established metrics for the LRTP in air, the CTD (Bennett et al., 1998) and the Spatial Range (Scheringer, 1997), rely on model calculations and are expressions of a modelled τ_{eff} (Bennett et al., 2001). Thus, fate- and transport models can be evaluated with respect to an important end-point of their application. However, the comparison of field-derived and model-based τ_{eff} is only valid if the region described by the model is similar to the region where the field measurements were made. For our two data sets, this is the case for the ELPOS model, and comparison of τ_{eff} from the model and from the two empirical data sets shows good agreement except for PCB-28. This is because in ELPOS at 5 °C, degradation in air dominates over deposition processes for tri-chlorinated PCBs (Beyer et al., 2003) and leads to a shorter modelled τ_{eff} for PCB-28. We interpret the general agreement of modelled and field-derived τ_{eff} values as a confirmation of the way in which the effective removal rate constant from air is parameterised in ELPOS. However, the discrepancy observed for PCB-28 is an indication that for lighter PCBs in temperate and cold environments, degradation by OH radicals is slower than assumed in the model. This, in turn, may have implications for the hemispheric mass budget of lighter PCBs, as discussed by Axelman and Gustafsson (2002).

Acknowledgements

We thank Jasmin Schuster for providing as yet unpublished data and for fruitful discussions about the intricacies of SPMD sampling.

4.6 Supporting information

4.6.1 Measurement locations

Tables 4.1 and 4.2 list the geographical locations of the TRANS and EMEP sites, respectively, the annual mean temperatures at the sites, calculated from the years 1998–2008 of the ERA-Interim reanalysis dataset (Berrisford et al., 2009), and the sites' RI values; RI is a measure of the effective distance from PCB emission sources.

station	latitude	longitude	location	RI	$\overline{T}$[°C]
1	50.75	−3.48	North Wyke	0.424	10.99
2	52.42	−4.06	Aberystwyth	0.450	10.44
3	54.03	−2.78	Hazelrigg	0.45	9.54
4	56.10	−6.17	Colonsay	0.629	9.70
5	58.05	−5.02	Ullapool	0.661	8.66
6	58.55	6.35	Ergesund	0.52	6.75
7	61.25	11.83	Rena	0.583	3.27
8	61.28	5.03	Askvoll	0.644	7.08
9	64.98	13.60	Røyvik	0.727	2.03
10	67.38	14.67	Bødo	0.797	3.94
11	69.83	25.03	Lakselv	0.808	0.60

Table 4.1: TRANS stations

station	latitude	longitude	location	m.a.s.l.	RI	$\overline{T}$[°C]
CZ0003R	49.58	15.08	Kosetice	534	0.216	8.32
FI0036R	68.00	24.25	Pallas/Matorova	340	0.742	0.79
FI0096G	68.00	24.15	Pallas/Särkijärvi	340	0.742	0.78
GB0014R	54.33	−0.81	High Muffles	267	0.444	10.11
IS0091R	63.40	−20.28	Storhofdi	118	0.990	5.93
NO0001R	58.38	8.25	Birkenes	190	0.509	7.28
NO0042G	78.90	11.88	Spitsbergen	474	1.154	−3.81
SE0012R	58.80	17.38	Aspvreten	20	0.464	7.43
SE0014R	57.39	11.91	Råö	5	0.443	8.50

Table 4.2: EMEP stations

4.6.2 Calculation of air concentrations from SPMD data

Deriving airborne-concentrations from SPMD-sequestered contaminant mass is fraught with uncertainties. In recent publications (Gioia et al., 2006; Moeckel et al., 2009) the loss of depuration compounds (carbon-13 labelled PCB congeners) was used for the calculation of air concentrations from SPMD sequestered amounts by inferring apparent effective air sampling rates, R_S, from the loss rates of the depuration compounds and use it in equation 4.1. For the three most recent sampling campaigns considered in this study, depuration compound loss data is available. However, an assumption for the depuration compound method presented by Moeckel et al. (2009) is that the SPMD uptake is air-side controlled. R_S can be expressed as $R_S = V_S k_0$, where k_0 is the bulk mass-transfer coefficient (MTC) across the interface and V_S is the SPMD volume. If the SPMD-air interface is described as a multilayer bottleneck boundary, k_0^{-1} is obtained as $k_0^{-1} = (k_s K_{SA})^{-1} + k_a^{-1}$, where k_s is the bulk MTC across the membrane and into the triolein, k_a is the MTC across the gas-phase laminar boundary layer, and K_{SA} is the bulk partition coefficient between SPMD and air. SPMD uptake is air-side controlled if $(k_s K_{SA})^{-1} \ll k_a^{-1}$ and vice versa. Under the conditions encountered here, k_a is temperature- and substance independent and therefore R_S should not vary for different ambient temperatures and different PCB congeners if uptake was indeed air-side controlled. Empirical evidence, however, suggests an increase of R_S with decreasing temperature, even if the temperature dependency of $\log K_{OA}$ is accounted for, and an increase of R_S at constant temperature for a sequence of PCBs with increasing $\log K_{OA}$ (Ockenden et al., 1998a). This evidence therefore indicates membrane-side control of the uptake with faster uptake for higher $\log K_{OA}$.

It has been suggested that k_S decreases with decreasing temperature, as the frequency of transient cavity formation in the non-porous SPMD membrane made of low-density polyethylene is temperature controlled (Huckins et al., 2006). In the case of membrane-side-controlled uptake, this effect would counteract the temperature effect on R_S described above. Huckins et al. (2006) summarise and quantitatively evaluate the available evidence and suggest that SPMD uptake of PCBs from air is partly membrane-side controlled and partly air-side controlled. The literature contains only vague speculations about the effect of the freezing of triolein (at $-4°C$) on SPMD uptake mechanisms. Levy et al. (2009), measuring organochlorine pesticides in the Alps with SPMDs and HiVol samplers, reported a correlation of air sampling rates with the number of days above $-4°$ C during

the sampling period. Apart from temperature, the air-flow conditions around the SPMD can influence R_S. However, the sampler deployment in Stevenson Screen Boxes is thought to equalise different wind conditions at different sites (Ockenden et al., 2001b).

4.6.3 Time trend analysis

To exploit the availability of data for a time span of 10 years, we conducted a regression analysis of the time trends of air concentrations for all congeners at all locations.

We removed all station/congener combinations for which fewer than two values above the detection limit were recorded. We then fitted a nested analysis of covariance model aimed at predicting the logarithmized concentration $\ln(C_{i,j,t})$ of congener j at sampling location i at time t:

$$\ln(C_{i,j,t}) = \beta_i^{(0)} + \beta_j^{(1)} + \beta^{(2)}t + \beta_i^{(3)}t + \beta_j^{(4)}t + \epsilon \quad , \tag{4.10}$$

using the routine `survreg` from the `survival` package of the statistical software R (Therneau and Lumley, 2009). $\beta_i^{(0)}$ and $\beta_j^{(1)}$ are constant effects of sampling location and congener, respectively. $\beta^{(2)}$, $\beta_i^{(3)}$ and $\beta_j^{(4)}$ represent the parts of the slope $\mathrm{d}\ln(C)/\mathrm{d}t$ that are attributable to the whole dataset, to the specific station, and to the specific congener, respectively. Time t has units of years. It turned out that the congener has no effect on the rate of log-concentration decrease over time, and we dropped the last term of equation 4.10. Figure 4.4 depicts the absolute residuals of this regression with respect to the sampling campaigns as a notched box plot. The median of the absolute residuals of the 2002–2004 campaign is the largest among all campaigns and the notches of this box do not overlap with any of the notches of the other campaigns' boxes. This indicates that the median of the absolute residuals of the 2002–2004 campaign is significantly different (at the 95% level) from that of every other campaign (McGill et al., 1978), and we consequently dropped this campaign from the dataset. The effect of location on the time trend $\mathrm{d}\ln(C)/\mathrm{d}t$ could not be rejected. The rate of decline over time is significantly less negative than the mean of $\mathrm{d}\ln(C)/\mathrm{d}t = -0.084$ (with C in units of $\mathrm{pg/m^3}$) at site 1, and more negative than the mean at site 7 (Figure 4.5). However, the site-specific rates of decline are not correlated with

either RI, average annual temperature, or latitude. The mean rate of decline corresponds to an "atmospheric half-life" of $t_{0.5} = 8.25$ years. That is a significantly slower decline of atmospheric concentrations than a previous estimate of $t_{0.5} = 4.1$ years based on the same dataset, but without the 2004–2008 data (Gioia et al., 2006), and also slower than the estimated (Breivik et al., 2007) average rate of decline of primary emissions from European sources of $0.118\,y^{-1}$, corresponding to $t_{0.5} = 5.87$ years (Figure 4.6). The individual time series of emission estimates by Breivik et al. (2007) from European sources are depicted in Figure 4.7

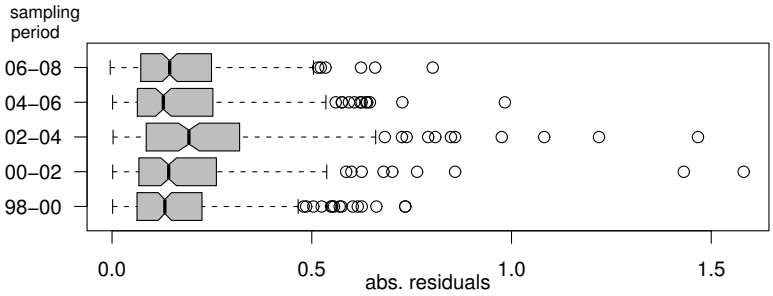

Figure 4.4: Absolute residuals of the time-trend regression for the different sampling campaigns. The absolute residuals on the x-axis have units of $\ln(C)$, with C in units of pg/m^3.

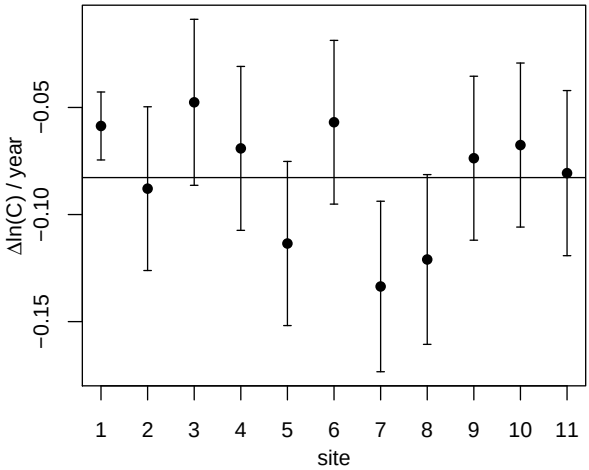

Figure 4.5: Rate constants of decline of atmospheric PCB concentrations for the TRANS sampling sites. The horizontal line marks the mean of $-0.084\,\ln(C)/\text{year}$. C has units of pg/m^3. Error bars represent 95% confidence intervals.

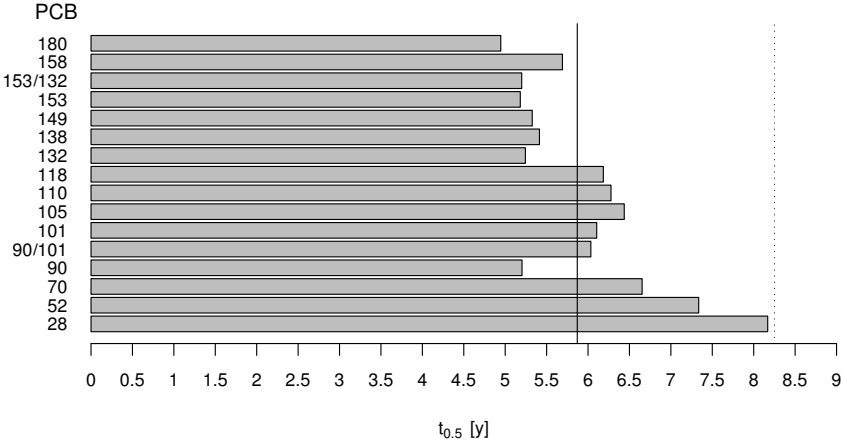

Figure 4.6: Half-lifes [y] of emission fluxes calculated from European emission estimates between 1998 and 2008 by Breivik et al. (2007). The full vertical line marks the average emission half-life, $t_{0.5}^{\text{em}} = 5.87$ y, and the dotted vertical line marks the average half-life of concentrations in the atmosphere, $t_{0.5}^{C_{\text{air}}} = 8.35$ y, calculated from the TRANS dataset.

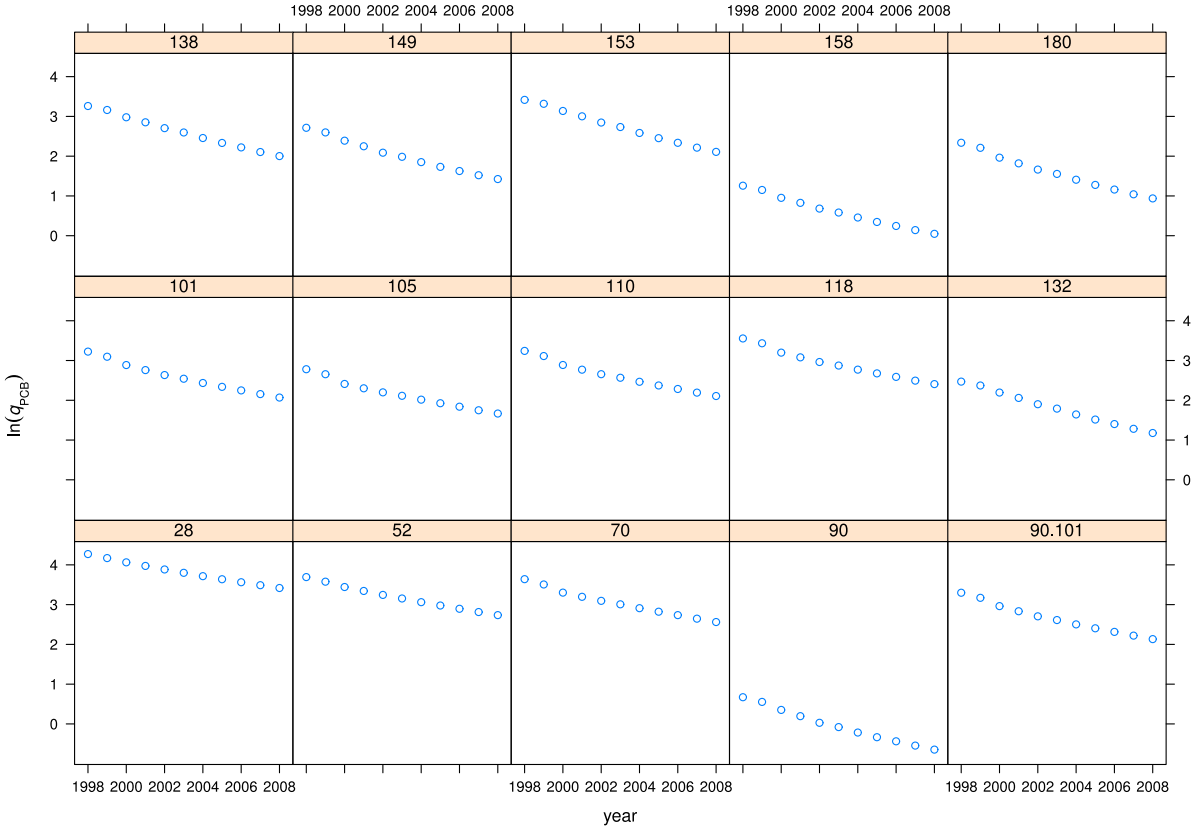

Figure 4.7: Time trends of logarithmized emission rates $\ln(q_{\mathrm{PCB}}\ [\mathrm{t/y}])$ for Europe, according to estimates by Breivik et al. (2007).

4.6.4 The CliMoChem experiment

We conducted an additional modelling experiment, similar to the one described in section 4.2.1. Figure 4.8 depicts the North-South fractionation of a PCB mixture in the atmosphere as predicted by CliMoChem, 100 years after a pulse release into air at the Arctic Circle. From the latitude of emission (67.5° N), fractionation occurs almost symmetrically northward and southward, but is even stronger towards the South, with increasing temperatures. No tendency of increased fractionation due to decreasing temperatures is evident. This result appears to contradict the *global distillation hypothesis* as well.

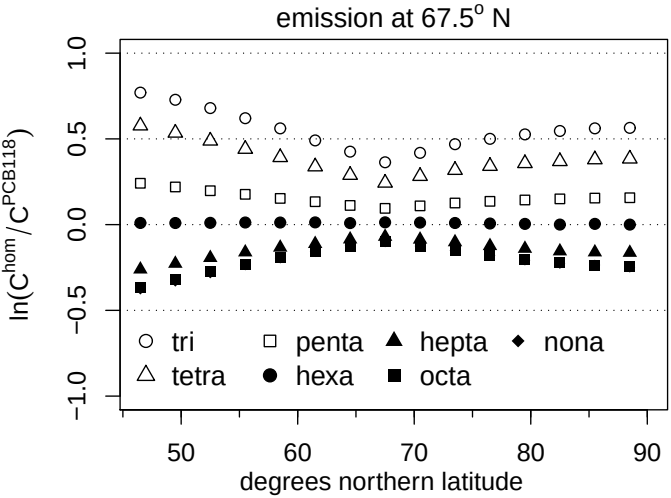

Figure 4.8: Fractionation of a PCB mixture after 100 years of continuous emissions at the Arctic Circle.

4.6.5 $\ln(C)$ versus RI and T

Figures 4.9 and 4.10 show the dependency of $\ln(C)$ on RI and T, respectively, for TRANS, and Figures 4.11 and 4.12 for EMEP. Figure 4.13 depicts the residuals of the multiple regression (equation 4.7), grouped with respect to measurement

sites for the TRANS (a) and the EMEP dataset (b). The high residuals at site 3 of the TRANS dataset led to the exclusion of this site.

4.6.6 Rank correlations

We compared Spearman's ρ between the measured log-concentrations and RI and T, respectively. The monotonic correlation measured with Spearman's ρ is stronger with RI than with T, except for PCBs 28 and 52 in the EMEP dataset and PCBs 87, 99, 110 and 118 in the TRANS dataset (4.14a). This finding is reflected in the plot of the p-values for ρ (4.14b).

4.6.7 Calculation of τ_{eff} from empirical data and comparison with modelled effective residence times in the atmosphere

Table 4.3 lists the regression results and the derived effective atmospheric residence times, τ_{eff}, for both datasets, along with τ_{eff} derived from the ELPOS model (Beyer et al., 2003). Figure 4.15 shows a comparison of $\ln(\tau_{eff}^{ELPOS})$ with the TRANS- and EMEP derived logarithmized effective residence times. The τ_{eff} for TRANS and EMEP can be considered proportional to τ_{eff}^{ELPOS}, only PCB-28 deviates from that relationship.

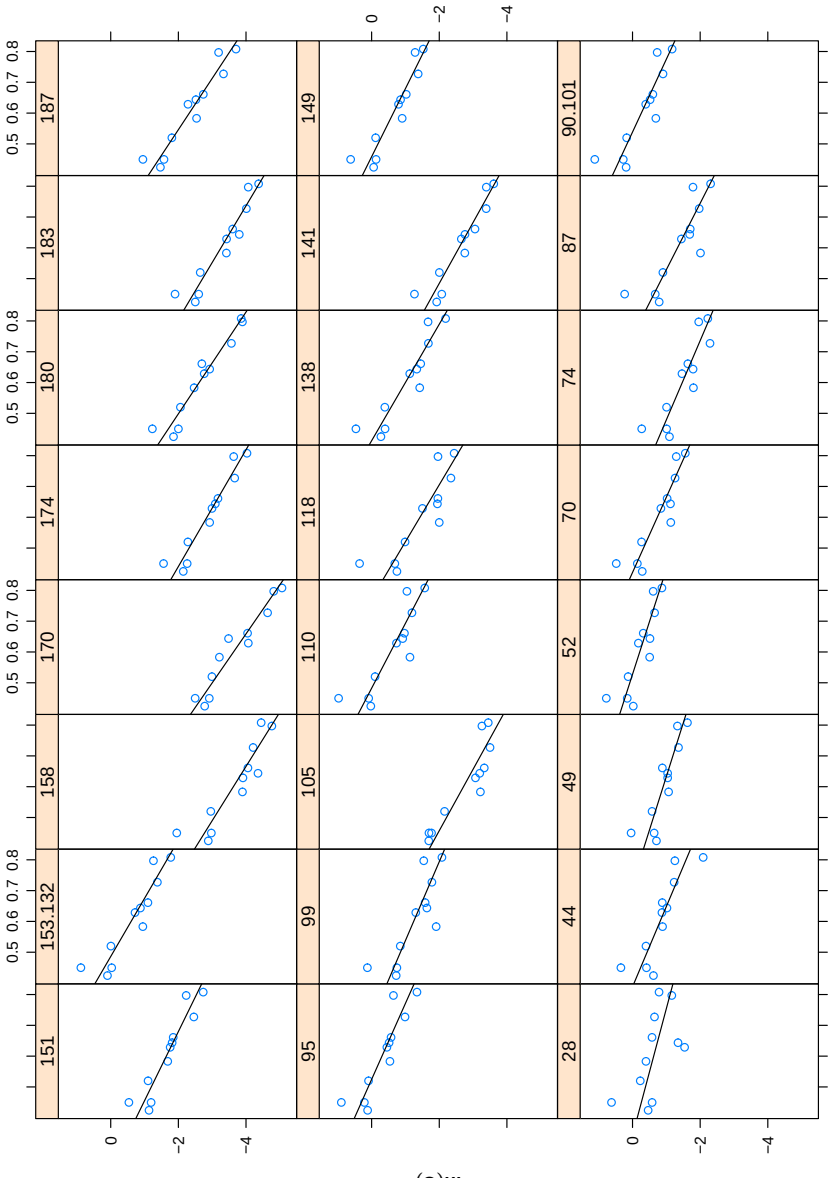

Figure 4.9: $\ln(C)$ versus RI for the TRANS dataset. C has units of pg/m^3.

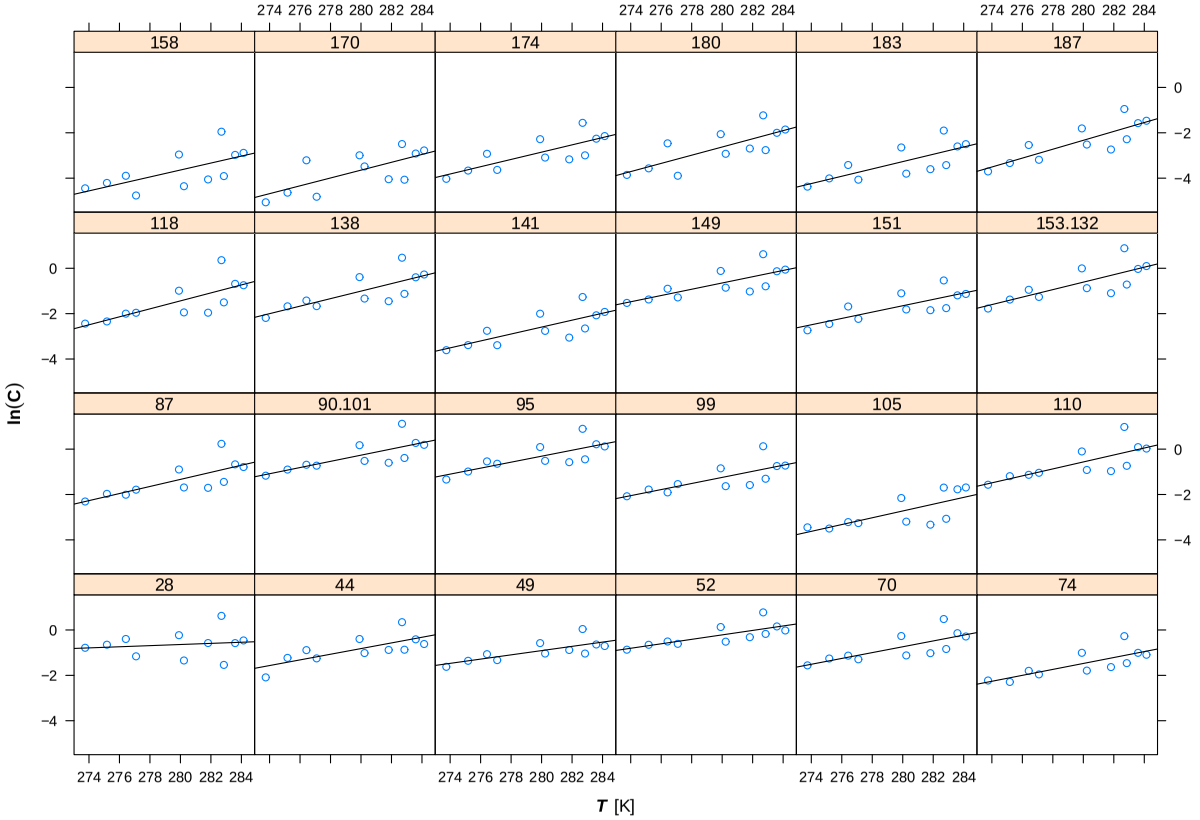

Figure 4.10: $\ln(C)$ versus T for the TRANS dataset. C has units of $\mathrm{pg/m^3}$.

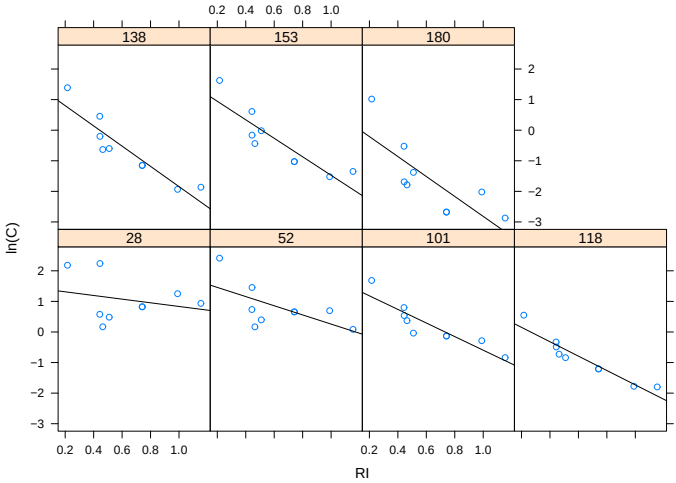

Figure 4.11: $\ln(C)$ versus RI for the EMEP dataset. C has units of $\mathrm{pg/m^3}$.

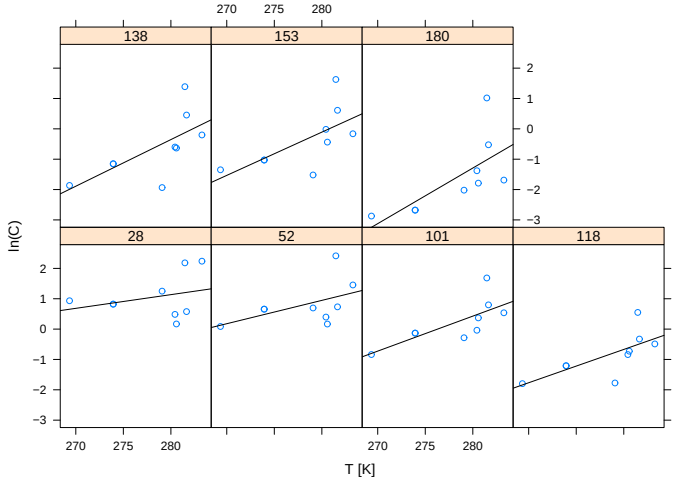

Figure 4.12: $\ln(C)$ versus T for the EMEP dataset. C has units of $\mathrm{pg/m^3}$.

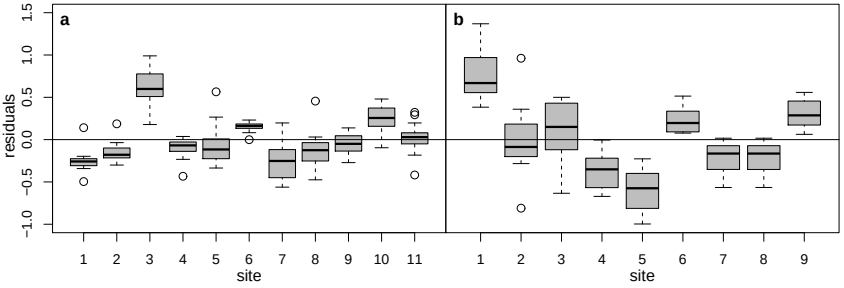

Figure 4.13: Residuals of the multiple regression of $\ln(C)$ versus RI and T of the TRANS dataset (a) and the EMEP dataset (b), grouped with respect to measurement sites. C has units of pg/m^3.

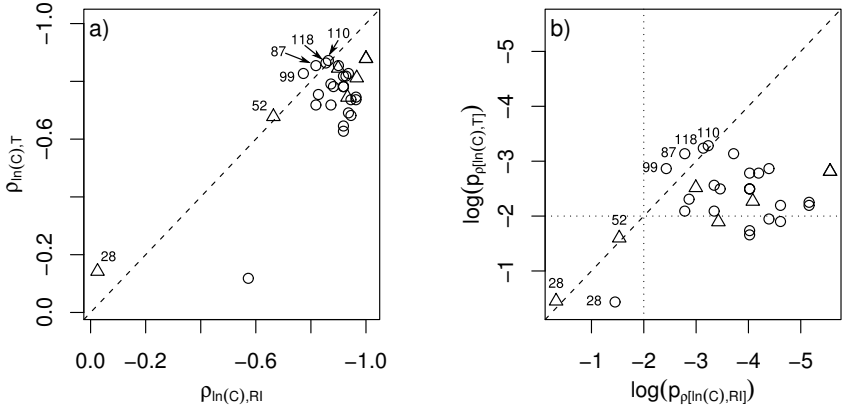

Figure 4.14: a): Comparison of Spearman's ρ between $\ln(C)$ and RI and between $\ln(C)$ and T; circles mark the TRANS dataset, triangles the EMEP dataset. b): Comparison of the p-values for ρ on a log scale; circles mark the TRANS dataset, triangles the EMEP dataset. Dotted lines in b) mark a p-value of 0.01.

PCB	DS	$\widehat{\alpha}$	$\widehat{\beta}$	$\widehat{\sigma}$	$\ln \tau_{eff}$	CI($\ln \tau_{eff}$)	τ_{eff}[d]	$\ln \tau_{eff}^{ELPOS}$	τ_{eff}^{ELPOS}[d]
28	T	0.14	−1.46	0.41	4.38	2 – 6.76	80	3.75	43
28	E	1.43	−0.6	0.75	5.24	3.15 – 7.34	189	3.75	43
44	T	1.03	−3.2	0.26	2.64	1.11 – 4.17	14	3.79	44
49	T	0.42	−2.31	0.15	3.53	2.65 – 4.41	34	NA	NA
52	T	1.12	−2.33	0.17	3.51	2.5 – 4.52	33	4.03	56
52	E	1.76	−1.5	0.6	4.34	2.65 – 6.04	77	4.03	56
70	T	1.25	−3.43	0.2	2.41	1.26 – 3.56	11	NA	NA
74	T	0.38	−3.21	0.23	2.63	1.32 – 3.93	14	NA	NA
87	T	0.78	−3.69	0.29	2.15	0.46 – 3.84	9	NA	NA
90/101	T	1.69	−3.41	0.21	2.43	1.21 – 3.64	11	NA	NA
95	T	1.66	−3.4	0.21	2.44	1.2 – 3.67	11	3.52	34
99	T	0.49	−3.05	0.29	2.79	1.1 – 4.49	16	NA	NA
101	E	1.63	−2.22	0.33	3.62	2.69 – 4.55	37	3.36	29
105	T	0.08	−4.72	0.34	1.12	−0.85 – 3.08	3	1.59	5
110	T	1.64	−3.84	0.26	2	0.48 – 3.51	7	3.14	23
118	T	1.05	−4.34	0.3	1.5	−0.23 – 3.23	4	2.06	8
118	E	0.62	−2.35	0.25	3.49	2.78 – 4.19	33	2.06	8
138	T	1.65	−4.55	0.23	1.29	−0.04 – 2.62	4	2.16	9
138	E	1.46	−3.31	0.45	2.53	1.27 – 3.8	13	2.16	9
141	T	0.01	−4.44	0.17	1.4	0.44 – 2.35	4	NA	NA
149	T	1.62	−3.88	0.17	1.96	1 – 2.91	7	NA	NA
151	T	0.69	−3.98	0.19	1.86	0.76 – 2.97	6	NA	NA
153	E	1.55	−3.03	0.5	2.81	1.41 – 4.22	17	2.34	10
153/132	T	2.03	−4.54	0.22	1.3	0.04 – 2.56	4	NA	NA
158	T	−0.86	−4.78	0.25	1.06	−0.37 – 2.49	3	NA	NA
170	T	−0.01	−6.08	0.26	−0.24	−1.72 – 1.25	1	NA	NA
174	T	−0.06	−4.74	0.14	1.1	0.26 – 1.94	3	NA	NA
180	T	0.65	−5.53	0.18	0.31	−0.72 – 1.33	1	1.76	6
180	E	0.44	−3.26	0.81	2.58	0.3 – 4.86	13	1.76	6
183	T	−0.42	−4.84	0.17	1	0 – 2	3	NA	NA
187	T	0.91	−5.49	0.2	0.35	−0.82 – 1.53	1	NA	NA

Table 4.3: Regression results for equation 4.8 and τ_{eff} derived from equation 4.9. DS indicates the dataset, T stands for TRANS and E for EMEP. $\widehat{\alpha}$ and $\widehat{\beta}$ are the estimates of the regression coefficients, and $\widehat{\sigma}$ is the estimate of the standard error. $\ln \tau_{eff}$ is the logarithmized effective residence time calculated from $\widehat{\beta}$ (equation 4.9), CI($\ln \tau_{eff}$) indicates the 95% confidence interval and τ_{eff} is the residence time in days. $\ln \tau_{eff}^{ELPOS}$ is the logarithmized effective residence time [days] derived from characteristic travel distances in Europe at 5° C calculated with the ELPOS model as reported by Beyer et al. (2003), and τ_{eff}^{ELPOS} is the associated effective residence time in days.

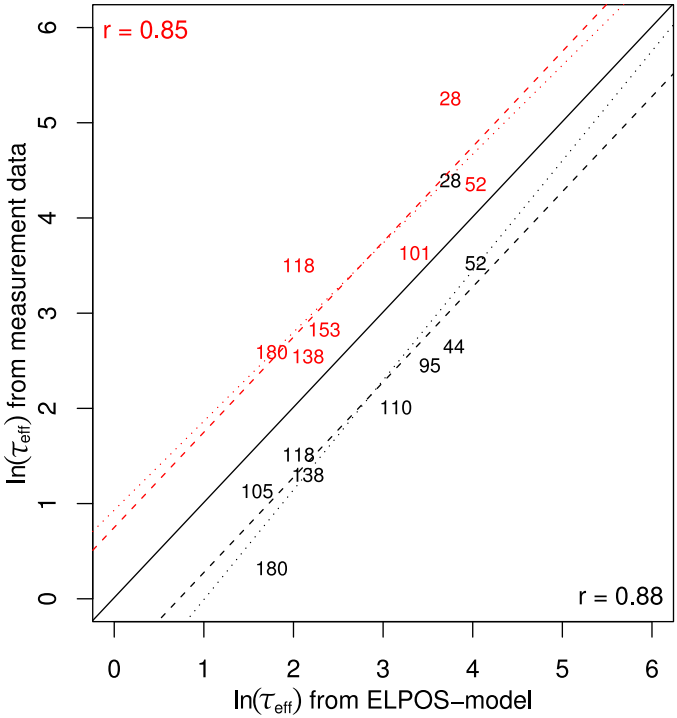

Figure 4.15: Logarithmized effective residence times in air from TRANS (black) and EMEP (red) versus $\ln(\tau_{eff})$ calculated with the ELPOS model (Beyer et al., 2003). The dotted lines are regression lines, the dashed lines mark the best fit with the slope forced to unity. τ_{eff} has units of days.

4.6.8 Inferring source strengths from measured concentrations

RI makes it possible to normalise measured concentrations in the field with respect to the effective distance to emission sources. We therefore can use concentration data from all sampling locations to estimate the concentration at, or very close to, the source by calculating $\ln(C)$ from equation 4.8, utilising a fixed, very small RI. That concentration should be related to the source strength. Since the emission source in our scenario is dispersed and since the range of RI does not include zero, we estimate $\ln(C)$ at $RI = 0.1626$, the minimum value encountered in the region of study, and compare it with the emission source strengths in Europe estimated by Breivik et al. (2007). Figure 4.16 shows that comparison, with concentrations at $RI = 0.1626$ derived from the TRANS dataset.

There is an intermediate yet highly significant correlation. PCB-28 has much higher emission source strength than calculated from the TRANS dataset and was excluded from the regression. The regression slope is not significantly different from one, indicating that emission source strength can be regarded as proportional to the atmospheric concentration close to sources, derived from field measurements.

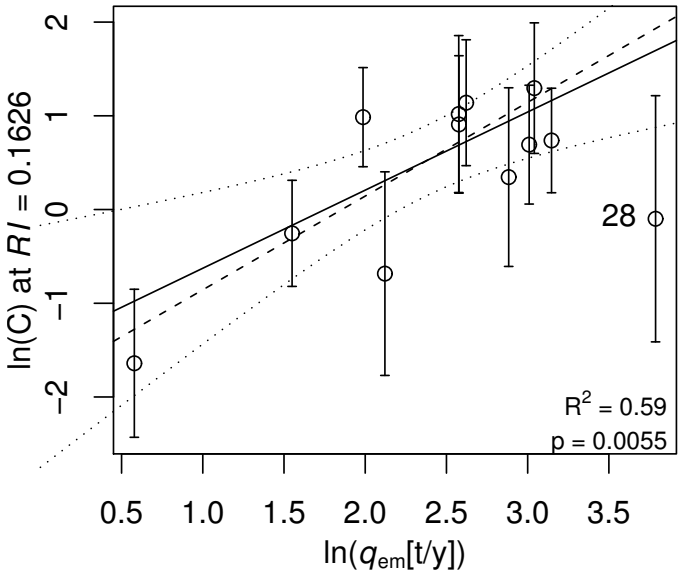

Figure 4.16: Predictions of $\ln(C)$ from equation 4.8 (TRANS) at the minimum $RI_{\min} = 0.1626$ versus the log-emission estimates for Europe according to Breivik et al. (2007). C has units of $\mathrm{pg/m^3}$. The error bars represent the 95% confidence intervals for the predictions of $\ln(C)$. PCB-28 was excluded from the regression. The continuous line marks the regression line, the dotted lines mark the 95% confidence interval and the dashed line represents the best fit with a slope forced to unity.

Chapter 5

Conclusions and outlook

5.1 Steady-state modelling

Mackay (1979) introduced a classification of models for the assessment of transport and transformation of toxic substances in the environment. This classification distinguishes four types of models ("Level I-IV") that describe a sequence of increasing complexity in the representation of the relevant processes. In today's landscape of models applied to POP fate- and transport, only two of Mackay's classes of models are relevant, i.e. the Level III and the Level IV model. The Level III model is the steady-state version of the Level IV model. Steady-state models have several advantages for the application as a screening tool in chemicals assessment:

- There is no need to specify and justify a particular point in time for the evaluation of the model output.

- Solving a multimedia mass balance model at steady-state means to solve a sparse system of linear equations; a computationally cheap task which can be carried out for thousands of substances on a current desktop computer in a matter of seconds or minutes.

- There is a broad consensus that the overall residence time at steady-state, τ^{ss}, is a meaningful metric for chemical screening assessments. The models potentially useful for chemicals assessment produce a variety of persistence metrics, but τ^{ss} is very well correlated with other metrics for persistence, including those calculated by dynamical models. (Fenner et al., 2005; Hollander et al., 2008).

- The most widely used LRTP-metrics, the *Characteristic Travel Distance* and the *Spatial Range* are based on steady-state concentration distributions.

It was shown in chapter 2 that the meaning of a steady-state solution extends beyond its identification with a natural system that is in steady-state. Natural endpoints of an exposure based assessment of organic chemicals, like τ^{ss}, *spatial range*, and *toxicity potential* are completely characterised by the steady-state solution of a linear time invariant system (LTI), even if emissions vary in time. The usefulness of indicators for regulatory purposes depends among other things on the ease and simplicity with which they can be calculated by non-technical people. An example is the the recent release of the *OECD P_{OV} & LRTP Screening Tool* (Wegmann et al., 2009), an extremely simple steady-state fate model, executed as Microsoft Excel macro. This thesis offers a theoretical result suited to strengthen the case for using simple steady-state models for exposure based risk assessments.

However, the result was derived under certain assumptions that might not be met in all areas of application. The most critical assumption is perhaps the time-invariance of the system under consideration. If diurnal and/or annual cycles of environmental parameters are considered, no steady-state solution exists. Further research should be directed towards the question whether the long-term behaviour of POP fate- and transport is adequately covered by a constant environment, represented by annually averaged values, or whether the long-term evolution of the time-invariant system can differ significantly from that of a system with time dependent coefficients. One possibility to answer this question are model experiments. Lammel (2004) conducted an exploratory simulation experiment and found that averaging environmental parameters could have a significant influence on the long-term evolution of the system. A more general approach to the problem could lie in the application of the *Floquet-Theory*, which states the existence of a periodic coordinate transformation that transforms a periodic linear system into a time-invariant one (Chicone, 1999). This could be exploited to systematically study the error induced by averaging environmental parameters in time.

5.2 Remoteness Index and LRTP

The exposure to a chemical at a particular location is determined by the geographical position of that location with respect to the emission sources of the chemical, and by properties of the chemical determining its fate- and transport behaviour. The *remoteness index*, RI, serves to separate these two elements.

Maps of RI can be used to better select sampling transects, for example to choose transects where expected concentration gradients are very steep to study loss processes during atmospheric transport, to identify areas with a similar remoteness from sources to study local influences on chemical concentrations, or to choose sampling locations that cover a representative range of remoteness. Maps of RI can be used to rank regions according to their vulnerability to chemical emissions from a distributed source, in a way that is independent of a particular chemical. Maps of this kind could contribute to more transparency in matters where environmental justice with respect to atmospheric pollutant transport are discussed.

RI serves to normalise measurements taken at different locations with respect to their remoteness from the emission source. This way, measurements of the same chemical at different locations can be combined to derive a chemical-specific measure for airborne long-range transport. Most importantly, RI provides a method to validate model calculated LRTP-indicators with field measurements and thus offers a possibility to strengthen the credibility of LRTP-indicators. It must be kept in mind that such an application relies on the assumption that the effective residence time in air can be considered constant across a region that covers the measurement locations. To apply RI on a regional scale, RI should be re-calculated for the region of interest to achieve a better precision. This is exemplified in the analysis of PCB measurements across Europe in Chapter 4.

The atmospheric-tracer transport model employed to derive the RI values used in Chapters 3 and 4 is fairly primitive. However, it is more realistic than the representations of atmospheric transport used in current spatially resolved multimedia box models for POP fate- and transport. It would be interesting to apply the method to derive RI to data generated by a more sophisticated tracer transport model. However, it is not clear whether such a dataset would allow for the definition of RI based on an expression as simple as equation 3.1.

A more direct calculation of *RI* could be achieved through the use of a Lagrangian particle transport model. In this approach, "particles" representing air-parcels would be released from the emission sources, the program would keep track of the age of the particles as they are transported through the atmosphere, and particles reaching the observation location would be recorded and then discarded. The average age of the particles reaching the observation location would substitute *RI*. The expected value of the traveltime of an air parcel would have the advantage of a physical meaning and the intuitively right unit, i.e. time. However, it appears computationally very challenging to carry out this proposal for a reasonably well resolved spatially distributed emission source, a representative time span, and enough observation locations to produce a map of expected traveltimes for an interesting region, e.g. Europe.

5.3 Global fractionation patterns

The *global distillation hypothesis* has stimulated and guided POP fate- and transport research since more than 15 years. The picture of a global distillation column has made its way into numerous publications and is part of the conceptual arsenal of many researchers in the field. In chapter 4, evidence is presented that observed fractionation patterns of PCB congeners between midlatitudinal Europe and the Arctic are likely not the result of a global distillation process, but rather reflect a gradient of increasing remoteness from emission sources.

The *global distillation hypothesis* as well as the here proposed mechanism of *differential removal* are strongly tied to the assessment of the LRTP of SVOCs. They both describe causative mechanisms that produce different spatial ranges for different SVOCs. This work indicates that the explaining power of the *global distillation hypothesis* has been overstated in some instances and that the remoteness from emission sources should be considered when interpreting observed patterns of SVOC fractionation. However, global distribution patterns of SVOCs that are compatible with *global distillation* but not with *differential removal* were observed for substances at the high vapour pressure end of the organohalogens considered here, e.g. hexachlorocyclohexane and hexachlorobenzene (Calamari et al., 1991; Simonich and Hites, 1995). Likely, both concepts need to be taken into account to arrive at a better description of large scale distribution patterns for all SVOCs.

A new hypothesis about the underlying mechanisms of large-scale fractionation patterns would combine *global distillation* and *differential removal*. For relatively volatile substances with long half-lifes in air, the global distribution in surface compartments might be dominated by the thermodynamic equilibrium between air and surface compartments. For less volatile substances like tetra- and higher chlorinated PCBs, the effective distance from sources might determine fractionation patterns. Future research should be directed at quantifying the contribution of each effect for different SVOCs, possibly as a function of vapour pressure and atmospheric half-life. Besides model experiments, field measurements along transects where a decreasing temperature does not correlate with increasing remoteness would help to better understand the mechanisms of global fractionation.

Nomenclature

Abbreviations

AhR 8
aryl hydrocarbon receptor

AMAP 27
Arctic Monitoring and Assessment Programme

AVHRR 29
Advanced Very High Resolution Radiometer

BCF 9
dimensionless bioconcentration factor

BETR-Global 5
Berkeley-Trent global contaminant fate model

CI 62
confidence interval

CliMoChem 5
Climate Zone Model for Chemicals

CROP 29
emission scenario associated with agricultural pesticide use

CTD 12
characteristic travel distance

DDT 3
dichlorodiphenyltrichloroethane

ECMWF 59
European Centre for Medium-Range Weather Forecasts

ECON 29
emission scenario associated with economic activity

EDC 8
endocrine disrupting chemical

ELPOS 63
environmental Long-range Transport and Persistence of Organic Substances Model

EMEP 36
European Monitoring and Evaluation Programme

EMEP 58
dataset of EMEP HiVol airsample measurements

ERA 59
ECMWF re-analysis project

EU 18
European Union

GAPS 36
Global Atmospheric Passive Sampling Network

GC-MS 57
gas chromatography-mass spectrometry

HCB 8
hexachlorobenzene

HCH 40
hexachlorocyclohexane

HiVol 55
high volume active sampler

L-BFGS 30
limited memory Broyden-Fletcher-Goldfarb-Shanno algorithm

LCA 24
Life Cycle Assessment

LCIA 19
Life Cycle Impact Assessment

LRTP 11
long-range transport potential

LTI 20
Linear Time Invariant (system)

m.a.s.l. 66
metre above sea level

NCAR 28
National Center for Atmospheric Research

NCEP 28
National Centers for Environmental Prediction

$NO_3\cdot$ 10
nitrate radical

NOAA 29
National Oceanic and Atmospheric Administration

NOAEL 9
No Adverse Effect Level

ODE 28
ordinary differential equation

OECD 20
Organisation for Economic Co-operation and Development

OH· 10
hydroxyl radical

PBDE 9
polybrominated diphenyl ether

PCB 3
polychlorinated biphenyl

PCDD 8
polychlorinated dibenzo-p-dioxins

PCDF 8
polychlorinated dibenzofuran

PCN 8
polychlorinated naphthalene

PFOS 3
perfluorooctane sulfonic acid

POP 2
persistent organic pollutant

QSPR 60
quantitative structure-property relationship

RI 26
Remoteness Index

SPMD 57
semipermeable membrane device

SR 12
spatial range

SVOC 2
semivolatile organic compound

TCDD 8
2,3,7,8-tetrachlorodibenzodioxin

TRANS 58
dataset of SPMD measurements along England-Norway transect

UNECE 18
United Nations Economic Commission for Europe

UNEP 18
United Nations Environment Programme

Mathematical operations

$\| \|_1$ 23
1-norm

$\delta(t)$ 21
Dirac delta function

$\mathcal{L}$ 22
Laplace transform

A^{-1} 20
inverse of matrix A

A^{T} 20
transpose of matrix A

Symbols

Depending on the use of the symbols in the main text, either units or dimensions (M for mass, T for time, and L for length) are given in brackets.

α 30
fitting parameter

β_i 30
fitting parameter

$\widehat{\beta}$ 60
estimate of regression parameter β

ΔU_{OA} [Jmol^{-1}] 57
internal energy of octanol-air transfer

$\mathcal{E}$ [ML^{-3}T] 19
environmental exposure

$\vec{\mathcal{E}}$ [ML^{-3}T] 20
n-vector of exposures, elements correspond to well-mixed volumes in environmental compartments

ϵ 60
error term in regression models

γ 30
fitting parameter

ω_j 60
weights for weighted regression

ρ 62
Spearman's rank-correlation coefficient

σ^2 60
variance

σ^2_{xx} [L^2T^{-2}] 28
zonal variance of wind velocities

σ^2_{yy} [L^2T^{-2}] 28
meridional variance of wind velocities

τ_{eff} [T] 28
effective residence time in air

τ^{ELPOS}_{eff} [d] 63
effective residence time in air, calculated with ELPOS

τ^{EMEP}_{eff} [d] 62
effective residence time in air, estimated from EMEP

τ^{TRANS}_{eff} [d] 62
effective residence time in air, estimated from TRANS

τ^{eq} [T] 24
equivalent width of concentration-time profile

τ_{ex} [T] 28
inter-hemispheric exchange time

τ_{max} [T] 31
maximum effective atmospheric residence time

τ^{ss} [T] 23
overall residence time at steady-state

θ 30
fitting parameter

$\vec{\vartheta} = (\vartheta_0, \vartheta_1)^T$ 59
vector of fitting parameters

$A = (a_{ij})$ [T^{-1}] 20
$n \times n$ matrix of first order rate constants

c [ML^{-3}] 19
contaminant concentration in a particular compartment

$\vec{c}$ [ML^{-3}] 20
n-vector of environmental contaminant concentrations, elements correspond to well-mixed volumes in environmental compartments

$\vec{c}_{ss}$ [ML^{-3}] 22
n-vector of steady-state concentrations in well-mixed environmental volumes

C_{air} [pg/m^3] 57
PCB concentration in air

C^{hom} [ML^{-3}] 61
average PCB homologue concentration in air

$C_{i,\tau_{eff}}$ [ML^{-3}] 30
contaminant concentration

D_{xx} [L^2T^{-1}] 28
zonal eddy-diffusivity

D_{yy} [L^2T^{-1}] 28
meridional eddy-diffusivity

I 22
$n \times n$ identity matrix

K_{AW} 53
dimensionless air-water partition coefficent

K_{OA} 2
dimensionless octanol-air partition coefficient

K_{OW} 9
dimensionless octanol-water partition coefficient

K_{SA} 57
dimensionless SPMD-air partition coefficient

k_0 [M/T] 67
bulk mass-transfer coefficient across the SPMD-air interface

k_a [M/T] 67
bulk mass-transfer coefficient across the gas-phase laminar boundary layer

k_{reac} [T^{-1}] 60
rate constant for removal from the atmosphere by reaction with OH radicals

k_s [M/T] 67
bulk mass-transfer coefficient across the SPMD membrane

m_N [M] 28
tracer mass in northern hemisphere

m_S [M] 28
tracer mass in southern hemisphere

m_S [pg] 57
SPMD-sequestered PCB mass

$\vec{m}$ [M] 20
n-vector of contaminant masses, elements correspond to well-mixed volumes in environmental compartments

$\vec{m}_e$ [M] 22
n-vector of total emitted contaminant masses

$\vec{m}_e^{\,pulse} = (m_e^1, \ldots, m_e^n)^T$ [M] 21
n-vector of contaminant masses emitted as a pulse

$\vec{m}_{ss}$ [M] 22
n-vector of steady-state masses in well-mixed environmental volumes

n 20
number of well-mixed volume elements

$q_{N\to S}$ [MT^{-1}] 28
north to south mass flow across the equator

q_{PCB} [ty^{-1}] 69
estimated PCB emission rates by Breivik et al. (2007)

$\vec{q}$ [MT^{-1}] 20
n-vector of emission rates, elements correspond to well-mixed volumes in environmental compartments

$\vec{q}_{ss}$ [MT^{-1}] 22
n-vector of emission rates from continuously emitting sources

r 63
Pearson's sample correlation coefficient

R [$JK^{-1}mol^{-1}$] 57
gas constant, 8.3145 $JK^{-1}mol^{-1}$

R^2 63
coefficient of determination

RI 26
Remoteness Index

R_S [m^3d^{-1}] 57
apparent SPMD air sampling rate

t [T] 19
time

$t_{0.5}$ [y] 69
half-life

T_0 [K] 57
standard temperature, 298.15 K

$\overline{T}_i$ [K] 57
average annual temperatures at sampling sites i

V_A [L^3] 31
volume of the atmosphere

V_S [m^3] 57
volume of SPMD, 4.525×10^{-6} m^3

V [L^3] 21
diagonal $n \times n$ matrix with the volumes of the well-mixed environmental volumes on its diagonal

Bibliography

Agrell, C., Okla, L., Larsson, P., Backe, C., and Wania, F. (1999). Evidence of latitudinal fractionation of polychlorinated biphenyl congeners along the baltic sea region. *Environmental Science and Technology*, 33(8):1149–1156.

AMAP (2004). *AMAP Assessment 2002: Persistent Organic Pollutants in the Arctic*. Arctic Monitoring and Assessment Programme (AMAP), Oslo, Norway.

Anderson, P. N. and Hites, R. A. (1996). OH radical reactions: The major removal pathway for polychlorinated biphenyls from the atmosphere. *Environmental Science and Technology*, 30(5):1756–1763.

Arnot, J. A. and Gobas, F. A. P. C. (2006). A review of bioconcentration factor (BCF) and bioaccumulation factor (BAF) assessments for organic chemicals in aquatic organisms. *Environmental Reviews*, 14(4):257–297.

Atkinson, R. (1990). Gas-phase tropospheric chemistry of organic compounds: A review. *Atmospheric Environment Part A*, 24(1):1 – 41.

Atkinson, R., Guicherit, R., Hites, R. A., Palm, W.-U., Seiber, J. N., and de Voogt, P. (1999). Transformations of pesticides in the atmosphere: A state of the art. *Water, Air, & Soil Pollution*, 115(1):219–243.

Axelman, J. and Gustafsson, O. (2002). Global sinks of PCBs: A critical assessment of the vapor-phase hydroxy radical sink emphasizing field diagnostics and model assumptions. *Global Biogeochemical Cycles*, 16(4):1111.

Beck, M. B., Ravetz, J. R., Mulkey, L. A., and Barnwell, T. O. (1997). On the problem of model validation for predictive exposure assessments. *Stochastic Hydrology and Hydraulics*, 11(3):229–254.

Bennett, D. H., McKone, T. E., Matthies, M., and Kastenberg, W. E. (1998). General formulation of characteristic travel distance for semivolatile organic chemicals in a multimedia environment. *Environmental Science and Technology*, 32(24):4023–4030.

Bennett, D. H., Scheringer, M., McKone, T. E., and Hungerbühler, K. (2001). Predicting long range transport: A systematic evaluation of two multimedia transport models. *Environmental Science and Technology*, 35(6):1181–1189.

Berrisford, P., Dee, D., Fielding, K., Fuentes, M., Kallberg, P., Kobayashi, S., and Uppala, S. (2009). The ERA-interim archive. Technical report, ECMWF, Shinfield Park, Reading.

Bertazzi, P. A., Consonni, D., Bachetti, S., Rubagotti, M., Baccarelli, A., Zocchetti, C., and Pesatori, A. C. (2001). Health effects of dioxin exposure: A 20-year mortality study. *American Journal Of Epidemiology*, 153(11):1031–1044.

Bessai, H. (2006). *MIMO Signals and Systems*. Springer, Berlin.

Beyer, A., Wania, F., Gouin, T., Mackay, D., and Matthies, M. (2003). Temperature dependence of the characteristic travel distance. *Environmental Science and Technology*, 37(4):766–771.

Bidleman, T. F. (1988). Atmospheric processes. *Environmental Science and Technology*, 22(4):361–367.

Brandes, L. J., den Hollander, H., and van de Meent, D. (1996). Simplebox 2.0: a nested multimedia fate model for evaluating the environmental fate of chemicals. RIVM Rapport 719101029, National Institute of Public Health and the Environment (RIVM), Bilthoven. Netherlands.

Bratseth, A. M. (2003). Zonal-mean transport characteristics of ECMWF reanalysis data. *Quarterly Journal of the Royal Meteorological Society*, 129:2331–2346.

Breivik, K., Sweetman, A., Pacyna, J. M., and Jones, K. C. (2002). Towards a global historical emission inventory for selected PCB congeners - a mass balance approach 1. global production and consumption. *Science of the Total Environment*, 290(1-3):181–198.

Breivik, K., Sweetman, A., Pacyna, J. M., and Jones, K. C. (2007). Towards a global historical emission inventory for selected PCB congeners – a mass balance approach: 3. an update. *Science of the Total Environment*, 377(2-3):296–307.

Brown, P. N., Byrne, G. D., and Hindmarsh, A. C. (1988). Vode: A variable coefficient ode solver. *SIAM Journal on Scientific and Statistical Computing*, 10:1038–1051.

Calamari, D., E., B., Focardi, S., Gaggi, C., Morosini, M., and Vighi, M. (1991). Role of plant biomass in the global environmental partitioning of chlorinated hydrocarbons. *Environmental Science and Technology*, 25(8):1489–1495.

Cartwright, N. (1997). Where do laws of nature come from? *Dialectica*, 51(1):65–78.

Chahine, M., Chen, L., Dimotakis, P., Jiang, X., Li, Q., Olsen, E., Pagano, T., Randerson, J., and Yung, Y. (2008). Satellite remote sounding of mid-tropospheric co2. *Geophysical Research Letters*, 35(17):L17807.

Chicone, C. (1999). *Ordinary Differential Equations with Applications*. Springer, New York.

Cleveland, W. S., Grosse, E., and Shyu, M. J. (1992). Local regression models. In Chambers, J. M. and Hastie, T., editors, *Statistical models in S*, pages 309–376. Chapman and Hall, New York.

Colborn, T., Dumanoski, D., and J.P., M. (1996). *Our Stolen Future*. Penguin Books.

Colborn, T., Saal, F. S. V., and Soto, A. M. (1993). Developmental effects of endocrine-disrupting chemicals in wildlife and humans. *Environmental Health Perspectives*, 101(5):378–384.

Committee to Review the Health Effects in Vietnam Veterans of Exposure to Herbicides (2004). *Veterans and Agent Orange - Update 2004*. The National Academies Press.

Costa, L. G. and Giordano, G. (2007). Developmental neurotoxicity of polybrominated diphenyl ether (PBDE) flame retardants. *Neurotoxicology*, 28(6):1047–1067.

Czeplak, G. and Junge, C. (1974). Studies of interhemispheric exchange in the troposphere by a diffusion model. *Advances in Geophysics*, 18:B57+.

Czub, G. and McLachlan, M. S. (2004). Bioaccumulation potential of persistent organic chemicals in humans. *Environmental Science and Technology*, 38(8):2406–2412.

Damstra, T., Barlow, S., Bergman, A., Kavlock, R., and Van Der Kraak, G. (2002). Global assessment of the state-of-the-science of endocrine disruptors (WHO/PCS/EDC/02.2). Technical report, The International Programme on Chemical Safety.

Doll, C. N. H., Muller, J. P., and Morley, J. G. (2006). Mapping regional economic activity from night-time light satellite imagery. *Ecological Economics*, 57(1):75–92.

Dreyfuss, R. (2000). Apocalypse still. *Mother Jones*, January/February Issue.

Drinker, C. K., Warren, M. F., and Bennett, G. A. (1937). The problem of possible systemic effects from certain chlorinated hydrocarbons. *Journal of Industrial Hygiene and Toxicology*, 19((7)):283–299.

Elvidge, C. D., Imhoff, M. L., Baugh, K. E., Hobson, V. R., Nelson, I., Safran, J., Dietz, J. B., and Tuttle, B. T. (2001). Night-time lights of the world: 1994-1995. *ISPRS Journal of Photogrammetry and Remote Sensing*, 56(2):81 – 99.

EMEP (2009). *EMEP POP data*. Retrieved July 12, 2009, from: `http://tarantula.nilu.no/projects/ccc/onlinedata/pops/index.html`.

European Parliament and Council of the EU (2006). Regulation (EC) No 1907/2006 of the European Parliament and of the Council concerning the Registration, Evaluation, Authorisation and Restriction of Chemicals (REACH).

Fenner, K., Scheringer, M., and Hungerbühler, K. (2000). Persistence of parent compounds and transformation products in a Level IV multimedia model. *Environmental Science and Technology*, 34(17):3809–3817.

Fenner, K., Scheringer, M., MacLeod, M., Matthies, M., McKone, T., Stroebe, M., Beyer, A., Bonnell, M., LeGall, A., Klasmeier, J., Mackay, D., van de Meent, D., Pennington, D., Scharenberg, B., Suzuki, N., and Wania, F. (2005). Comparing estimates of persistence and long-range transport potential among multimedia models. *Environmental Science and Technology*, 39(7):1932–1942.

Gaylor, D. W. (2000). The use of Haber's law in standard setting and risk assessment. *Toxicology*, 149(1):17–19.

Gioia, R., Steinnes, E., Thomas, G. O., Mejier, S. N., and Jones, K. C. (2006). Persistent organic pollutants in european background air: derivation of temporal and latitudinal trends. *Journal of Environmental Monitoring*, 8(7):700–710.

Goodhead, R. and Tyler, C. (2009). Endocrine-disrupting chemicals and their environmental impacts. In Walker, C., editor, *Organic Pollutants - An Ecotoxicological Perspective*. CRC Press.

Guinée, J. and Heijungs, R. (1993). A proposal for the classification of toxic substances within the framework of life cycle assessment of products. *Chemosphere*, 26(10):1925–1944.

Guo, Y. L. L., Lambert, G. H., Hsu, C. C., and Hsu, M. M. L. (2004). Yucheng: health effects of prenatal exposure to polychlorinated biphenyls and dibenzofurans. *International Archives Of Occupational And Environmental Health*, 77(3):153–158.

Haag, D. and Kaupenjohann, M. (2001). Parameters, prediction, post-normal science and the precautionary principle - a roadmap for modelling for decision-making. *Ecological Modelling*, 144(1):45–60.

Haag, D. and Matschonat, G. (2001). Limitations of controlled experimental systems as models for natural systems: a conceptual assessment of experimental practices in biogeochemistry and soil science. *Science Of The Total Environment*, 277(1-3):199–216.

Hazewinkel, M., editor (2002). *Encyclopaedia of Mathematics*. Springer.

Heijungs, R. (1995). Harmonization of methods for impact assessment. *Environmental Science and Pollution Research*, 2(4):217–224.

Hertwich, E. G. (2001). Fugacity superposition: a new approach to dynamic multimedia fate modeling. *Chemosphere*, 44(4):843–853.

Hertwich, E. G., Mateles, S. F., Pease, W. S., and McKone, T. E. (2001). Human toxicity potentials for life-cycle assessment and toxics release inventory risk screening. *Environmental Toxicology and Chemistry*, 20(4):928–939.

Hollander, A., Scheringer, M., Shatalov, V., Mantseva, E., Sweetman, A., Roemer, M., Baart, A., Suzuki, N., Wegmann, F., and van de Meent, D. (2008). Estimating overall persistence and long-range transport potential of persistent organic pollutants: a comparison of seven multimedia mass balance models and atmospheric transport models. *Journal Of Environmental Monitoring*, 10(10):1139–1147.

Homberger, E., Reggiani, G., Sambeth, J., and Wipf, H. K. (1979). The Seveso accident: Its nature, extent and consequences. *The Annals of Occupational Hygiene*, 22(4):327–370.

Hotchkiss, A. K., Rider, C. V., Blystone, C. R., Wilson, V. S., Hartig, P. C., Ankley, G. T., Foster, P. M., Gray, C. L., and Gray, L. E. (2008). Fifteen years after "Wingspread" - environmental endocrine disrupters and human and wildlife health: Where we are today and where we need to go. *Toxicological Sciences*, 105(2):235–259.

Huckins, J. N., Petty, J. D., and Kees, B. (2006). *Monitors of organic chemicals in the environment: Semipermeable Membrane Devices*. Springer, New York.

Huijbregts, M. A. J., Thissen, U., Guinee, J. B., Jager, T., Kalf, D., van de Meent, D., Ragas, A. M. J., Sleeswijk, A. W., and Reijnders, L. (2000). Priority assessment of toxic substances in life cycle assessment. Part I: Calculation of toxicity potentials for 181 substances with the nested multi-media fate, exposure and effects model USES-LCA. *Chemosphere*, 41(4):541–573.

Humphreys, P. (2004). *Extending Ourselves: Computational Science, Empiricism, and Scientific Method*. Oxford University Press.

Jacob, D. J., Prather, M. J., Wofsy, S. C., and McElroy, M. B. (1987). Atmospheric distribution of Kr-85 simulated with a general circulation model. *Journal of Geophysical Research, [Atmospheres]*, 92(D6):6614–6626.

Jaward, F., Meijer, S., Steinnes, E., Thomas, G., and Jones, K. (2004). Further studies on the latitudinal and temporal trends of persistent organic pollutants in Norwegian and U.K. background air. *Environmental Science and Technology*, 38(9):2523–2530.

Jones, P. W. (1999). First- and second-order conservative remapping schemes for grids in spherical coordinates. *Monthly Weather Review*, 127(9):2204–2210.

Jorgenson, J. L. (2001). Aldrin and Dieldrin: A review of research on their production, environmental deposition and fate, bioaccumulation, toxicology and epidemiology in the United States. *Environmental Health Perspectives*, 109:113–139.

Kallenborn, R., Oehme, M., Wynn-Williams, D. D., Schlabach, M., and Harris, J. (1998). Ambient air levels and atmospheric long-range transport of persistent organochlorines to Signy Island, Antarctica. *Science of the Total Environment*, 220(2-3):167–180.

Kalnay, E., Kanamitsu, M., Kistler, R., Collins, W., Deaven, D., Gandin, L., Iredell, M., Saha, S., White, G., Woollen, J., Zhu, Y., Chelliah, M., Ebisuzaki,

W., Higgins, W., Janowiak, J., Mo, K. C., Ropelewski, C., Wang, J., Leetmaa, A., Reynolds, R., Jenne, R., and Joseph, D. (1996). The NCEP/NCAR 40-year reanalysis project. *Bulletin of the American Meteorological Society*, 77(3):437–471.

Kelly, B. C., Ikonomou, M. G., Blair, J. D., Morin, A. E., and Gobas, F. A. P. C. (2007). Food web-specific biomagnification of persistent organic pollutants. *Science*, 317(5835):236–239.

Krimsky, S. (2000). *Hormonal Chaos*. The Johns Hopkins University Press.

Kuhn, T. (1962). *The Structure of Scientific Revolutions*. University of Chicago Press.

Lammel, G. (2004). Effects of time-averaging climate parameters on predicted multicompartmental fate of pesticides and POPs. *Environmental Pollution*, 128(1-2):291–302.

Lemaire, G., Mnif, W., Mauvais, P., Balaguer, P., and Rahmani, R. (2006). Activation of alpha- and beta-estrogen receptors by persistent pesticides in reporter cell lines. *Life Sciences*, 79(12):1160–1169.

Levy, W., Henkelmann, B., Pfister, G., Bernhoft, S., Kirchner, M., Jakobi, G., Bassan, R., Krauchi, N., and Schramm, K. W. (2009). Long-term air monitoring of organochlorine pesticides using semi permeable membrane devices (SPMDs) in the alps. *Environmental Pollution*, 157(12):3272–3279.

Li, Y. F. (1999). Global gridded technical hexachlorocyclohexane usage inventories using a global cropland as a surrogate. *Journal of Geophysical Research, [Atmospheres]*, 104(D19):23785–23797.

Lioy, P. J. (1990). Assessing total human exposure to contaminants - a multidisciplinary approach. *Environmental Science and Technology*, 24(7):938–945.

Liu, D. C. and Nocedal, J. (1989). On the limited memory BFGS method for large-scale optimization. *Mathematical Programming*, 45(3):503–528.

Loveland, T. R., Reed, B. C., Brown, J. F., Ohlen, D. O., Zhu, Z., Yang, L., and Merchant, J. W. (2000). Development of a global land cover characteristics database and IGBP DISCover from 1 km AVHRR data. *International Journal of Remote Sensing*, 21(6-7):1303–1330.

Macdonald, R. W., Barrie, L. A., Bidleman, T. F., Diamond, M. L., Gregor, D. J., Semkin, R. G., Strachan, W. M. J., Li, Y. F., Wania, F., Alaee, M., Alexeeva, L. B., Backus, S. M., Bailey, R., Bewers, J. M., Gobeil, C., Halsall, C. J., Harner, T., Hoff, J. T., Jantunen, L. M. M., Lockhart, W. L., Mackay, D., Muir, D. C. G., Pudykiewicz, J., Reimer, K. J., Smith, J. N., Stern, G. A., Schroeder, W. H., Wagemann, R., and Yunker, M. B. (2000). Contaminants in the Canadian Arctic: 5 years of progress in understanding sources, occurrence and pathways. *Science of the Total Environment*, 254(2-3):93–234.

Mackay, D. (1979). Finding fugacity feasible. *Environmental Science and Technology*, 13(10):1218–1223.

Mackay, D. (1982). Correlation of bioconcentration factors. *Environmental Science and Technology*, 16(5):274–278.

Mackay, D. and Fraser, A. (2000). Bioaccumulation of persistent organic chemicals: mechanisms and models. *Environmental Pollution*, 110(3):375–391.

MacLeod, M., Riley, W., and McKone, T. (2005). Assessing the influence of climate variability on atmospheric concentrations of polychlorinated biphenyls using a global-scale mass balance model (BETR-Global). *Environmental Science and Technology*, 39:6749–6756.

MacLeod, M., Scheringer, M., and Hungerbühler, K. (2007). Estimating enthalpy of vaporization from vapor pressure using Trouton's Rule. *Environmental Science and Technology*, 41(8):2827–2832.

Maeder, M. and Neuhold, B. (2007). *Practical data analysis in chemistry*. Elsevier, Amsterdam.

Matthies, M., Klasmeier, J., Beyer, A., and Ehling, C. (2009). Assessing persistence and long-range transport potential of current-use pesticides. *Environmental Science and Technology*, 43(24):9223–9229.

McGill, R., Tukey, J. W., and Larsen, W. A. (1978). Variations of box plots. *American Statistician*, 32(1):12–16.

Meadows, D., Randers, J., and Meadows, D. (2004). *Limits to growth. The 30-year update*. Chelsa Green.

Meijer, S. N., Ockenden, W. A., Steinnes, E., Corrigan, B. P., and Jones, K. C. (2003). Spatial and temporal trends of POPs in Norwegian and UK background air: Implications for global cycling. *Environmental Science and Technology*, 37(3):454–461.

Meijer, S. N., Steinnes, E., Ockenden, W. A., and Jones, K. C. (2002). Influence of environmental variables on the spatial distribution of PCBs in Norwegian and UK soils: Implications for global cycling. *Environmental Science and Technology*, 36(10):2146–2153.

Minh, T. B., Nakata, H., Watanabe, M., Tanabe, S., Miyazaki, N., Jefferson, T. A., Prudente, M., and Subramanian, A. (2000). Isomer-specific accumulation and toxic assessment of polychlorinated biphenyls, including coplanar congeners, in cetaceans from the north pacific and asian coastal waters. *Archives of Environmental Contamination and Toxicology*, 39(3):398–410.

Moeckel, C., Harner, T., Nizzetto, L., Strandberg, B., Lindroth, A., and Jones, K. C. (2009). Use of depuration compounds in passive air samplers: Results from active sampling-supported field deployment, potential uses, and recommendations. *Environmental Science and Technology*, 43(9):3227–3232.

Morrison, M. C. (1998). Modelling nature: Between physics and the physical world. *Philosophia naturalis*, 35(1):65–85.

Muir, D. C. G., Omelchenko, A., Grift, N. P., Savoie, D. A., Lockhart, W. L., Wilkinson, P., and Brunskill, G. J. (1996). Spatial trends and historical deposition of polychlorinated biphenyls in Canadian midlatitude and Arctic lake sediments. *Environmental Science and Technology*, 30(12):3609–3617.

Muir, D. C. G., Teixeira, C., and Wania, F. (2004). Empirical and modeling evidence of regional atmospheric transport of current-use pesticides. *Environmental Toxicology and Chemistry*, 23(10):2421–2432.

Murgatroyd, R. J. (1969). Estimations from geostrophic trajectories of horizontal diffusivity in the mid-latitude troposphere and lower stratosphere. *Quarterly Journal of the Royal Meteorological Society*, 95(403):40–62.

Ngo, A. D., Taylor, R., Roberts, C. L., and Nguyen, T. V. (2006). Association between Agent Orange and birth defects: systematic review and meta-analysis. *Int. J. Epidemiol.*, 35(5):1220–1230.

NOAA (2002). Documentation for the world radiance calibrated images 1996–1997, derived from DMSP OLS nighttime imagery. http://www.ngdc.noaa.gov/dmsp/data/rad_cal/rad_cal.tar.

Ockenden, W., Lohmann, R., Shears, J., and Jones, K. (2001a). The significance of PCBs in the atmosphere of the southern hemisphere. *Environmental Science and Pollution Research*, 8(3):189–194.

Ockenden, W. A., Breivik, K., Meijer, S. N., Steinnes, E., Sweetman, A. J., and Jones, K. C. (2003). The global re-cycling of persistent organic pollutants is strongly retarded by soils. *Environmental Pollution*, 121(1):75–80.

Ockenden, W. A., Corrigan, B. P., Howsam, M., and Jones, K. C. (2001b). Further developments in the use of semipermeable membrane devices as passive air samplers: Application to pcbs. *Environmental Science and Technology*, 35(22):4536–4543.

Ockenden, W. A., Prest, H. F., Thomas, G. O., Sweetman, A., and Jones, K. C. (1998a). Passive air sampling of pcbs: Field calculation of atmospheric sampling rates by triolein-containing semipermeable membrane devices. *Environmental Science and Technology*, 32(10):1538–1543.

Ockenden, W. A., Sweetman, A. J., Prest, H. F., Steinnes, E., and Jones, K. C. (1998b). Toward an understanding of the global atmospheric distribution of persistent organic pollutants: The use of semipermeable membrane devices as time-integrated passive samplers. *Environmental Science and Technology*, 32(18):2795–2803.

OECD (2004). Guidance document on the use of multimedia models for estimating overall environmental persistance and long-range transport. OECD Series on Testing and Assessment 45, OECD.

Olson, W. H. and Cumming, R. B. (1981). Chemical mutagens - dosimetry, Haber's rule and linear-systems. *Journal of Theoretical Biology*, 91(3):383–395.

Pozo, K., Harner, T., Wania, F., Muir, D. C. G., Jones, K. C., and Barrie, L. A. (2006). Toward a global network for persistent organic pollutants in air: Results from the gaps study. *Environmental Science and Technology*, 40(16):4867–4873.

Prather, M., McElroy, M., Wofsy, S., Russell, G., and Rind, D. (1987). Chemistry of the global troposphere - fluorocarbons as tracers of air motion. *Journal of Geophysical Research, [Atmospheres]*, 92(D6):6579–6613.

Ravetz, J. R. (1999). What is post-normal science ? *Futures*, 31(7):647–653.

Ritter, L., Solomon, K., and Forget, J. (1995). Pesistent organic pollutants. Technical report, The International Programme on Chemical Safety (IPCS).

Rockstrom, J., Steffen, W., Noone, K., Persson, A., Chapin, F. S., Lambin, E. F., Lenton, T. M., Scheffer, M., Folke, C., Schellnhuber, H. J., Nykvist, B., de Wit, C. A., Hughes, T., van der Leeuw, S., Rodhe, H., Sorlin, S., Snyder, P. K., Costanza, R., Svedin, U., Falkenmark, M., Karlberg, L., Corell, R. W., Fabry, V. J., Hansen, J., Walker, B., Liverman, D., Richardson, K., Crutzen, P., and Foley, J. A. (2009). A safe operating space for humanity. *Nature*, 461(7263):472–475.

Rozman, K. K. and Doull, J. (2001). Paracelsus, Haber and Arndt. *Toxicology*, 160(1-3):191–196.

Schantz, S. L. (1996). Developmental neurotoxicity of pcbs in humans: What do we know and where do we go from here? *Neurotoxicology and Teratology*, 18(3):217 – 227.

Schecter, A., Birnbaum, L., Ryan, J. J., and Constable, J. D. (2006). Dioxins: An overview. *Environmental Research*, 101(3):419–428.

Schenker, U., MacLeod, M., Scheringer, M., and Hungerbühler, K. (2005). Improving data quality for environmental fate models: A least-squares adjustment procedure for harmonizing physicochemical properties of organic compounds. *Environmental Science and Technology*, 39(21):8434–8441.

Scheringer, M. (1996). Persistence and spatial range as endpoints of an exposure-based assessment of organic chemicals. *Environmental Science and Technology*, 30(5):1652–1659.

Scheringer, M. (1997). Characterization of the environmental distribution behavior of organic chemicals by means of persistence and spatial range. *Environmental Science and Technology*, 31(10):2891–2897.

Scheringer, M. (2002). *Persistence and Spatial Range of Environmental Chemicals*. Wiley-VCH, Weinheim.

Scheringer, M. (2008). *The fate of persistent organic pollutants in the environment*, pages 189–203. NATO science for peace and security series C: Environmental security. Springer.

Scheringer, M. (2009). Long-range transport of organic chemicals in the environment. *Environmental Toxicology and Chemistry*, 28(4):677–690.

Scheringer, M., Boschen, S., and Hungerbühler, K. (2006). Will we know more or less about chemical risks under reach? *Chimia*, 60(10):699–706.

Scheringer, M., Salzmann, M., Stroebe, M., Wegmann, F., Fenner, K., and Hungerbühler, K. (2004). Long-range transport and global fractionation of POPs: insights from multimedia modeling studies. *Environmental Pollution*, 128(1-2):177 – 188.

Scheringer, M., Wegmann, F., Fenner, K., and Hungerbühler, K. (2000). Investigation of the cold condensation of persistent organic pollutants with a global multimedia fate model. *Environmental Science and Technology*, 34:1842–1850.

Schreiber, T., Gassmann, K., Gotz, C., Hubenthal, U., Moors, M., Krause, G., Merk, H. F., Nguyen, N. H., Scanlan, T. S., Abel, J., Rose, C. R., and Fritsche, E. (2010). Polybrominated diphenyl ethers induce developmental neurotoxicity in a human in vitro model: Evidence for endocrine disruption. *Environmental Health Perspectives*, 118(4):572–578.

Schuster, J. K., Gioia, R., Breivik, K., Steinnes, E., and Jones, K. C. (2010). Trends in European background air reflect reductions in primary emissions of PCBs and PBDEs. *Environmental Science and Technology*. in Review.

Schwarzenbach, R. P., Gschwend, P. M., and Imboden, D. M. (2003). *Environmental organic chemistry*. Wiley.

Selin, H. and Eckley, N. (2003). Science, politics, and persistent organic pollutants: The role of scientific assessments in international environmental cooperation. *International Environmental Agreements: Politics, Law and Economics*, 3(1):17–42.

Semeena, V. S., Feichter, J., and Lammel, G. (2006). Impact of the regional climate and substance properties on the fate and atmospheric long-range transport of persistent organic pollutants - examples of DDT and γ-HCH. *Atmospheric Chemistry and Physics*, 6:1231–1248.

Shen, L., Wania, F., Ying, D. L., Teixeira, C., Muir, D. C. G., and Xiao, H. (2006). Polychlorinated biphenyls and polybrominated diphenyl ethers in the North American atmosphere. *Environmental Pollution*, 144(2):434 – 444.

Shoeib, M. and Harner, T. (2002). Characterization and comparison of three passive air samplers for persistent organic pollutants. *Environmental Science and Technology*, 36(19):4142–4151.

Siegenthaler, U. and Oeschger, H. (1978). Predicting future atmospheric carbondioxide levels. *Science*, 199(4327):388–395.

Simonich, S. L. and Hites, R. A. (1995). Global distribution of persistent organochloride compounds. *Science*, 269(5232):1851–1854.

Sobek, A. and Gustafsson, O. (2004). Latitudinal fractionation of polychlorinated biphenyls in surface seawater along a 62 degrees N – 89 degrees N transect from the southern Norwegian Sea to the North Pole area. *Environmental Science and Technology*, 38(10):2746–2751.

Spivakovsky, C. M., Logan, J. A., Montzka, S. A., Balkanski, Y. J., Foreman-Fowler, M., Jones, D. B. A., Horowitz, L. W., Fusco, A. C., Brenninkmeijer, C. A. M., Prather, M. J., Wofsy, S. C., and McElroy, M. B. (2000). Three-dimensional climatological distribution of tropospheric OH: Update and evaluation. *Journal Of Geophysical Research-Atmospheres*, 105(D7):8931–8980.

Stellman, J. M., Stellman, S. D., Christian, R., Weber, T., and Tomasallo, C. (2003). The extent and patterns of usage of agent orange and other herbicides in vietnam. *Nature*, 422(6933):681–687.

Stroebe, M., Scheringer, M., and Hungerbühler, K. (2004). Measures of overall persistence and the temporal remote state. *Environmental Science and Technology*, 38(21):5665–5673.

Sutton, P., Roberts, D., Elvidge, C., and Baugh, K. (2001). Census from heaven: An estimate of the global human population using night-time satellite imagery. *International Journal of Remote Sensing*, 22(16):3061–3076.

Tang, C. Y., Fu, Q. S., Robertson, A. P., Criddle, C. S., and Leckie, J. O. (2006). Use of reverse osmosis membranes to remove perfluorooctane sulfonate (PFOS) from semiconductor wastewater. *Environmental Science and Technology*, 40(23):7343–7349.

Therneau, T. and Lumley, T. (2009). *survival: Survival analysis, including penalised likelihood.* R package version 2.35-4.

Toppari, J., Larsen, J. C., Christiansen, P., Giwercman, A., Grandjean, P., Guillette, L. J., Jegou, B., Jensen, T. K., Jouannet, P., Keiding, N., Leffers, H., McLachlan, J. A., Meyer, O., Muller, J., RajpertDeMeyts, E., Scheike, T., Sharpe, R., Sumpter, J., and Skakkebaek, N. E. (1996). Male reproductive health and environmental xenoestrogens. *Environmental Health Perspectives*, 104:741–803.

UNECE (1998). Aarhus protocol on persistent organic pollutants. http://www.unece.org/env/lrtap/full%20text/1998.POPs.e.pdf.

UNEP (2001). Stockholm convention on persistent organic pollutants. http://www.pops.int.

UNEP (2007). UNEP/POPS/COP.3/INF/14 - Guidance on the Global Monitoring Plan for Persistent Organic Pollutants, Preliminary version.

Vallack, H. W., Bakker, D. J., Brandt, I., Brostrom-Lunden, E., Brouwer, A., Bull, K. R., Gough, C., Guardans, R., Holoubek, I., Jansson, B., Koch, R., Kuylenstierna, J., Lecloux, A., Mackay, D., McCutcheon, P., Mocarelli, P., and Taalman, R. D. F. (1998). Controlling persistent organic pollutants - what next? *Environmental Toxicology And Pharmacology*, 6(3):143–175.

Van Oostdam, J., Donaldson, S. G., Feeley, M., Arnold, D., Ayotte, P., Bondy, G., Chan, L., Dewaily, E., Furgal, C. M., Kuhnlein, H., Loring, E., Muckle, G., Myles, E., Receveur, O., Tracy, B., Gill, U., and Kalhok, S. (2005). Human health implications of environmental contaminants in Arctic Canada: A review. *Science Of The Total Environment*, 351:165–246.

von Waldow, H., MacLeod, M., Scheringer, M., and Hungerbühler, K. (2010). Quantifying remoteness from emission sources of persistent organic pollutants on a global scale. *Environmental Science and Technology*, 44(8):2791–2796.

Walker, C. (2009). *Organic Pollutants - An Ecotoxicological Perspective*. CRC Press.

Wania, F. and Mackay, D. (1993). Global fractionation and cold condensation of low volatility organochlorine compounds in polar regions. *Ambio*, 22(1):10–18.

Wania, F. and Mackay, D. (1995). A global distribution model for persistent organic chemicals. *Science of the Total Environment*, 161:211–232.

Wania, F. and Mackay, D. (1996). Tracking the distribution of persistent organic pollutants. *Environmental Science and Technology*, 30(9):A390–A396.

Wania, F. and Mackay, D. (1999). The evolution of mass balance models of persistent organic pollutant fate in the environment. *Environmental Pollution*, 100(1-3):223 – 240.

Wania, F. and Su, Y. S. (2004). Quantifying the global fractionation of polychlorinated biphenyls. *Ambio*, 33(3):161–168.

Wegmann, F., Cavin, L., MacLeod, M., Scheringer, M., and Hungerbühler, K. (2009). The OECD software tool for screening chemicals for persistence and long-range transport potential. *Environmental Modelling and Software*, 24(2):228 – 237.

Welshons, W. V., Thayer, K. A., Judy, B. M., Taylor, J. A., Curran, E. M., and vom Saal, F. S. (2003). Large effects from small exposures. I. mechanisms for endocrine-disrupting chemicals with estrogenic activity. *Environmental Health Perspectives*, 111(8):994–1006.

Witschi, H. (1999). Some notes on the history of Haber's law. *Toxicological Sciences*, 50(2):164–168.

Xiao, H. and Wania, F. (2003). Is vapor pressure or the octanol-air partition coefficient a better descriptor of the partitioning between gas phase and organic matter? *Atmospheric Environment*, 37(20):2867–2878.